UNIVERSITY OF CALIFORNIA

Los Angeles

Analysis of Glial Transcriptomes in Health and Disease

A dissertation submitted in partial satisfaction of the requirements for the degree Doctor of Philosophy in Neuroscience

by

Mitchell Krawczyk

2023

ABSTRACT OF THE DISSERTATION

Analysis of Glial Transcriptomes in Health and Disease

by

Mitchell Krawczyk

Doctor of Philosophy in Neuroscience

University of California, Los Angeles, 2023

Professor Ye Zhang, Chair

Glia are integral components of the central nervous system. Astrocytes, microglia, oligodendrocytes, and oligodendrocyte progenitor cells are numerous, ubiquitous cells that perform vital and wide-ranging functions from ion homeostasis to immune defense. However, neuroscience research historically adopted a neuron-centric framework, so tools and techniques developed to understand neuronal biology were not as quickly applied to glia. This dissertation utilizes next generation sequencing of RNA from various glial cell types to expand our understanding of glial biology in a several different contexts. In the first chapter, I examined the transcriptomic signatures of acutely purified human astrocytes at baseline and in pathological contexts because little is known about the biology of astrocytes in humans in health and disease. Peritumor astrocytes had decreased expression of synapse-related genes as well as a number of cell surface receptors, suggesting that astrocytes contribute to circuit dysfunction in the tumor microenvironment. I also mapped how gene expression of human astrocytes changes during maturation and aging, and identified sex-specific gene signatures of human

astrocytes. In the second chapter, I tested whether altering the peripheral immune system would alter glia in the brain. In recent years, there has been a boom in research uncovering interactions between the immune system and the brain, which was previously considered an immune-privileged organ. I performed RNA sequencing on four classes of glia in immunodeficient *Rag2*$^{-/-}$ mice that lack mature T and B cells required for adaptive immune responses. These mice had altered RNA expression in oligodendrocytes without notable changes in other cell types, including microglia, the brain-resident immune cells. These results revealed novel interactions between lymphocytes and oligodendrocytes. In the third and final chapter, I tested whether the gene *Serpine2* was important for glial transcription in astrocytes and microglia. *Serpine2* is substantially expressed in multiple brain cell types, particularly astrocytes, and it codes for a secreted serine protease inhibitor that regulates several enzymes, including thrombin. Microglia upregulated antimicrobial genes in the absence of *Serpine2*, revealing a novel mechanism by which microglial antimicrobial genes are regulated. In contrast astrocyte transcriptome did not change in the absence of *Serpine2*. Intriguingly, I did not find any gene expression associated with *Serpine2* in microglia or astrocytes after presenting an inflammatory stimulus. In total, this dissertation represents multiple lines of inquiry that improves our understanding of glial transcriptome in health and disease.

The dissertation of Mitchell Krawczyk is approved.

Baljit S. Khakh

Jessica Rexach

Michael Victor Sofroniew

Ye Zhang, Committee Chair

University of California, Los Angeles

2023

TABLE OF CONTENTS

List of Figures and Tables

Chapter 1:

Chapter 2:

Chapter 3:

Supplementary Information

ACKNOWLEDGEMENTS

First and foremost, I have to thank Dr. Ye Zhang for her mentorship and guidance over the last six years. She made a work culture centering optimism and compassion while leading by example with her own incredible work ethic. It was an honor and a pleasure learning from someone whose enthusiasm easily matches (if not exceeds) that of her trainees. As her first graduate student, I am amazed at the research program she has built from the ground up.

I am also hugely grateful to the Zhang lab members for the community and scientific support they provided throughout this process. Our team was small but mighty, and I leaned on every single lab mate at some point for questions, advice, or just a sympathetic ear. I have to specifically recognize Jiwen, Marlesa, and Lin, who were all reliable comrades for nearly the entire length of my PhD work. I learned from you all.

My particular journey also included a number of generous collaborators. It took a village for the human astrocyte project in particular to obtain such rare and valuable tissue samples. Special thanks to some of my closest collaborators, Samuel Reyes and Dr. Julia Chang, for their diligent work; despite the hectic nature of obtaining fresh, human tissue samples, they were always a source of calm and cheer. Thank you to all the talented surgeons who managed to collect samples for this valuable research while also handling the awesome responsibility of their patients' wellbeing. And of course, thank you to the people who consented to donate their brain tissue to this research. In the midst of harrowing personal circumstances, they made a selfless choice for the benefit of us all.

Thank you to the members of my committee, Drs. Baljit Khakh, Jessica Rexach, Michael Sofroniew, and formerly Michael Gandal. It astounds me that researchers of your stature and experience would bring your talents to bare on my humble work. I and my research are made better by your generosity and wisdom.

The community at UCLA played an important role during this long, challenging process. Dr. Felix Schweizer and Jenny Lee go above and beyond to provide support to the

neuroscience students. This program and this campus also gave me so many friends who helped make the last six years so much more than a degree: Jill, Ty, Megan, Tanya, Kelly, Amy, Lyle, Cassie, and Catherine to name a few (there are so many more).

Of course, there are many more people who filled my life and helped keep me sane throughout grad school. I can never apologize enough for all the time you had to spend listening to me talk about grad school. Thank you to Katie, Katelyn, Maddy, Sierra, Hadley, Emma, Larkin, Eliza, Kate, Michael, Ashley, Nick, John, Sixtine, Nisha, Marilyn, and many more for all the love and laughter that kept me going. My special thanks goes to Elizabeth Cooke for being my partner in crime. I shared more of this adventure with you than anyone else, and my memory of this time will always be tied to the memory of our friendship.

Lastly, I have to thank my family. To my mom, Tracy Krawczyk, and my dad, Paul Krawczyk, you have given me everything I needed to get me this far. To my sister, Olivia Krawczyk, you are an example to me in so many ways. The words “love” and “support” are too small to describe everything you all give me. To my grandmother, Patricia Cope, I know you would have loved to see this, and you are dearly missed.

Chapter 1 was originally published in *Journal of Neuroscience* in February of 2022 (Volume 42, Issue 8), presented here with minor formatting changes. As the primary author, I executed nearly all experiments, analysis, figure making, and writing myself, with the following contributions: Lin Pan, Rana Khankan, and Ye Zhang helped harvest some human astrocyte samples, Jillian Haney and Michael Gandal advised on analysis of RNAseq data, and Ye Zhang participated in writing and editing the manuscript.

Chapter 2 is currently in press in *PLOS ONE*, as of January 2023. Again, I performed the majority of experiments and analysis, and wrote the resulting manuscript myself with the following contributions: Lin Pan performed western blots and their quantification (Fig 2-3B), Alice Zhang aided in animal husbandry, and Ye Zhang assisted in editing the manuscript.

Chapter 3 will be submitted for publication shortly. I performed the majority of experiments, analysis, and manuscript preparation. Paul Vander performed immunohistochemistry of *Serpine2* mice, including the staining, imaging, and quantification of microglial markers presented in Figure 3-3. Once again, Alice Zhang assisted in animal husbandry, and Ye Zhang participated in editing and revising the manuscript.

Finally, I would like to acknowledge the financial support that made this work possible. I received funds from the lab of Ye Zhang, the ARCS Foundation, and the Neurobehavioral Genetics T32.

VITA

EDUCATION

BS Neurobiology, Psychology; University of Washington (*summa cum laude*) 2012-2016

RESEARCH EXPERIENCE

University of California, Los Angeles, CA 2016-present
Laboratory of Dr. Ye Zhang

University of California, Los Angeles, CA 2016
Laboratory of Dr. Felix Schweizer

University of Washington, Seattle, WA 2014-2016
Laboratory of Dr. Martha Bosma

RESEARCH GRANTS AND FELLOWSHIPS

2018-2022 ARCS Scholar
2021-2022 Neurobehavioral Genetics T32

PUBLICATIONS

M Krawczyk, A Zhang, & Y Zhang. Lymphocyte deficiency alters the transcriptomes of oligodendrocytes, but not astrocytes or microglia. *PLOS One* (in press)

D Sapkota, M Kater, K Sakers, K Nygaard, Y Liu, S Koester, S Bass, A Lake, R Khazanchi, R Khankan, **M Krawczyk**, A Smit, S Maloney, M Verheijen, Y Zhang, & J Dougherty. Activity dependent translation dynamically alters the proteome of the perisynaptic astrocyte process. *Cell Reports* (2022)

K Leng, I Rose, H Kim, W Xia, W Romero-Fernandez, B Rooney, M Koontz, E Li, Y Ao, S Wang, **M Krawczyk**, J TCW, A Goate, Y Zhang, E Ullian, M Sofroniew, S Fancy, M Schrag, E Lippmann, & M Kampmann. CRISPRi screens in human iPSC-derived astrocytes elucidate regulators of distinct inflammatory reactive states. *Nature Neuroscience* (2022) preprint: https://doi.org/10.1101/2021.08.23.457400

M Krawczyk, JR Haney, et al. Human astrocytes exhibit tumor microenvironment-, age-, and sex-related transcriptomic signatures. *Journal of Neuroscience* (2022) https://doi.org/10.1523/JNEUROSCI.0407-21.2021

J Li, R Khankan, C Caneda, MI Godoy, MS Haney, **M Krawczyk**, MC Bassik, SA Sloan, and Y Zhang. Astrocyte-to-astrocyte contact and a positive feedback loop of growth factor signaling regulate astrocyte maturation. *Glia* (2019) https://doi.org/10.1002/glia.23630

KE Miller, K Barr, **M Krawczyk**, & E Covey. Seasonal variations in auditory processing in the inferior colliculus of Eptesicus fuscus. *Hearing Research* (2016) https://doi.org/10.1016/j.heares.2016.07.014

Chapter 1

Human Astrocytes Exhibit Tumor Microenvironment-, Age-, and Sex-Related Transcriptomic Signatures

1.1 Abstract

Astrocytes are critical for the development and function of synapses. There are notable species differences between human astrocytes and commonly used animal models. Yet, it is unclear whether astrocytic genes involved in synaptic function are stable or exhibit dynamic changes associated with disease states and age in humans, which is a barrier in understanding human astrocyte biology and its potential involvement in neurological diseases. To better understand the properties of human astrocytes, we acutely purified astrocytes from the cerebral cortices of over 40 humans across various ages, sexes, and disease states. We performed RNA sequencing to generate transcriptomic profiles of these astrocytes and identified genes associated with these biological variables. We found that human astrocytes in tumor-surrounding regions downregulate genes involved in synaptic function and sensing of signals in the microenvironment, suggesting involvement of peri-tumor astrocytes in tumor-associated neural circuit dysfunction. In aging, we also found downregulation of synaptic regulators and upregulation of markers of cytokine signaling, while in maturation we identified changes in ionic transport with implications for calcium signaling. In addition, we identified subtle sexual dimorphism in human cortical astrocytes, which has implications for observed sex differences across many neurological disorders. Overall, genes involved in synaptic function exhibit dynamic changes in the peritumor microenvironment and aging. This data provides powerful new insights into human astrocyte biology in several biologically relevant states, that will aid in generating novel testable hypotheses about homeostatic and reactive astrocytes in humans.

1.2 Introduction

Astrocytes are a major component of the central nervous system. Though astrocytes were long regarded as passive support cells, studies of murine astrocytes found they have active functions that are critical for the development and function of synapses. For example, astrocyte-secreted factors powerfully induce the formation of functional synapses *in vivo* and *in*

vitro, which otherwise largely fails to occur [1-10]. In addition to important roles in synapse formation, astrocytes contribute to engulfment and elimination of synapses in development [11-14]. Moreover, astrocytes maintain extracellular potassium levels [15-17] and participate in recycling neurotransmitters [18], thus maintaining homeostasis at synapses. There is now a variety of evidence showing that astrocytes help shape circuit functions and behavior [19-27]. Various groups have demonstrated that altering intracellular astrocyte signaling *in vivo* can induce abnormal behavior or correct phenotypic behavior in disease models [15, 28-34]. Astrocytes are molecularly and functionally heterogeneous, potentially adapting to diverse roles they play in different brain regions [35-42].

Astrocyte biology faces an added layer of complexity considering their significant dynamism in response to insult or injury [43]. Astrocytes undergoing reactive astrogliosis in response to a challenge can display stark morphological changes, including hypertrophy and retraction of processes, in addition to a plethora of intracellular alterations [44]. Reactivity is observed in many neurological disorders including traumatic brain injury, stroke, epilepsy, and neurodegenerative diseases, and there appears to be disease-specific aspects to this response [29, 45-49].

Given their many and varied roles in the central nervous system (CNS), astrocytes are frequently implicated in neurological pathologies [26, 50-57]. Recently, transcriptomic analysis of neuropsychiatric disease found astrocytic genes included in the gene signatures of autism spectrum disorder, bipolar disorder, and schizophrenia [58, 59]. Astrocyte reactivity is also prominent in several neurodegenerative diseases, including Alzheimer disease and Parkinson disease [48]. In amyotrophic lateral sclerosis (ALS), reactive astrogliosis occurs around degenerating motor neurons, and this reactivity precedes motor neuron death in the rat SOD1 model of ALS [60]. Further investigation found that overexpressing GLT1 in astrocytes improved neuronal survival and delayed disease onset in the mSOD1 mouse model of ALS [61].

Our understanding of human astrocytes significantly trails our knowledge of murine astrocytes [62]. Although the majority of major astrocyte functions appear to be shared between mice and humans, it is still imperative to narrow this gap in knowledge as researchers continue to identify important differences between these species in the CNS. Firstly, human astrocytes are notably larger with more elaborate branching than rodent astrocytes *in vivo* and *in vitro* [63-65]. At the molecular level, previous characterization of human and mouse astrocyte transcriptomes found many genes specifically expressed by human astrocytes [65, 66]. At a functional level, behavioral differences were observed *in vivo* when human glial progenitors were transplanted into mice [67]. Animal studies have produced, and continue to produce, a remarkable body of knowledge concerning the many vital astrocytic functions in the brain (e.g. synapse formation, circuit functions). It is because animal models clearly demonstrate the importance of astrocyte biology that complementary analysis is also required in humans.

Given the importance of astrocytes in synaptic function, a key question that needs to be answered is whether genes involved in astrocyte-synapse interactions are stable or exhibit dynamic changes associated with disease states and age in humans. With the advent of improved astrocyte purification methodologies, we can now extract highly pure populations of human astrocytes by targeting the astrocytic cell surface protein HepaCAM using antibodies. By employing an immunopanning technique, we previously published human astrocyte transcriptomes of twelve human cortical samples between the ages of 8 and 63 years old [65]. In this study, we acutely purified samples from over 40 patients, which now include astrocytes from healthy and diseased brain regions. For the first time, we are also presenting samples under the age of 8, allowing for analysis of human astrocyte maturation, as well as other biological variables of interest. Here, we describe some of the first transcriptomic data of human astrocytes in the tumor microenvironment, as well as changes in astrocyte gene expression associated with maturation, aging, and sex. Among our findings, we see downregulation of synaptic genes in peritumor astrocytes as well as aging astrocytes.

1.3 Materials and Methods

Human Tissue

Human tissue was obtained with informed consent and the approval of the UCLA Institutional Review Board. We obtained tissue primarily from brain surgeries at UCLA to treat epilepsy and tumors, plus one postmortem sample with short postmortem interval (<18 hours). All samples were from the cerebral cortex, primarily from the temporal lobe (n = 31), but several samples came from the frontal (n = 9) or parietal lobes (n = 5), or the insula (n =2). Tissue was immersed in 4° C media (saline or Hibernate-A medium) before transfer to the lab for dissection and dissociation. Six samples were obtained from surgeries offsite, which were shipped overnight in 4°C media for dissection and dissociation in the lab. The final cohort includes 7 peritumor samples, 30 epilepsy samples, and 12 controls totaling 49 samples from 41 patients (see SI1-1). No affected samples came from the same patient that provided a control sample.

Vertebrate Animals

All mouse experimental procedures were performed with approval from the UCLA Chancellor's Animal Research Committee in compliance with all federal and state laws and policies. For *in situ* hybridization of mouse brain tissue, we used mice at postnatal day 71 (2 females, 1 male) from a C57/BL6 FVB mixed background.

Purification of Human Astrocytes

Human astrocytes were purified using immunopanning, as described in [65]. Briefly, we dissected gray matter from cortical tissue and enzymatically digested the tissue with papain (20 units/mL) for 80 minutes at 34.5°C. We then rinsed the tissue in a protease inhibitor solution. We gently triturated the tissue to generate a single-cell suspension, and we passed the cells over a series of plastic petri dishes that were precoated with antibody. The cell suspension was incubated at room temperature for 10-15 minutes on each dish, which contained anti-CD45 antibody (BD Pharmingen 550539) to deplete microglia, O4 hybridoma to deplete

oligodendrocyte precursor cells, GalC hybridoma to deplete oligodendrocytes and myelin, or anti-Thy1 (BD Pharmingen 550402) to deplete neurons. Finally, the astrocyte-enriched cell suspension was incubated for 20 minutes at room temperature on a dish coated with anti-HepaCAM antibody (R&D Systems MAB4108) to bind astrocytes. We washed the bound astrocytes with PBS to remove contaminants, and we immediately harvested RNA by applying 700 μL of TRIzol solution (Thermo Fisher Scientific 15596018). TRIzol solution was then flash frozen in liquid nitrogen and stored at -80°C to await RNA purification. The total time from receiving tissue to storing astrocyte RNA took approximately 4 hours.

RNA Library Construction and Sequencing

RNA was extracted from frozen TRIzol using the miRNeasy kit (Qiagen 217004), according to the manufacturer's protocol. We checked RNA quality with the 2200 TapeStation System (Agilent G2964AA) and the RNA high sensitivity assay (Agilent 5067-5579). All RNA integrity numbers were ≥ 6.5, except RNA samples that were not concentrated enough for accurate measurement. We then used the Nugen Ovation RNAseq System V2 (Nugen 7102-32) to generate cDNA libraries, and we fragmented the cDNA using a Covaris S220 focused-ultrasonicator (Covaris 500217). We amplified and prepared these libraries for sequencing with the NEB Next Ultra RNA Library Prep Kit (New England Biolabs E7530S) and NEBNext multiplex oligos for Illumina (NEB E7335S). We performed end repair and adapter ligation, and we amplified the final libraries using 10 cycles of PCR. The sequencing libraries were verified using the TapeStation D1000 assay (Agilent 5067-5582). Indexed libraries were pooled and sequenced using the Illumina HighSeq 4000 sequencer and obtained 18.9 million ± 1.6 million (mean ± SEM) single end, 50 bp reads across four batches.

Read Alignment and Quantification

We mapped reads using the STAR package [68] and genome assembly GRCh38 (Ensembl, release 91), and obtained 77.0% ± 5.8% (mean ± standard deviation) uniquely aligned reads in all samples. Reads were counted using the HTSeq package [69], and reads

were subsequently quantified by Reads Per Kilobase of transcript per Million mapped reads (RPKM) using EdgeR-limma packages in R (SI1-2).

Differential Gene Expression Analysis of Disease and Sex

We analyzed differential gene expression of disease and sex using the DESeq2 package in R, see Figures 2-1, 4-1, & 6-1 [70]. In this analysis, we included all samples and used the following command to create our linear model: ~ factor(Diagnosis) + Age + factor(Sex) + MicroPC + Batch, where Diagnosis was a factor with values [Control, Peritumor, Epilepsy], Age was a numeric value in years, Sex was a factor with values [Male, Female], and MicroPC was numeric value measuring microglia contamination. To calculate the "microPC", we first determined the gene expression of microglia-specific genes (>10x enriched in microglia vs. astrocytes) in all samples, using the data from [65]. Then, we performed principal component analysis (PCA) using the prcomp function in R on the scaled microglia gene expression, and we took the first principal component (PC1) as a summary measure of microglial gene expression in each sample. Results were cross-checked with leave-one-out validation, where the analysis was reiterated with the removal of one sample in each round for a total of 49 iterations. To determine how robust the analysis is to the effect of brain region, we reran the analysis using only temporal lobe tissue, see results in SI1-4. We further assessed the effect of brain region by performing differential gene expression analysis of region in samples from temporal lobe and frontal lobe (peritumor samples excluded, see SI1-5). We used the linear model: ~ factor(Region) + Age + factor(Sex) + MicroPC + Batch.

Analysis of Human Aging Genes

To identify genes associated with aging astrocytes, we began with genes significantly associated with Age in the DESeq2 analysis of disease and sex, as described above. In order to separate genes that change in aging (i.e. later life) from genes that change in development (early life), we categorized samples in 3 categories, excluding peritumor samples: 0-21 years old (n = 34), 21-50 years old (n = 3), and 50+ years old (n = 5). We compared younger adults

(21-50) to older adults (50+), and we narrowed the gene list to those with an average expression > 0.01 RPKM and 1.5-fold differences in the average expression between groups. This yielded a list of 394 gene entries, 277 of which were protein-coding, see SI1-12.

Analysis of Human Astrocyte Maturation

We analyzed differential gene expression across astrocyte maturation using a two-step process. First, we performed DESeq2 on samples ≤ 21 years old, excluding peritumor samples (n = 35). Model: ~ factor(Diagnosis) + Age + factor(Sex) + MicroPC + OligPC + factor(Batch). The "oligPC" was calculated in the same manner as the microPC using gene expression of oligodendrocyte-specific genes identified using data from [65]. While it is necessary to use cell-type specific filters to exclude contamination, excluding oligodendrocyte-enriched genes may obscure potential lineage relationships between astrocytes and oligodendrocytes [71]. Thus, we only used these filters for differential expression analysis and included the unfiltered complete dataset in SI1-2. Finally, we filtered out genes that were 10x enriched in human neurons over human astrocytes, using data from [65]. This yielded 1,463 gene entries significantly associated with maturation. We also performed a leave-one-out reanalysis to assess the robustness of the maturation gene expression findings, see SI1-4.

The DESeq2 analysis included samples as young as 7 months old, but we could capture changes from earlier stages in development by using our recently published transcriptomic profiles of fetal human astrocytes. We compared 4 fetal samples with our near-adult human samples between 13-21 years old (excluding peritumor, n = 11). For each sample, gene expression was converted to a percentile, where the most highly expressed gene = 1 and the least expressed gene = 0. Next, we conducted parallel t-tests with a Benjamini-Hochberg correction for multiple tests, performed in GraphPad Prism v8. This generated over 10,000 hits. Finally, we combined the two gene lists using an equal number of genes from each list, (i.e. we filtered results from the second analysis to the 1,463 top hits by p-value to match the first

analysis), producing a final list of 2,749 genes associated with human astrocyte maturation, see SI1-10.

Analysis of Disease-Associated Genes

We tested whether peritumor or maturation gene signatures were enriched with disease-associated genes. We obtained gene lists for various neurological diseases from a curated database, Phenopedia [72]. Using these gene lists, we performed Fisher's exact tests on differentially expressed genes in peritumor astrocytes and corrected for multiple comparisons using the Benjamini-Hochberg method. The results are in SI1-6.

Mouse Aging Genes and Human Comparison

We accessed mouse astrocyte RNAseq data from the BioProject database (www.ncbi.nlm.nih.gov/bioproject), accession no. PRJNA417856 [73]. We downloaded FASTQ files of sequenced cortical astrocytes at ages postnatal day 7 (n = 3), 10 weeks (n = 3), and 2 years (n = 2). Reads were aligned with STAR 2.6.0 and genome assembly GRCm38 (Ensembl release 100). All samples had >70% uniquely mapped reads. We used HTSeq to generate counts, and then we determined differential gene expression between two ages (day 7 vs. 10 weeks & 10 weeks vs. 2 years) using DESeq2. Model = ~ factor(Age), where Age is a binary factor.

We used the STRING database (string-db.org) to find and visualize protein-protein interactions in human and mouse aging-associated genes. For mouse aging genes, we combined the results of three studies of mouse astrocytes [73-75].

Gene Ontology (GO)

To identify patterns in our various differentially expressed gene lists, we used the online platform Metascape (metascape.org, [76]). We input all protein-coding genes from our gene sets, and conducted an enrichment analysis with default settings, with the following adjustments: reference data sets were limited to GO datasets (Molecular Functions, Biological Processes, and Cellular Components), and we defined a list of background genes (i.e. the set of

genes expressed in astrocytes that are included in this analysis) as follows: for human analyses, the background gene list consisted of all genes with expression ≥0.05 RPKM in 30+% of our samples. For mouse analyses, the background list consisted of genes with ≥0.05 RPKM in 30+% in the mouse samples from [73].

We used Fisher's exact test to individually test differentially expressed genes in peritumor astrocytes for enrichment of GO gene sets that were reportedly found in tumor-core astrocytes [77]: Positive regulation of receptor signaling via JAK/STAT (GO:0046427/GO:2000366), Negative regulation of receptor signaling via JAK/STAT (GO:0046426, GO:2000365), Interleukin-6 mediated signaling pathway (GO:0070102), and Response to interferon gamma (GO:0034341).

Pro- and anti-inflammatory genes were identified using GO annotations for positive regulation of inflammatory response (GO:0050729) and negative regulation of inflammatory response (GO:0050728) [78-80].

RNAScope In Situ Hybridization

RNAScope in situ hybridization was performed on fresh frozen human tissue collected from surgeries and fresh frozen mouse tissue harvested after a 10-minute transcardial perfusion of phosphate buffered saline. Tissues were embedded in OCT compound (Fisher Scientific 23-730-571) and cut into 20-30 μm-thick sections. RNAScope Multiplex Fluorescent V2 Assay (ACDBio 323100) was performed per manufacturer's protocols. Probes were purchased from ACDBio for human and mouse *SLC1A3* and *TLR4*. Images were captured using the Zeiss LSM 800 confocal microscope using at equal power and exposure across all samples stained with the same set of probes. Photoshop v22.1 was used to enhance brightness for publication.

Statistical Analyses

Differential gene expression was analyzed using DESeq2. Enrichment of GO terms was analyzed using Metascape. Enrichment of disease-associated genes and peritumor genes was

analyzed with Fisher's exact test in R using fisher.text(). All analyses are detailed under the corresponding sections above.

Data Deposition

All human RNAseq data is deposited on the Gene Expression Omnibus and will be made public before publication.

1.4 Results

Purification of Human Cortical Astrocytes in Health and Disease

We obtained human cortical tissue from patients undergoing neurological surgery. Our final analysis includes 49 samples from 41 patients, with ages ranging from 7 months to 65 years old. Twelve of these samples were taken from normal regions of cortex that were resected *en route* to deep-seated pathologies. Nine of these normal specimens were obtained during surgery for deep epileptogenic foci. In these cases, we confirmed that normal specimens taken did not include abnormal-appearing tissue using MRI-registered frameless stereotaxy, did not show abnormal interictal activity on invasive electrode recordings, and did not demonstrate abnormal histopathologic findings. Two other cases from which normal specimens were collected were encapsulated, benign tumors, where normal-appearing brain tissue based on MRI-registered frameless stereotaxy was collected outside a 1 cm margin from the tumor. Finally, one normal tissue specimen was obtained from a patient at the time of death from a cardiac condition, without other intracranial pathologies. A similar cohort of control human astrocytes were sequenced and analyzed previously, where the authors characterized the baseline characteristics of the human astrocyte transcriptome (Zhang et al., 2016); of note, we used remaining RNA from 7 of these samples in this study. From this point forward, we refer to normal brain tissue samples from these sources as "controls".

In the current study, we sought to compare normal astrocytes against disease-affected astrocytes. Affected samples included in the analysis fall into two categories of diagnosis: 1) 30

included brain tissue showing epileptiform activity on intra-operative electrode recordings surrounding resected focal cortical dysplasia (FCD), a developmental form of epilepsy; and 2) 7 included brain tissue immediately surrounding a brain tumor (including glioblastoma, low grade glioma, and metastatic breast cancer) based on MRI and visual inspection at the time of surgery (referred to here as “peritumor”). Specific pathologic diagnoses are presented in SI1-1.

We purified human cortical astrocytes using immunopanning (Fig 1-1A). We removed white matter and generated a single cell suspension with mechanical and enzymatic digestion. The single cell suspension passes over antibody-coated Petri dishes that bind contaminating cell types with cell type specific antigens. This immunopanning protocol uses anti-CD45 antibodies to pull down myeloid cells (i.e. microglia and macrophages), anti-GalC hybridoma cell supernatant to pull down oligodendrocytes and myelin debris, anti-O4 hybridoma cell supernatant to bind oligodendrocyte precursor cells (OPCs), and anti-Thy1 antibodies to bind neurons. Finally, the enriched suspension passes onto a dish coated in anti-HepaCAM antibodies, a cell-surface glycoprotein enriched in astrocytes. We harvested the astrocyte RNA from this dish and used it to perform RNA sequencing (RNAseq). The sequenced samples show high expression of astrocyte marker genes such as GFAP and SLC1A2, and extremely low expression of neuronal, myeloid, and endothelial genes. There are only slight traces of some oligodendrocyte-lineage marker genes (Fig 1-1B). Using immunopanning, we obtained RNA highly enriched for human cortical astrocytes in healthy and diseased states for bulk RNAseq (SI1-2).

Glioblastoma cells infiltrate surrounding brain tissue. To determine whether our purified astrocytes from the peritumor regions are bona fide astrocytes or infiltrating glioblastoma cells, we examined the expression of a glioblastoma marker gene AVIL [81] and did not detect expression in our peritumor astrocyte samples (SI1-2). Furthermore, we compared gene expression of astrocytes surrounding glioblastoma tissue (infiltrating) and astrocytes surrounding low grade glioma or metastatic tumors (non-infiltrating). Peritumor astrocyte

signature genes described below are not more highly expressed by glioblastoma-surrounding astrocytes than non-infiltrating tumor-surrounding astrocytes (SI1-2). Although we cannot rule out contamination from a small number of infiltrating glioblastoma cells, the gene signatures of peritumor astrocytes are likely from predominantly bona fide astrocytes instead of infiltrating cells.

Peritumor astrocytes downregulate genes involved in synaptic function and genes encoding cell surface receptors

After sequencing RNA from human astrocytes in FCD and peritumor regions, we employed differential gene expression analysis to examine their molecular signatures using the analysis package DESeq2 in R. We used a linear model that included variables for diagnosis, sequencing batch, age, and sex. To control for potential variance from low level microglial contamination, we included an additional variable that quantified microglial marker gene expression by performing principal components analysis (PCA) on microglial marker gene expression in our dataset. Including the first principal component in the linear model effectively eliminated significant differential expression of microglial genes.

First, we examined the effect of the brain tumor microenvironment on astrocyte gene expression. Brain tumors drive considerable changes in the surrounding microenvironment, and astrocytes themselves are known to readily change state in response to a variety of stimuli [82, 83]. However, transcriptomic changes of peritumor astrocytes in humans have not been reported, to the best of our knowledge. Using our DESeq2 pipeline, we found 3,131 genes differentially expressed in peritumor astrocytes, providing a new resource for elucidating astrocytic changes in the brain tumor microenvironment (SI1-3). The vast majority of these findings were robust under leave-one-out validation (SI1-4) where the analysis was reiterated with the removal of one sample in each round.

Synaptic gene signatures in peritumor astrocytes

Many genes related to synaptic function are downregulated in the peritumor region (Fig 1-2A-D), such as the glutamate transporters SLC1A2 and SLC1A3, which take up the excitatory neurotransmitter glutamate from the synaptic cleft and maintains excitation-inhibition balance in the brain [84]. SLC1A2-knockout mice suffer from epileptic seizures and die prematurely [85]. Also downregulated is the gene KCNJ10 encoding the inwardly rectifying potassium channel Kir4.1, which takes up potassium from the extracellular space after neuronal firing, buffers potassium levels in the astrocytic syncytium, and modulates neuronal excitability [86]. Patients with mutations in the KCNJ10 gene suffer from seizure disorders [87]. A large proportion of human patients with brain tumors also suffer from epileptic seizures, which reduce their quality of life and sometimes cause death [88]. Our observation of strong reductions of SLC1A2, SLC1A3, and KCNJ10 in peritumor astrocytes suggest potential involvement of astrocytes in tumor-associated seizures and reveal astrocytes as novel potential targets for treating these seizures. A study in a rat model of glioma supports the feasibility of this approach [89]. Furthermore, astrocyte secreted molecules that regulate synapse formation and maturation, SPARCL1, CHRDL1, and GPC5 are also downregulated in peritumor astrocytes (Fig 1-2B, 2D). Together, these findings suggest decreased support of synapses in the tumor microenvironment that could contribute to dysregulation of synaptic activity and emergent clinical symptoms like seizures. Upregulated genes in peritumor astrocytes include the reactivity-associated genes GFAP, TIMP1 and VIM, suggesting that astrocytes in the peritumor microenvironment are reactive in humans.

Cell surface receptors in peritumor astrocytes

Cell surface receptors mediate sensing of signals in the microenvironment. To examine the expression of genes encoding receptors located on the plasma membrane by peritumor astrocytes, we used a list of experimentally validated and in silico predicted genes encoding cell surface receptors [90]. We determined the complete set of transmembrane receptors present in human astrocytes (SI1-7). We found 157 transmembrane receptor genes expressed by human

astrocytes (average RPKM >1). Of these genes, peritumor astrocytes downregulate one fourth (40/157) and upregulate only 3/157, suggesting that peritumor astrocytes are impaired in their ability to receive and respond to external cues (Fig 1-2G).

Synaptic genes and cell surface receptors downregulated in peritumor astrocytes are associated with psychiatric disease risk

Having discovered genes up- and down-regulated in peritumor astrocytes, we next assessed whether these genes are involved in other diseases. We used the Phenopedia dataset for genes associated with various neurological diseases [72] and tested whether genes up and downregulated in peritumor astrocytes are significantly enriched in genes associated with the risk of each neurological disorder using Fisher's exact test followed by correction for multiple comparisons (Methods). Genes that were downregulated in peritumor astrocytes were enriched for genes with genetic links to several neurological diseases (SI1-6). Interestingly, these associations existed primarily among psychiatric disorders (bipolar disorder, schizophrenia, mood disorders, obsessive-compulsive disorder, depressive disorder, and anxiety disorder). In addition, genes downregulated in peritumor astrocytes also significantly overlap with Alzheimer's disease risk genes, but not with other neurodegenerative disorders (Parkinson Disease, ALS, Frontotemporal Dementia, and Huntington Disease).

Next, we asked whether synaptic and receptor genes contributed to the association between peritumor genes and genes associated with psychiatric disease. We tested whether synaptic genes and receptor genes downregulated in peritumor astrocytes were enriched in genes associated with risks of the aforementioned six psychiatric disorders and Alzheimer's Disease. We found that both synaptic and receptor genes downregulated in peritumor astrocytes are enriched in genes associated with all six psychiatric disorders, whereas Alzheimer's Disease only associated with synaptic genes (SI1-6). We conclude that peritumor astrocytes downregulate receptor and synaptic genes that are associated with psychiatric

disease risk, highlighting the potential importance of this core group of astrocytic genes in neural circuit development and function.

Gene ontology of peritumor astrocyte signatures

To find larger patterns in the data, we performed pathway analysis with the online tool Metascape to identify gene ontology (GO) terms that are enriched in our gene lists (SI1-8). Among upregulated genes, we found highly significant enrichment of GO terms related to cell cycle and protein translation, consistent with the presence of proliferative reactive astrocytes in the peritumor region. Meanwhile, downregulated genes were enriched for an array of functional terms related to synaptic function as well as cation transport (Fig 1-2C), further supporting the hypothesis that peritumor astrocytes are defective in supporting or participating in normal synaptic signaling. Interestingly, both up- and downregulated gene lists are enriched for extracellular matrix genes (Fig 1-2E), which is notable considering the importance of extracellular remodeling in tumor expansion and migration as well as synaptic plasticity [91, 92]. Broadly, we see peritumor astrocytes alter extracellular matrix gene expression while upregulating genes necessary for cell division and translation, and downregulating expression of genes related to synaptic transmission and ionic homeostasis, revealing potential contribution of astrocytes to neural circuit dysfunction associated with brain tumors.

Peritumor astrocytes differ from tumor-core astrocytes

To assess whether peritumor astrocytes resemble tumor-core associated astrocytes, we compared our peritumor astrocyte dataset to a previously published tumor-core associated astrocyte dataset [77]. Heiland and colleagues reported that tumor-core astrocytes contribute to an immunosuppressive environment in part due to increased JAK/STAT pathway activation. Among peritumor astrocytes, however, we did not find significant enrichment of the JAK/STAT pathway among differentially expressed genes. We also failed to find enrichment of interferon gamma response genes and interleukin-6 response genes, which were also identified by Heiland et al. When we examined pro- and anti-inflammatory genes that are differentially

expressed in peritumor astrocytes, we found that the majority of pro-inflammatory genes were upregulated (10/11, Fig 1-2F), and the majority of anti-inflammatory genes were downregulated (16/26, Fig 1-2F). Taken together, these findings suggest a contrast between an anti-inflammatory signature of tumor-core astrocytes, and an at least partly pro-inflammatory signature of peritumor astrocytes.

Peritumor astrocytes attenuate core astrocytic genes

To assess whether peritumor astrocytes may lose normal astrocyte function, we examined genes highly expressed by astrocytes and found that peritumor astrocytes downregulate several known markers of mature astrocytes (Fig 1-2D). Furthermore, we examined a list of the top 50 astrocyte markers identified in a meta-analysis of human gene expression [93]. Peritumor astrocytes significantly downregulated 41/50 genes, with 50/50 trending downward (Fig 1-2H). These results are consistent with a possible loss of normal astrocytic functions in the peritumor microenvironment.

TLR4 is expressed by human astrocytes and not mouse astrocytes

To assess changes of peritumor astrocytes using an orthogonal approach, we performed *in situ* hybridization with RNAscope. Based on RNAseq, we found that toll-like receptor 4 (TLR4) was downregulated in peritumor astrocytes. TLR4 is a member of the toll-like receptor family of pattern recognition receptors, which recognize pathogen-associated molecular patterns and initiate innate immune responses [94]. Specifically, TLR4 encodes a transmembrane protein that binds bacterial lipopolysaccharides and triggers innate immune responses to bacterial infection. Moreover, TLR4 also recognizes endogenous ligands, such as heat shock proteins and lipoproteins from damaged cells [95]. Previous studies in mice found that TLR4 was highly enriched in myeloid cells, such as microglia in the brain, but we detected significant mRNA expression of TLR4 in astrocytes in humans (this study and Zhang et al. 2016). To directly compare TLR4 expression between species, we performed RNAscope *in situ* hybridization on human and mouse cortical tissue. Whereas a small minority of mouse astrocytes expressed

TLR4 (7%, 4/58 cells, n = 3), a majority of human astrocytes showed expression of TLR4 (62%, 18/29 cells, n = 2, Fig 1-3A, B). Even more strikingly, TLR4$^+$ astrocytes in humans contain larger numbers of TLR4$^+$ mRNA puncta than did TLR4$^+$ astrocytes in mice (Fig 1-3C). Though the small sample size does not provide a definitive conclusion, we find evidence of human-specific expression of TLR4 in astrocytes that corroborates findings from RNAseq, suggesting enhanced ability of human astrocytes to detect TLR4 ligands, such as signals from bacteria and damaged cells, compared with mouse astrocytes. Furthermore, this mode of signaling is notably reduced in peritumor astrocytes.

The transcriptomes of astrocytes in FCD and control do not differ

Next, we examined the transcriptional signature of FCD. FCD is characterized by abnormalities in neuronal migration during development. Patients with FCD display abnormal radial and/or tangential lamination in a local region of cerebral cortex. More severe cases include dysmorphic neurons, and others also develop large and often multi-nucleated cells called balloon cells [96]. Our DESeq2 analysis found only 24 protein-coding genes significantly associated with epilepsy, and all but one of those genes (SCN4B) had low expression (an average expression <1 RPKM; see SI1-9). Samples from FCD patients did not separate from controls in PCA, hierarchical clustering, or expression of reactive astrocyte markers (data not shown). Therefore, astrocytes in FCD in humans do not exhibit robust gene expression changes. However, we cannot exclude the possibility that a small subpopulation of astrocytes immediately adjacent to FCD lesions have gene expression changes that were undetectable at the population level. Given the lack of robust differences between control samples and epilepsy samples, they were used along with control samples in subsequent analyses.

Genes involved in ion transport and calcium signaling change with astrocyte maturation

Developing and mature brains have drastically different cognitive capacities, learning potentials, and susceptibilities to disease. Astrocytes are critical for the development of neural circuits, maintenance of homeostasis in adults, and responses and repair in neurological

diseases [11, 97, 98]. However, cellular and molecular changes of astrocytes during brain development and maturation in humans are unclear. Previous studies have performed transcriptome profiling of a small number of samples of human astrocytes from fetuses, children ≥8 years old, and adults [65]. The gene expression profiles of astrocytes during an important period of development, birth to 8 years, remain unknown. Therefore, molecular knowledge of astrocyte development and maturation in humans is incomplete. Here, we recruited patients throughout development and adulthood (n=16 samples between 0-5 years old; 6 samples between 6-10 years old; 12 samples between 11-17 years old; and 8 adult samples, excluding peritumor; SI1-1), purified astrocytes, and performed RNA-seq. We analyzed maturation-associated genes based on our new RNAseq data using a linear model (DESeq2 R package, detailed in Methods) and also included fetal data from our previous study [66] after normalizing data from two studies using percentiles (detailed in Methods). Our final results find 1509 upregulated genes and 1240 downregulated genes associated with astrocyte maturation across human development (Fig 1-4C, SI1-10). Major astrocyte markers were not highly expressed in fetal astrocytes, but even the youngest postnatal samples (7 months) showed high expression of most markers. However, postnatal gene expression continued to evolve. Notably, top genes changing in the postnatal epoch displayed a shift in expression starting around 8 years old (Fig 1-4A).

To assess the changes associated with astrocyte maturation, we analyzed gene ontology of up- and downregulated astrocyte maturation genes using Metascape (see SI1-11). Upregulated genes showed significant enrichment for several GO terms related to ion homeostasis, as well as lipid metabolism (Fig 1-4B). Many of the genes pertaining to ion transport are specifically related to calcium transport and signaling (Fig 1-4D), which is intriguing given the importance of calcium as a signaling molecule, particularly in astrocytes. Therefore, immature and mature astrocytes may differ in ion transport and calcium signaling, thus altering many downstream signaling pathways that affect both astrocytes and surrounding neurons in

development. Downregulated GO terms are almost entirely related to cell cycle and cell division, which is expected to decline throughout development (Fig 1-4B). We also observe a general upward trend for several astrocyte marker genes that we would also expect to increase across maturation (Fig 1-4D).

Characterizing the maturation of human astrocytes directly contributes to our understanding of human astrocyte biology and brain development, but most existing knowledge is derived from animal studies. Therefore, it is vital to determine which aspects of human biology are recapitulated by animal models and which are wholly unique. We compared our analysis of human astrocyte maturation with a published study that measured mouse astrocyte gene expression across several ages [73]. We compared astrocyte gene expression data from mice at an early developmental age, postnatal day 7 (P7), and a young adult timepoint, 10 weeks, and identified 4,417 genes associated with mouse astrocyte maturation. Most of the mouse and human astrocyte maturation genes we found were not direct orthologues (Fig 1-4C), and yet both gene lists had remarkably similar patterns based on gene ontology (Fig 1-4B). Both species downregulate cell division and upregulate ionic transport and calcium signaling genes across maturation. The conservation of these patterns in evolution suggests the importance of these astrocytic developmental changes. Based on this analysis, we find that human and mouse astrocytes share broad outcomes in maturation but differences concerning the exact pattern of molecular changes. While mouse models may not recapitulate every aspect of human biology, our data suggest that the maturation of astrocytes in humans can be accurately modeled in mice.

Human astrocytes downregulate genes involved in synaptic function in aging

Aging is associated with increased risk of cognitive decline and increased susceptibility to neurodegeneration and stroke. Astrocytes are important for maintaining homeostasis of the brain. Yet, aging-associated changes in human astrocytes are largely unknown. Characterizing these changes is the first step in elucidating potential involvement of astrocytes in aging-

associated cognitive decline and neurodegeneration and developing astrocyte-targeted treatments. To identify genes with aging-associated expression, we began with genes significantly associated with age in the DESeq2 analysis of all samples that we also used to identify disease-related genes. To identify genes specifically associated with aging (changes after completing maturation) rather than general age (changes across the entire lifespan), we grouped samples into groups by age: 0-20 years old; 21-50 years old; and 50+ years old. From our list of age-associated genes, we extracted genes with average expression >1.5x higher or lower in the 50+ group vs. the 21-50 group. We further filtered by minimum RPKM level of 0.01 to exclude lowly expressed genes. Thus, we identified 394 (277 protein-coding) genes significantly associated with aging (SI1-12).

As in peritumor astrocytes, we find decreased expression of genes mediating astrocyte-synaptic interactions in older astrocytes (Fig 1-5A). Most notably, there is a reduction of SLC1A3, a glutamate transporter that clears glutamate from the extracellular space. Under normal conditions, SLC1A3 is a highly expressed core marker of adult astrocytes [65]. There is also a decline in CHRDL1, which codes for an astrocyte-secreted factor that drives synapse maturation [10]. Aging astrocytes also have lower expression of two genes coding for glycoproteins found in the extracellular matrix. The first, CSPG5, shapes neurite growth and localizes around GABAergic and glutamatergic synaptic terminals [99], while the second, OLMF1, binds synaptic proteins such as synaptophysin and AMPA receptors [100]. Declining expression of synaptic genes raises important questions about astrocytic roles in age-related cognitive decline and neurological disease.

Subjects over 50 show additional decreases in genes associated with energy metabolism (Fig 1-5A). These include genes involved in mitochondrial generation of ATP such as ATP5A1, an ATP-synthase subunit, MRPL35, a mitochondrial ribosomal component, and SLC25A5, a transporter that carries ATP out of the mitochondria. We also observe lower expression of the glycolytic enzyme PGAM1, and SLC13A5, a citrate transporter. Astrocytes

are known to secrete citrate into the extracellular space where citrate has the ability to chelate calcium and magnesium ions, which are important to neuronal NMDA signaling [101]. Together, these gene expression changes are consistent with decreased production of ATP in aging human astrocytes.

Lastly, we also observe an increase of several genes involved in cytokine signaling and senescence. These include the cytokines LIF, IL6, and CCL2, as well as cytokine regulator SOCS3 (Fig 1-5B), which are also found in reactive astrocytes in mice [102]. Therefore, these changes suggest that aging astrocytes may exhibit differences in interactions with neuronal synapses, altered energy metabolism, and increased cytokine signaling.

To assess the similarity between human and mouse astrocyte aging, we returned to the mouse aging dataset from [73]. They reported a list of 58 age-associated genes in mouse cortical astrocytes. We wanted to determine whether mice recapitulated human changes related to metabolism, synapses, cytokines and senescence. Due to the short length of the mouse gene list, we sought to identify trends in the whole dataset. To do so, we first chose relevant GO terms that captured the trends we observed in humans (“ATP metabolic process”, “synapse”, “cytokine-mediated signaling pathway”, and “cellular senescence”). Using these gene lists, we plotted differences in gene expression of all genes between the ten-week-old and two-year-old mice (Fig 1-5C). There is a prominent right skew in cytokine signaling genes, and we observe a slight left shift in ATP metabolism genes, suggesting mouse astrocytes also show signs of upregulating cytokine signaling genes while downregulating metabolic genes in old age. The distributions for synaptic and senescence genes were highly symmetrical, suggesting no broad trends associated with age. However, mouse astrocytes could show important changes in smaller subsets of synaptic or senescence genes upon further analysis. In total, we see evidence that mouse astrocytes share metabolic and cytokine features of human astrocyte aging.

Next, we examined changes in protein-protein interactions in aging astrocytes from humans and mice using the online tool STRING (string-db.org). We combined differentially expressed genes from three different studies of aging mouse astrocytes [73-75]. Again, we see downregulation of mitochondrial ATP metabolism genes in both species, and both species also upregulated genes involved in inflammation such as cytokine signaling, the complement pathway, and interferon response pathway (Fig 1-5D). Furthermore, in aging human astrocytes, inositol triphosphate-calcium signaling pathway and senescence genes are upregulated whereas growth factor signaling genes are downregulated. In aging mouse astrocytes, mRNA splicing genes are upregulated and ribosomal translation genes are downregulated.

Region-specific gene signatures in astrocytes

Studies in mice have found regional differences in gene expression, but little is known about potential differences across the human brain. We compared expression in temporal lobe (n = 27) and frontal lobe samples (n = 8) and found 64 differentially expressed genes. Interestingly, Sema3a, a gene expressed at higher levels in ventral than in dorsal spinal cord astrocytes and repels axons from ventral spinal cords in mice [39] is expressed at higher levels in the frontal lobe than in the temporal lobe in humans, suggesting potentially conserved roles of astrocytic Sema3a in region specific axon guidance.

Subtle sexual dimorphism in astrocyte gene signatures

Female and male brains differ in their susceptibility to neurological disorders. For example, intellectual disability, autism spectrum disorder and Parkinson disease are more prevalent in men than in women [103, 104], whereas multiple sclerosis, Alzheimer disease, and anxiety disorder are more prevalent in women than in men [105-107]. The cellular and molecular mechanisms underlying sexually dimorphic susceptibility to neurological and psychiatric disorders are largely unknown. While understanding of sexually dimorphic properties of other brain cells, particularly microglia, is increasing, sexual dimorphism in human astrocytes has not yet been reported. In our differential gene expression analysis of all 49

samples, we found 105 genes (40 protein coding) with expression levels significantly associated with sex (Fig 1-6, SI1-13). This gene list represents the first evidence of sexual dimorphism in human cortical astrocytes, to the best of our knowledge. Some of these genes are transcription factors (POU5F1B, HOXC10) or epigenetic factors, which may globally regulate gene expression. For example, the lysine demethylases KDM6A and KDM5C located on the X-chromosome are expressed at higher levels by female than male astrocytes. Females have two copies of X-chromosome genes and males only have one copy. Most X-chromosome genes are subjected to X-inactivation in females, where only one copy of the gene is expressed, thus making expression levels comparable in males and females. Interestingly, KDM6A and KDM5C expression in female astrocytes are approximately twice as high as in male astrocytes, likely by escaping from X-inactivation, as has been reported in other cell types [108]. KDM6A demethylates histone 3 lysine 27 trimethylation, a repressive mark found in promoters and enhancers, thus contributing to gene activation. KDM5C demethylates histone 3 lysine 4 methylation associated with active promoters and enhancers, thus contributing to gene repression. Both KDM6A and KDM5C are associated with risk of intellectual disability, a disease more common in males than in females [109]. Lower expression of these genes in male astrocytes may make them more susceptible to mutations that reduce demethylase activity, leading to astrocyte gene regulation defects, neural circuit dysfunction, and intellectual disability. We also observed a diverse array of differentially expressed genes whose protein products are located in the plasma membrane, though their functions in astrocytes remain mysterious (TMEM176B, TMEM143, CD99). Together, this data represents the first evidence that human astrocytes display a subtle sexual dimorphism at the molecular level.

1.5 Discussion

We generated transcriptomic data of over 40 samples of acutely purified human astrocytes. These samples vary in age, sex, and disease state, allowing us to analyze these

features in humans for the first time with RNAseq. Overall, genes associated with synaptic function change in multiple conditions, highlighting dynamism in astrocyte-synapse interactions in humans. Together, this data elucidates several fundamental aspects of human astrocyte biology in health and disease, as well as drawing important comparisons to murine astrocytes.

Molecular Profile of Astrocytes in Human Disease

Prior to the advent of the immunopanning technique, astrocyte purification mainly relied on serum-selection [110]. In these methods, heterogenous collections of cells were cultured with serum-containing media that preferentially allowed survival and propagation of astrocytes. However, these conditions were not physiological, as serum is a component of the blood that does not cross the blood brain barrier in healthy brain tissue. Astrocytes placed under these conditions upregulate reactive markers and adopt fibroblast-like morphology in culture [102, 111]. Using this method, it was challenging to study *in vivo* reactive astrocyte states, as the signal was masked by the response to serum during *in vitro* purification. Immunopanning allows for acute purification without the use of cell culture or serum, maintaining astrocytes in a near-physiological state [65]. This technique allowed us to characterize the transcriptomic profile of human astrocytes from two *in vivo* neurological disorders, FCD, and brain tumor.

Despite previous evidence that some forms of epilepsy can induce astrocyte reactivity [47], our analysis does not find notable changes in the astrocytes in FCD. This may reflect differences in disease progression across different kinds of epilepsy. A human study of patients with FCD only observed astrocyte reactivity in the center of the disorganized cortex, not in outer regions with milder neuronal phenotypes [112]. Therefore, it is conceivable that human astrocytes in this epileptic context would not necessarily demonstrate reactivity, and our findings in FCD should not be generalized to all forms of epilepsy. Additionally, bulk RNA-seq may miss reactive changes of a small subset of astrocytes.

In stark contrast, peritumor astrocytes demonstrate a robust change in gene expression. Peritumor astrocytes strongly decrease expression of glutamate transporters (SLC1A2 and

SLC1A3) that are normally highly expressed in astrocytes and help maintain the excitation-inhibition balance of the brain. Seizure activity is common in individuals with brain tumors, and seizures are often the precipitating event that leads to medical treatment [88]. Astrocytes may contribute to unregulated excitation in the brain by downregulating these important glutamate transporters. Excessive excitation not only causes harmful seizures; there is recent evidence that neurons form synaptic structures with tumor cells, and neuronal activity drives further proliferation and infiltration of tumor cells [113-115]. This raises the exciting possibility of therapeutically targeting glutamate uptake in astrocytes, in addition to existing anti-seizure medications. In future studies, it will be vital to determine whether these general patterns hold for the various classes and origins of brain tumors, and at what stage of disease progression they appear. Beyond glutamate transporters, peritumor astrocytes downregulate several other genes that normally support synaptic function, suggesting further impacts on circuit function.

Indeed, our findings portray a general loss of function in peritumor astrocytes. There is a strong upregulation of cellular proliferation markers in conjunction with near-universal downregulation of core astrocyte genes. We specifically identified a widespread reduction of astrocyte receptor genes, which may limit their ability to sense and respond to their environment.

Interestingly, there may be one important gain-of-function in peritumor astrocytes. A study of human astrocytes from tumor cores concluded that astrocytes contributed to an immune-suppressive environment that permitted tumor proliferation and infiltration. Tumor-core astrocytes showed changes in the JAK/STAT and interferon gamma response as well as upregulation of the anti-inflammatory cytokine Il-10 [77], which were not present in the peritumor astrocytes. On the contrary, peritumor astrocytes upregulate many pro-inflammatory genes and downregulate anti-inflammatory genes. Although loss of synaptic support from peritumor astrocytes may contribute to circuit disruption and tumor-associated seizure activity, an increase

in pro-inflammatory signaling may play a vital role in containing tumor growth and migration by promoting an immune response.

Human Astrocyte Maturation

Human brain development proceeds through a cascade of complex and reciprocal interactions between several maturing cell types. For example, neurons largely fail to make functional synapses in the absence of astrocytes, and astrocytes lack morphological complexity without the presence of neurons [6, 9]. The developmental trajectory of most major brain cells has been described by the presence of cell-specific transcription factors that drive cells toward a specific fate, such as NEUROD1 in neurons and OLIG2 in oligodendrocytes. Although some important regulators have been identified, astrocyte development and maturation remain less well understood [36, 116-118]. Previous work compared fetal astrocytes to postnatal astrocytes that helped identify markers of mature versus immature astrocytes, and here we extend that work by creating a developmental timeline across postnatal astrocyte maturation in humans. This provides some of the first insight into how human astrocytes mature past the early stages of development. We found a shift in astrocytic gene expression around 8 years old that persists into early adulthood. This time frame coincides with the onset of increased synaptic pruning in the cortex, as evidenced by a decline in cortical synaptic spine density beginning around puberty [119-121]. Based on this data, astrocytes adopt functions for the support and maintenance of synapses before birth, but they adopt new roles in synaptic remodeling during postnatal maturation. These data also provide new markers to use in untangling astrocytic gene networks and molecular mechanisms that related to increased synaptic pruning. Pathway analysis of astrocyte maturation genes identified downregulation of proliferative pathways and upregulation of pathways related to ion homeostasis and lipid metabolism. We also find these patterns of astrocyte maturation preserved in mice, even though mice and humans showed divergent sets of maturation-related genes. This suggests mice and human astrocytes share many aspects of their developmental arcs, though they may express different sets of genes to

achieve the same functional goal. Future studies should aim to identify the signaling mechanisms that drive astrocyte maturation, as aberrations in astrocyte maturation could contribute to dysfunction in neural circuits and ultimately neurodevelopmental disorders.

Aging in Human Astrocytes

Astrocytes become reactive in age-related neurological diseases such as Alzheimer Disease [48]. It is important to determine whether reactivity is induced purely by disease progression or whether astrocyte reactivity occurs in the course of normal aging, which may further contribute to aspects of disease progression. We observe declining expression of synaptic genes, including the glutamate transporter gene SLC1A3. As we noted in peritumor astrocytes, altered expression of this gene product would impact the balance of excitation-inhibition in the brain and impair circuit function. Two separate animal studies have identified increasing expression of reactive markers across age in the mouse brain, both in the cortex and subcortical regions [73, 74]. We find corresponding evidence in our analysis of aging human astrocytes where several genes involved in cytokine signaling are upregulated, including CCL2, IL6, and SOCS3. We also observe a modest increase in senescence markers CDKN1A and CDKN2A. As our cohort only extends to age 65, further study of astrocytes at more advanced ages could uncover much larger changes in the astrocyte transcriptome throughout the aging process. While reactive and senescence markers increase, we observe a decrease in genes related to energy metabolism. Astrocytes typically provide metabolic support to aid in proper neuronal function and signaling, so these changes may contribute to age-related declines in cognition. An important question for further examination is whether a decrease in neuronal support is reflective of astrocytic dysfunction or declining demand from neurons. Our study does not have a large cohort of patients in the aging adult group. Given the higher variability of human data caused by greater genetic and environmental diversity compared with laboratory mice, future studies with large sample sizes will further expand our understanding of astrocyte aging in humans.

Sexual Dimorphism of Human Astrocytes

Many neurological diseases have differences in incidence and prognosis depending on sex, but little is known about the mechanisms that underlie these differences. Recently, multiple findings identified sex differences in microglia, but sex differences in astrocytes remain elusive despite their extensive interactions with microglia. Slight differences in astrocyte number and morphology were reported in sub-cortical regions of the brain in rats, such as the amygdala [122, 123]. Here, we report the first evidence of sexual dimorphism in human astrocytes, to the best of our knowledge. Female cortical astrocytes have higher transcription of several plasma membrane proteins, including somatostatin receptor SSTR2, a transcriptional target of p53, PERP, and transmembrane protein TMEM176B. We also observe differential expression of genes encoding epigenetic regulators located on sex chromosomes, such as demethylases KDM5C and KDM6A. Though healthy astrocytes demonstrate relatively few sex differences, further studies should investigate whether underlying differences in epigenetic state could contribute to sex-specific responses to insult or injury and ultimately underlie sex differences in neurological disease.

Naturally, limited access to fresh brain tissue limits many studies of the human brain, including this one, and our findings are not an exhaustive list of changes in human astrocytes. Further studies are needed to clarify context-dependent expression in human astrocytes in other diseases and patient populations to identify astrocytic roles in human health and disease. Our discovery of changes in genes involved in synaptic function across multiple conditions in human astrocytes is an important step in that direction, and our dataset will provide valuable insight for further investigation of human biology and novel approaches for neurological disease.

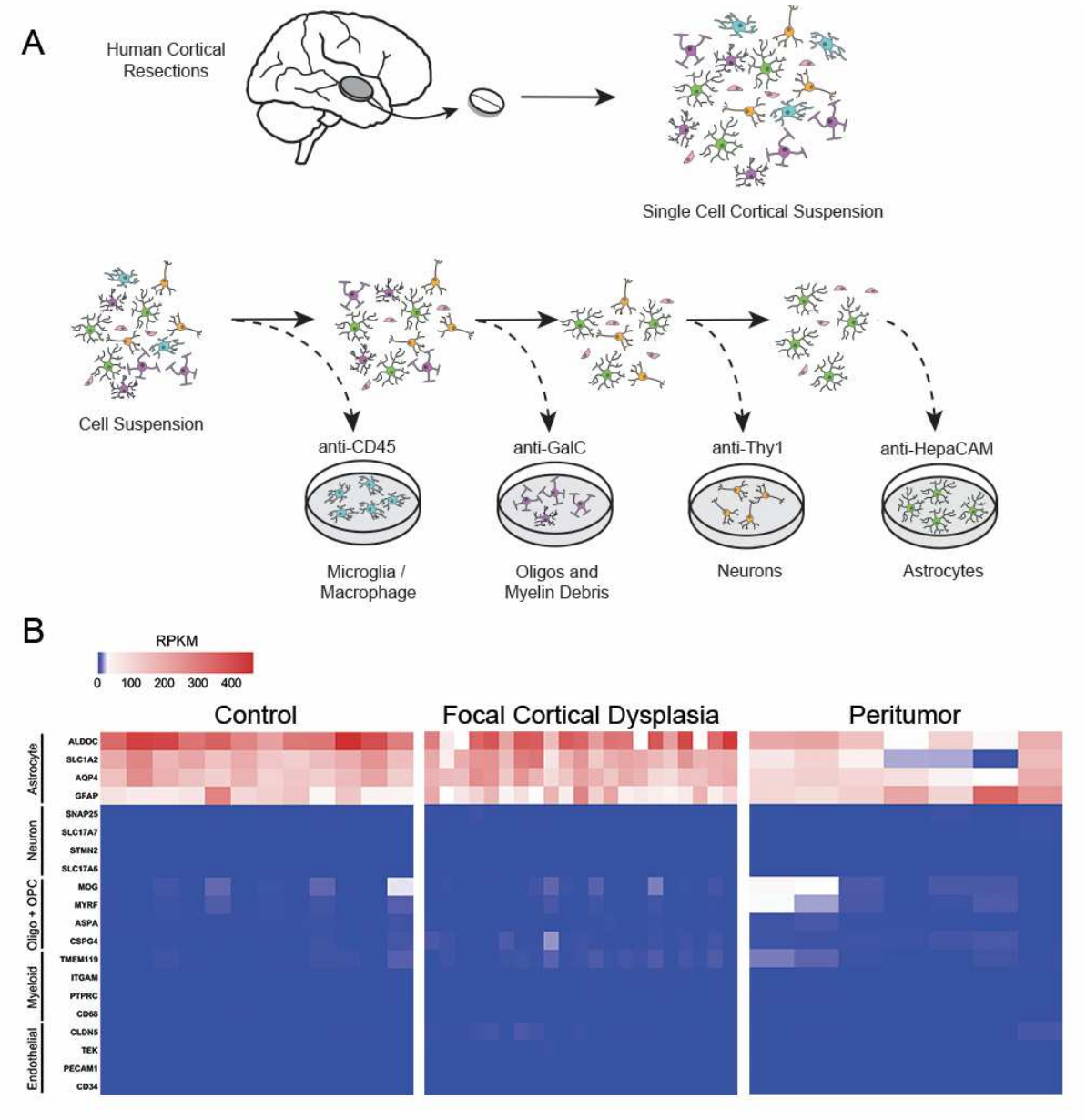

Figure 1-1. Acute purification of human astrocytes from cerebral cortex. A) Diagram of human astrocyte purification by immunopanning. Surgically resected tissue underwent enzymatic digestion and gentle mechanical digestion to generate a single cell suspension. These cells were passed over a series of plates coated with cell-type-specific antibodies to deplete microglia, oligodendrocyte-lineage cells, and neurons before finally passing to a plate that specifically binds astrocytes using an anti-HepaCAM antibody. B) Heatmaps showing the expression of cell type specific genes in RPKM after RNA sequencing of immunopanned

astrocytes. All samples are highly enriched in astrocytic genes (red), with little to no expression of gene markers for neurons, myeloid cells (i.e. microglia or macrophages), oligodendrocyte-lineage cells, or endothelial cells. Detailed sample info and total gene expression are detailed in SI1-1 and 1-2.

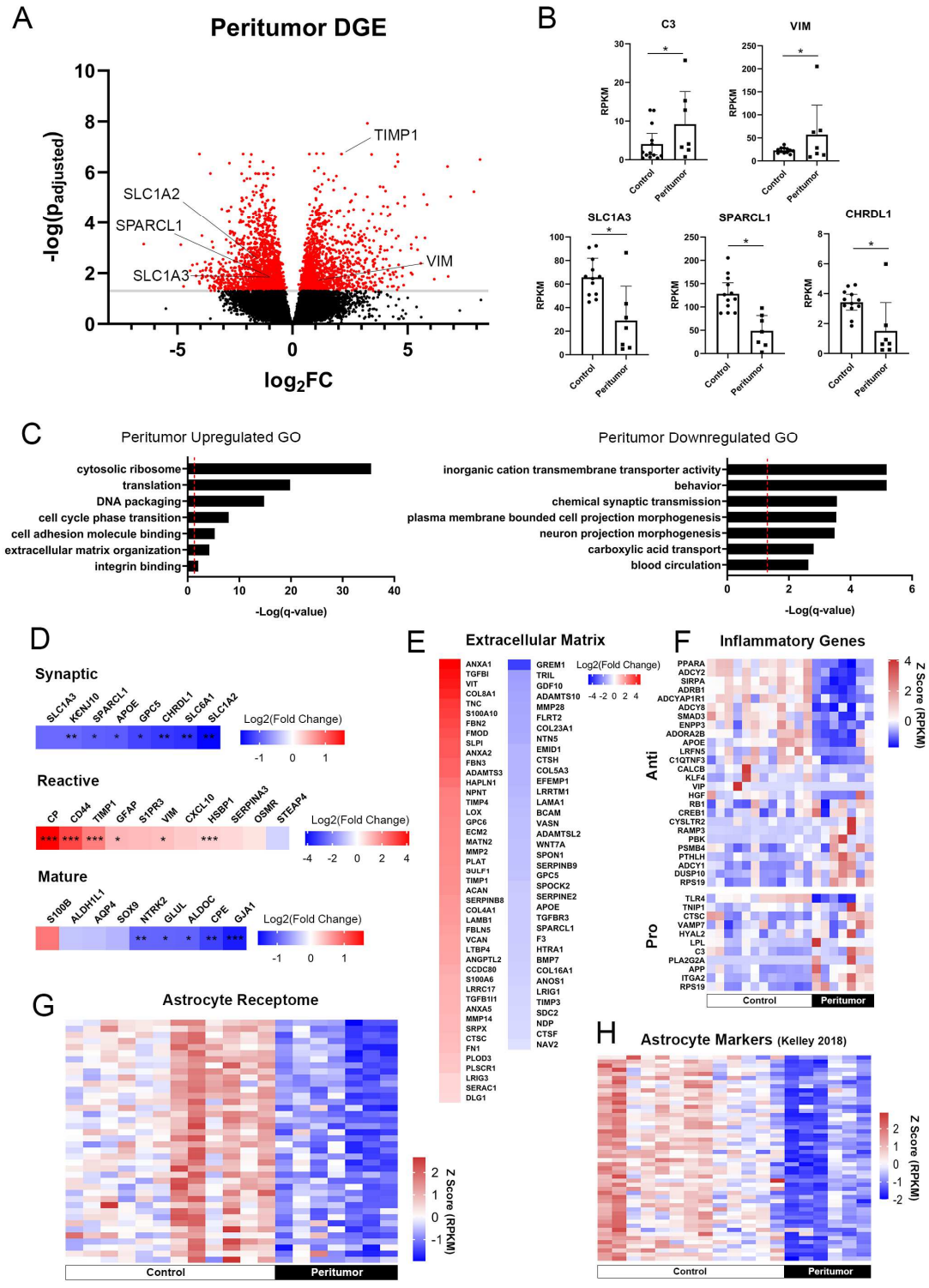

Figure 1-2. Transcriptomic signature of human astrocytes in the peritumor microenvironment. A) Volcano plot showing differential gene expression in human peritumor astrocytes vs. controls; red = $p < 0.05$. Full DGE in SI1-3; cross-validation in SI1-4; effects of

brain region in SI1-5. B) Bar plots of astrocyte genes with changing expression in the peritumor microenvironment. C) Selected gene ontology terms that are significantly enriched in up- (left) and downregulated (right) genes in peritumor astrocytes; dashed lines: $p < 0.05$. Full GO results in SI1-8. Analysis of synaptic genes and disease-associated genes in SI1-6. D) Heatmaps of differential gene expression in peritumor astrocytes related to (top) synaptic function, (middle) astrocyte reactivity, and (bottom) mature astrocyte markers. E) Heatmaps of extracellular matrix genes with increased (red) or decreased (blue) expression in peritumor astrocytes, all significant at $p < 0.05$. F) Normalized gene expression of anti-inflammatory (top) and pro-inflammatory (bottom) genes that are differentially expressed in peritumor astrocytes ($p < 0.05$). G) Normalized gene expression of plasma membrane receptors that are differentially expressed in peritumor astrocytes ($p < .05$). Full gene list in SI1-7. H) Normalized gene expression of the top 50 astrocyte marker genes, identified by Kelley, Nakao-Inoue (93), in peritumor and control astrocytes. * $p < 0.05$, ** $p < 0.01$, *** $p < 0.001$.

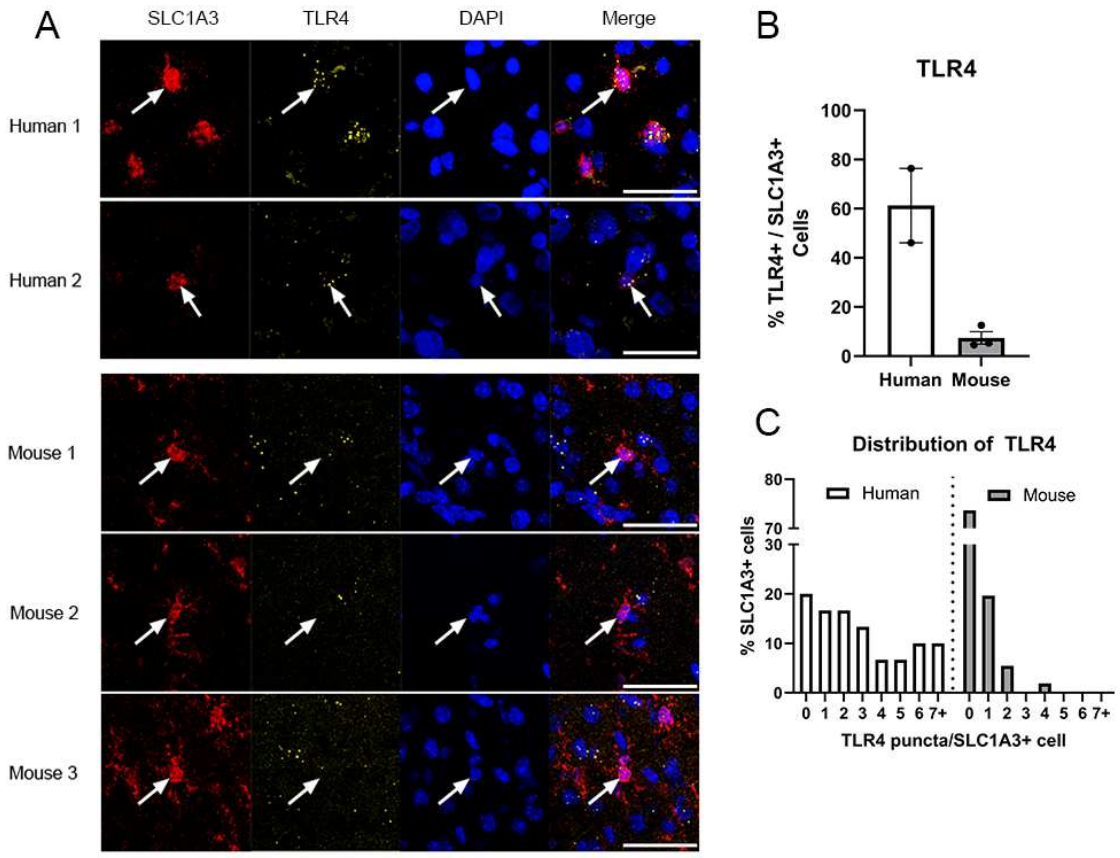

Figure 1-3. In situ hybridization validation of human astrocyte RNAseq. A) RNAscope in situ hybridization of TLR4 (yellow) in astrocytes (SLC1A3, red) in both human and mouse tissues. Scale bar = 50 μm. B) Quantification of TLR4+ astrocytes in human and mouse cortical tissue. Error bars = standard error. C) Histogram depicting the number of TLR4+ puncta in an astrocytic cell body labeled by SLC1A3 in human and mouse cortical tissue.

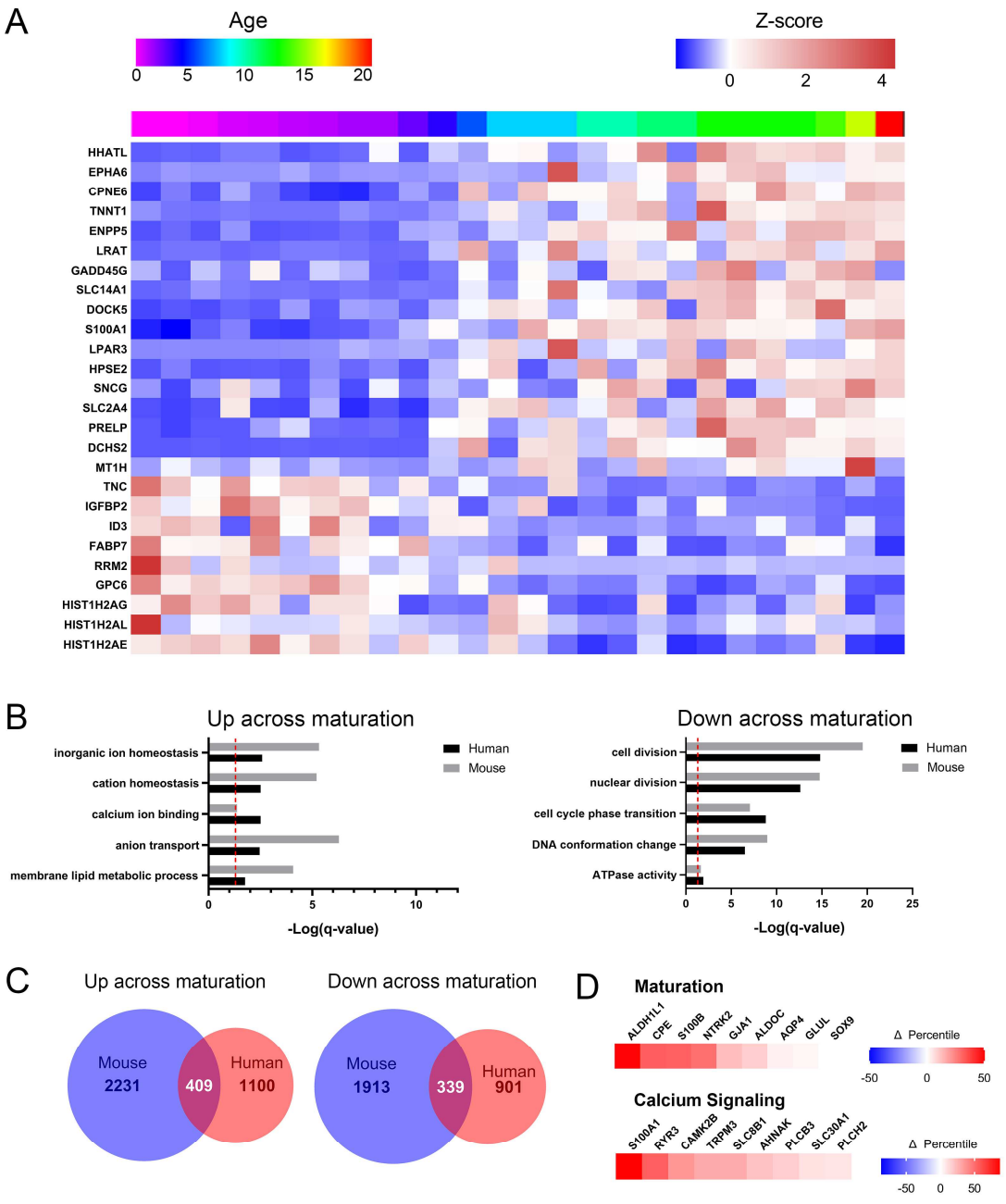

Figure 1-4. Molecular characterization of human astrocyte maturation. Full maturation DGE results in SI1-10, including FCD samples as they were not substantially different from controls (SI1-9). A) Heatmap of representative genes with changing expression across maturation (7 months – 21 years old, n = 26). Astrocytic gene expression approaches the mature pattern around 8 years of age. Plotted as Z-score of gene expression (RPKM); top bar:

rainbow index of sample ages. B) Selected gene ontology terms enriched in genes that are up- (left) or downregulated (right) across maturation in both human astrocytes (black bars) and mouse astrocytes (grey bars, from [73]). Dashed lines: $p < 0.05$. Full results reported in SI1-11. C) Venn diagrams quantifying astrocyte maturation-associated genes that are up- (left) and downregulated (right) in humans (red) and mice (blue). D) Top: heatmap of selected astrocyte maturation markers colored by percentile change of RNA expression (e.g. Δ percentile = +100 demonstrates a gene went from the least expressed gene to the most expressed gene) from fetal human astrocytes [66] to mature human astrocytes (13-21 years old). Bottom: heatmap of selected calcium signaling genes, same quantification as the heatmap above.

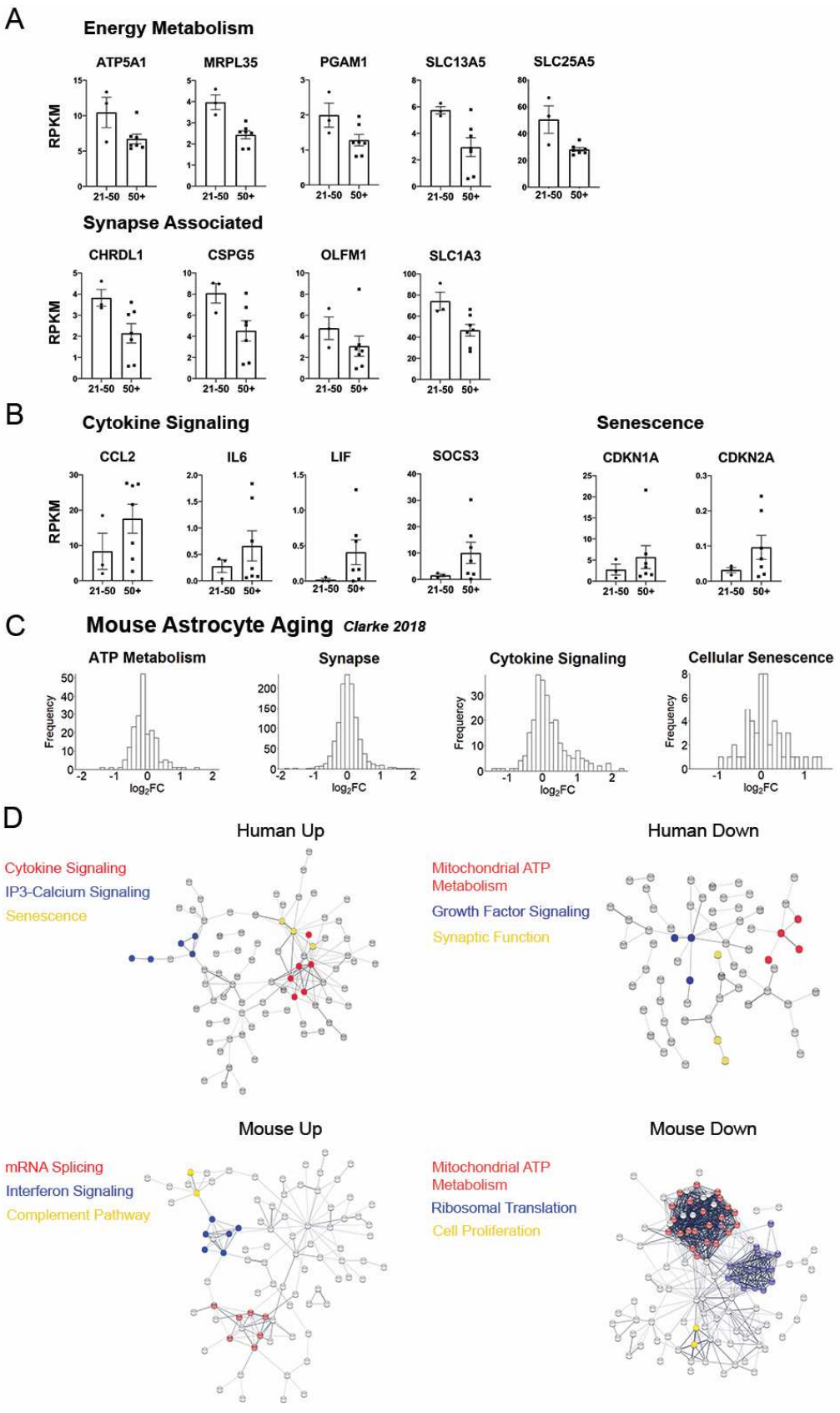
A
Energy Metabolism
ATP5A1
MRPL35
PGAM1
SLC13A5
SLC25A5
RPKM
21-50
50+
Synapse Associated
CHRDL1
CSPG5
OLFM1
SLC1A3
B
Cytokine Signaling
CCL2
IL6
LIF
SOCS3
Senescence
CDKN1A
CDKN2A
C
Mouse Astrocyte Aging Clarke 2018
ATP Metabolism
Synapse
Cytokine Signaling
Cellular Senescence
Frequency
log2FC
D
Human Up
Cytokine Signaling
IP3-Calcium Signaling
Senescence
Human Down
Mitochondrial ATP Metabolism
Growth Factor Signaling
Synaptic Function
Mouse Up
mRNA Splicing
Interferon Signaling
Complement Pathway
Mouse Down
Mitochondrial ATP Metabolism
Ribosomal Translation
Cell Proliferation

Figure 1-5. Age-associated genes in human astrocytes. Full expression data presented in SI1-12. A) Expression of age-associated human astrocyte genes with decreased expression in older adults (50+ years old) compared to younger adults (21-50 years old). B) Age-associated human astrocyte genes with increased expression in older adults compared to younger adults. All genes shown are significantly associated with age, and at least 1.5-fold enriched in younger or older adults. C) Change in RNA expression of mouse astrocytes (10 weeks old vs. 2 years old, from [73]) in various gene ontology categories. Gene lists derived from the following GO annotations, from left to right: GO:0046034, GO:0045202, GO:0019221 and GO:0090398. D) Protein-protein interaction networks among human (top) and mouse (bottom) age-associated genes.

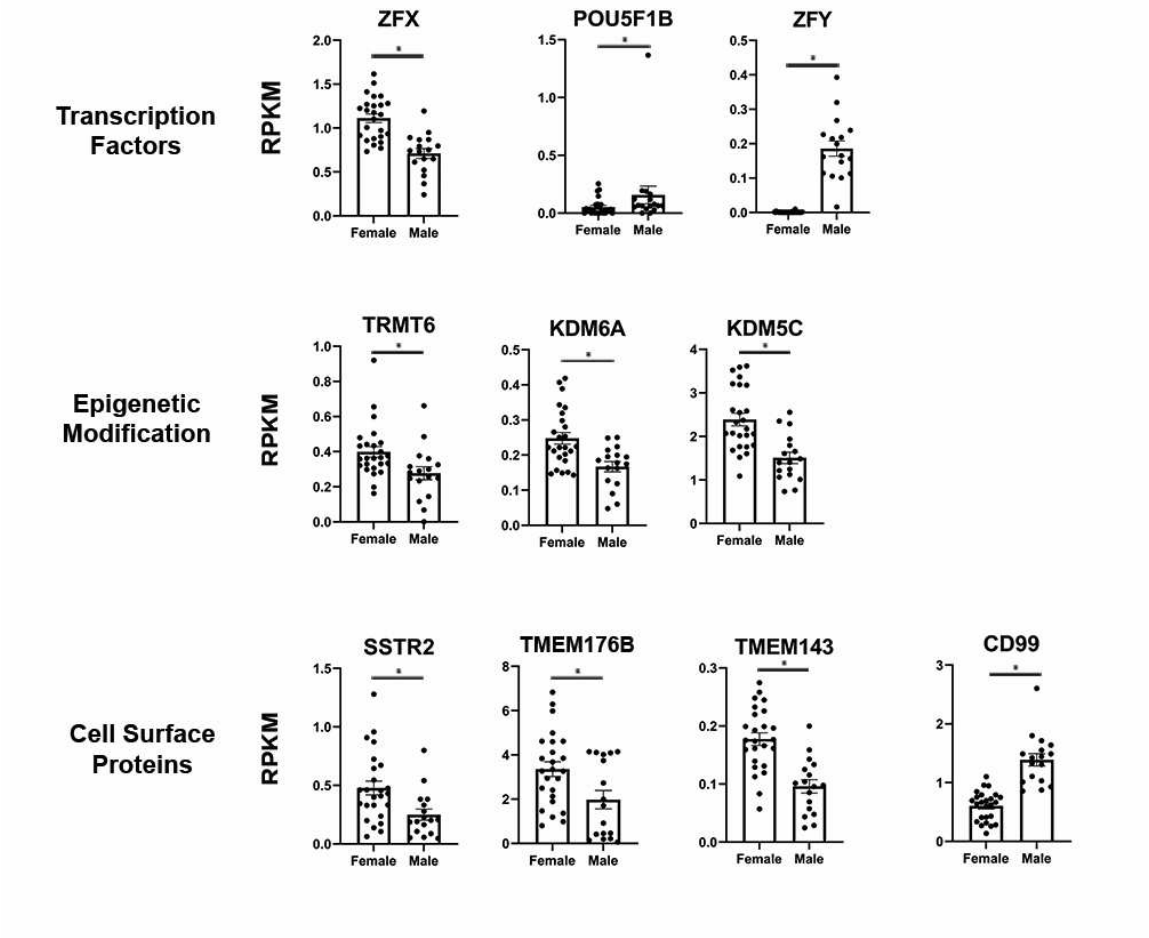

Figure 1-6. Sexually dimorphic genes in human astrocytes. Selected genes that are significantly associated with sex, including genes encoding transcription factors, epigenetic modifying enzymes, and proteins localized to the plasma membrane. Full DGE results presented in SI1-13.

1.6 References

1. Allen NJ, Bennett ML, Foo LC, Wang GX, Chakraborty C, Smith SJ, et al. Astrocyte glypicans 4 and 6 promote formation of excitatory synapses via GluA1 AMPA receptors. Nature. 2012;486(7403):410-4. Epub 2012/06/23. doi: 10.1038/nature11059. PubMed PMID: 22722203; PubMed Central PMCID: PMCPMC3383085.
2. Christopherson KS, Ullian EM, Stokes CC, Mullowney CE, Hell JW, Agah A, et al. Thrombospondins are astrocyte-secreted proteins that promote CNS synaptogenesis. Cell. 2005;120(3):421-33. Epub 2005/02/15. doi: 10.1016/j.cell.2004.12.020. PubMed PMID: 15707899.
3. Ullian EM, Sapperstein SK, Christopherson KS, Barres BA. Control of synapse number by glia. Science. 2001;291(5504):657-61. Epub 2001/02/07. doi: 10.1126/science.291.5504.657. PubMed PMID: 11158678.
4. Kucukdereli H, Allen NJ, Lee AT, Feng A, Ozlu MI, Conatser LM, et al. Control of excitatory CNS synaptogenesis by astrocyte-secreted proteins Hevin and SPARC. Proc Natl Acad Sci U S A. 2011;108(32):E440-9. Epub 2011/07/27. doi: 10.1073/pnas.1104977108. PubMed PMID: 21788491; PubMed Central PMCID: PMCPMC3156217.
5. Krencik R, Seo K, van Asperen JV, Basu N, Cvetkovic C, Barlas S, et al. Systematic Three-Dimensional Coculture Rapidly Recapitulates Interactions between Human Neurons and Astrocytes. Stem Cell Reports. 2017;9(6):1745-53. Epub 2017/12/05. doi: 10.1016/j.stemcr.2017.10.026. PubMed PMID: 29198827; PubMed Central PMCID: PMCPMC5785708.
6. Banker GA. Trophic interactions between astroglial cells and hippocampal neurons in culture. Science. 1980;209(4458):809-10. Epub 1980/08/15. doi: 10.1126/science.7403847. PubMed PMID: 7403847.
7. Singh SK, Stogsdill JA, Pulimood NS, Dingsdale H, Kim YH, Pilaz LJ, et al. Astrocytes Assemble Thalamocortical Synapses by Bridging NRX1alpha and NL1 via Hevin. Cell.

2016;164(1-2):183-96. Epub 2016/01/16. doi: 10.1016/j.cell.2015.11.034. PubMed PMID: 26771491; PubMed Central PMCID: PMCPMC4715262.

8. Farhy-Tselnicker I, van Casteren ACM, Lee A, Chang VT, Aricescu AR, Allen NJ. Astrocyte-Secreted Glypican 4 Regulates Release of Neuronal Pentraxin 1 from Axons to Induce Functional Synapse Formation. Neuron. 2017;96(2):428-45 e13. Epub 2017/10/13. doi: 10.1016/j.neuron.2017.09.053. PubMed PMID: 29024665; PubMed Central PMCID: PMCPMC5663462.

9. Stogsdill JA, Ramirez J, Liu D, Kim YH, Baldwin KT, Enustun E, et al. Astrocytic neuroligins control astrocyte morphogenesis and synaptogenesis. Nature. 2017;551(7679):192-7. Epub 2017/11/10. doi: 10.1038/nature24638. PubMed PMID: 29120426; PubMed Central PMCID: PMCPMC5796651.

10. Blanco-Suarez E, Liu TF, Kopelevich A, Allen NJ. Astrocyte-Secreted Chordin-like 1 Drives Synapse Maturation and Limits Plasticity by Increasing Synaptic GluA2 AMPA Receptors. Neuron. 2018;100(5):1116-32 e13. Epub 2018/10/23. doi: 10.1016/j.neuron.2018.09.043. PubMed PMID: 30344043; PubMed Central PMCID: PMCPMC6382071.

11. Chung WS, Clarke LE, Wang GX, Stafford BK, Sher A, Chakraborty C, et al. Astrocytes mediate synapse elimination through MEGF10 and MERTK pathways. Nature. 2013;504(7480):394-400. Epub 2013/11/26. doi: 10.1038/nature12776. PubMed PMID: 24270812; PubMed Central PMCID: PMCPMC3969024.

12. Vainchtein ID, Chin G, Cho FS, Kelley KW, Miller JG, Chien EC, et al. Astrocyte-derived interleukin-33 promotes microglial synapse engulfment and neural circuit development. Science. 2018;359(6381):1269-73. Epub 2018/02/09. doi: 10.1126/science.aal3589. PubMed PMID: 29420261; PubMed Central PMCID: PMCPMC6070131.

13. Tasdemir-Yilmaz OE, Freeman MR. Astrocytes engage unique molecular programs to engulf pruned neuronal debris from distinct subsets of neurons. Genes Dev.

2014;28(1):20-33. Epub 2013/12/24. doi: 10.1101/gad.229518.113. PubMed PMID: 24361692; PubMed Central PMCID: PMCPMC3894410.

14. Lee JH, Kim JY, Noh S, Lee H, Lee SY, Mun JY, et al. Astrocytes phagocytose adult hippocampal synapses for circuit homeostasis. Nature. 2020. Epub 2020/12/29. doi: 10.1038/s41586-020-03060-3. PubMed PMID: 33361813.
15. Kelley KW, Ben Haim L, Schirmer L, Tyzack GE, Tolman M, Miller JG, et al. Kir4.1-Dependent Astrocyte-Fast Motor Neuron Interactions Are Required for Peak Strength. Neuron. 2018;98(2):306-19 e7. Epub 2018/04/03. doi: 10.1016/j.neuron.2018.03.010. PubMed PMID: 29606582; PubMed Central PMCID: PMCPMC5919779.
16. Kuffler SW, Nicholls JG, Orkand RK. Physiological properties of glial cells in the central nervous system of amphibia. J Neurophysiol. 1966;29(4):768-87. Epub 1966/07/01. doi: 10.1152/jn.1966.29.4.768. PubMed PMID: 5966434.
17. Olsen ML, Sontheimer H. Functional implications for Kir4.1 channels in glial biology: from K+ buffering to cell differentiation. J Neurochem. 2008;107(3):589-601. Epub 2008/08/12. doi: 10.1111/j.1471-4159.2008.05615.x. PubMed PMID: 18691387; PubMed Central PMCID: PMCPMC2581639.
18. Rothstein JD, Dykes-Hoberg M, Pardo CA, Bristol LA, Jin L, Kuncl RW, et al. Knockout of glutamate transporters reveals a major role for astroglial transport in excitotoxicity and clearance of glutamate. Neuron. 1996;16(3):675-86. Epub 1996/03/01. doi: 10.1016/s0896-6273(00)80086-0. PubMed PMID: 8785064.
19. Papouin T, Dunphy JM, Tolman M, Dineley KT, Haydon PG. Septal Cholinergic Neuromodulation Tunes the Astrocyte-Dependent Gating of Hippocampal NMDA Receptors to Wakefulness. Neuron. 2017;94(4):840-54 e7. Epub 2017/05/10. doi: 10.1016/j.neuron.2017.04.021. PubMed PMID: 28479102; PubMed Central PMCID: PMCPMC5484087.

20. Dowling C, Allen NJ. Mice Lacking Glypican 4 Display Juvenile Hyperactivity and Adult Social Interaction Deficits. Brain Plast. 2018;4(2):197-209. Epub 2019/01/02. doi: 10.3233/BPL-180079. PubMed PMID: 30598870; PubMed Central PMCID: PMCPMC6311356.

21. Halassa MM, Florian C, Fellin T, Munoz JR, Lee SY, Abel T, et al. Astrocytic modulation of sleep homeostasis and cognitive consequences of sleep loss. Neuron. 2009;61(2):213-9. Epub 2009/02/03. doi: 10.1016/j.neuron.2008.11.024. PubMed PMID: 19186164; PubMed Central PMCID: PMCPMC2673052.

22. Mu Y, Bennett DV, Rubinov M, Narayan S, Yang CT, Tanimoto M, et al. Glia Accumulate Evidence that Actions Are Futile and Suppress Unsuccessful Behavior. Cell. 2019;178(1):27-43 e19. Epub 2019/06/25. doi: 10.1016/j.cell.2019.05.050. PubMed PMID: 31230713.

23. Nagai J, Rajbhandari AK, Gangwani MR, Hachisuka A, Coppola G, Masmanidis SC, et al. Hyperactivity with Disrupted Attention by Activation of an Astrocyte Synaptogenic Cue. Cell. 2019;177(5):1280-92 e20. Epub 2019/04/30. doi: 10.1016/j.cell.2019.03.019. PubMed PMID: 31031006; PubMed Central PMCID: PMCPMC6526045.

24. Nedergaard M. Direct signaling from astrocytes to neurons in cultures of mammalian brain cells. Science. 1994;263(5154):1768-71. Epub 1994/03/25. doi: 10.1126/science.8134839. PubMed PMID: 8134839.

25. Parpura V, Basarsky TA, Liu F, Jeftinija K, Jeftinija S, Haydon PG. Glutamate-mediated astrocyte-neuron signalling. Nature. 1994;369(6483):744-7. Epub 1994/06/30. doi: 10.1038/369744a0. PubMed PMID: 7911978.

26. Robel S, Buckingham SC, Boni JL, Campbell SL, Danbolt NC, Riedemann T, et al. Reactive astrogliosis causes the development of spontaneous seizures. J Neurosci. 2015;35(8):3330-45. Epub 2015/02/27. doi: 10.1523/JNEUROSCI.1574-14.2015. PubMed PMID: 25716834; PubMed Central PMCID: PMCPMC4339349.

27. Huang AY, Woo J, Sardar D, Lozzi B, Bosquez Huerta NA, Lin CJ, et al. Region-Specific Transcriptional Control of Astrocyte Function Oversees Local Circuit Activities. Neuron. 2020;106(6):992-1008 e9. Epub 2020/04/23. doi: 10.1016/j.neuron.2020.03.025. PubMed PMID: 32320644; PubMed Central PMCID: PMCPMC7879989.

28. Nagai J, Yu X, Papouin T, Cheong E, Freeman MR, Monk KR, et al. Behaviorally consequential astrocytic regulation of neural circuits. Neuron. 2021;109(4):576-96. Epub 2021/01/02. doi: 10.1016/j.neuron.2020.12.008. PubMed PMID: 33385325; PubMed Central PMCID: PMCPMC7897322.

29. Yu X, Nagai J, Marti-Solano M, Soto JS, Coppola G, Babu MM, et al. Context-Specific Striatal Astrocyte Molecular Responses Are Phenotypically Exploitable. Neuron. 2020;108(6):1146-62 e10. Epub 2020/10/22. doi: 10.1016/j.neuron.2020.09.021. PubMed PMID: 33086039; PubMed Central PMCID: PMCPMC7813554.

30. Yu X, Taylor AMW, Nagai J, Golshani P, Evans CJ, Coppola G, et al. Reducing Astrocyte Calcium Signaling In Vivo Alters Striatal Microcircuits and Causes Repetitive Behavior. Neuron. 2018;99(6):1170-87 e9. Epub 2018/09/04. doi: 10.1016/j.neuron.2018.08.015. PubMed PMID: 30174118; PubMed Central PMCID: PMCPMC6450394.

31. Ng FS, Sengupta S, Huang Y, Yu AM, You S, Roberts MA, et al. TRAP-seq Profiling and RNAi-Based Genetic Screens Identify Conserved Glial Genes Required for Adult Drosophila Behavior. Front Mol Neurosci. 2016;9:146. Epub 2017/01/10. doi: 10.3389/fnmol.2016.00146. PubMed PMID: 28066175; PubMed Central PMCID: PMCPMC5177635.

32. Ma Z, Stork T, Bergles DE, Freeman MR. Neuromodulators signal through astrocytes to alter neural circuit activity and behaviour. Nature. 2016;539(7629):428-32. Epub 2016/11/10. doi: 10.1038/nature20145. PubMed PMID: 27828941; PubMed Central PMCID: PMCPMC5161596.

33. Chen N, Sugihara H, Kim J, Fu Z, Barak B, Sur M, et al. Direct modulation of GFAP-expressing glia in the arcuate nucleus bi-directionally regulates feeding. Elife. 2016;5. Epub 2016/10/19. doi: 10.7554/eLife.18716. PubMed PMID: 27751234; PubMed Central PMCID: PMCPMC5068968.

34. Ung K, Tepe B, Pekarek B, Arenkiel BR, Deneen B. Parallel astrocyte calcium signaling modulates olfactory bulb responses. J Neurosci Res. 2020;98(8):1605-18. Epub 2020/05/20. doi: 10.1002/jnr.24634. PubMed PMID: 32426930.

35. Chai H, Diaz-Castro B, Shigetomi E, Monte E, Octeau JC, Yu X, et al. Neural Circuit-Specialized Astrocytes: Transcriptomic, Proteomic, Morphological, and Functional Evidence. Neuron. 2017;95(3):531-49 e9. Epub 2017/07/18. doi: 10.1016/j.neuron.2017.06.029. PubMed PMID: 28712653; PubMed Central PMCID: PMCPMC5811312.

36. Glasgow SM, Zhu W, Stolt CC, Huang TW, Chen F, LoTurco JJ, et al. Mutual antagonism between Sox10 and NFIA regulates diversification of glial lineages and glioma subtypes. Nat Neurosci. 2014;17(10):1322-9. Epub 2014/08/26. doi: 10.1038/nn.3790. PubMed PMID: 25151262; PubMed Central PMCID: PMCPMC4313923.

37. John Lin CC, Yu K, Hatcher A, Huang TW, Lee HK, Carlson J, et al. Identification of diverse astrocyte populations and their malignant analogs. Nat Neurosci. 2017;20(3):396-405. Epub 2017/02/07. doi: 10.1038/nn.4493. PubMed PMID: 28166219; PubMed Central PMCID: PMCPMC5824716.

38. Miller SJ, Philips T, Kim N, Dastgheyb R, Chen Z, Hsieh YC, et al. Molecularly defined cortical astroglia subpopulation modulates neurons via secretion of Norrin. Nat Neurosci. 2019;22(5):741-52. Epub 2019/04/03. doi: 10.1038/s41593-019-0366-7. PubMed PMID: 30936556; PubMed Central PMCID: PMCPMC6551209.

39. Molofsky AV, Kelley KW, Tsai HH, Redmond SA, Chang SM, Madireddy L, et al. Astrocyte-encoded positional cues maintain sensorimotor circuit integrity. Nature.

2014;509(7499):189-94. Epub 2014/04/30. doi: 10.1038/nature13161. PubMed PMID: 24776795; PubMed Central PMCID: PMCPMC4057936.

40. Morel L, Chiang MSR, Higashimori H, Shoneye T, Iyer LK, Yelick J, et al. Molecular and Functional Properties of Regional Astrocytes in the Adult Brain. J Neurosci. 2017;37(36):8706-17. Epub 2017/08/20. doi: 10.1523/JNEUROSCI.3956-16.2017. PubMed PMID: 28821665; PubMed Central PMCID: PMCPMC5588463.

41. Tsai HH, Li H, Fuentealba LC, Molofsky AV, Taveira-Marques R, Zhuang H, et al. Regional astrocyte allocation regulates CNS synaptogenesis and repair. Science. 2012;337(6092):358-62. Epub 2012/06/30. doi: 10.1126/science.1222381. PubMed PMID: 22745251; PubMed Central PMCID: PMCPMC4059181.

42. Diaz-Castro B, Bernstein AM, Coppola G, Sofroniew MV, Khakh BS. Molecular and functional properties of cortical astrocytes during peripherally induced neuroinflammation. Cell Rep. 2021;36(6):109508. Epub 2021/08/12. doi: 10.1016/j.celrep.2021.109508. PubMed PMID: 34380036.

43. Poskanzer KE, Molofsky AV. Dynamism of an Astrocyte In Vivo: Perspectives on Identity and Function. Annu Rev Physiol. 2018;80:143-57. Epub 2017/11/23. doi: 10.1146/annurev-physiol-021317-121125. PubMed PMID: 29166242; PubMed Central PMCID: PMCPMC5811396.

44. Sofroniew MV. Astrocyte Reactivity: Subtypes, States, and Functions in CNS Innate Immunity. Trends Immunol. 2020;41(9):758-70. Epub 2020/08/21. doi: 10.1016/j.it.2020.07.004. PubMed PMID: 32819810; PubMed Central PMCID: PMCPMC7484257.

45. Burda JE, Bernstein AM, Sofroniew MV. Astrocyte roles in traumatic brain injury. Exp Neurol. 2016;275 Pt 3:305-15. Epub 2015/04/02. doi: 10.1016/j.expneurol.2015.03.020. PubMed PMID: 25828533; PubMed Central PMCID: PMCPMC4586307.

46. Panickar KS, Norenberg MD. Astrocytes in cerebral ischemic injury: morphological and general considerations. Glia. 2005;50(4):287-98. Epub 2005/04/23. doi: 10.1002/glia.20181. PubMed PMID: 15846806.

47. Binder DK, Steinhauser C. Functional changes in astroglial cells in epilepsy. Glia. 2006;54(5):358-68. Epub 2006/08/04. doi: 10.1002/glia.20394. PubMed PMID: 16886201.

48. Beach TG, Walker R, McGeer EG. Patterns of gliosis in Alzheimer's disease and aging cerebrum. Glia. 1989;2(6):420-36. Epub 1989/01/01. doi: 10.1002/glia.440020605. PubMed PMID: 2531723.

49. Liddelow SA, Guttenplan KA, Clarke LE, Bennett FC, Bohlen CJ, Schirmer L, et al. Neurotoxic reactive astrocytes are induced by activated microglia. Nature. 2017;541(7638):481-7. Epub 2017/01/19. doi: 10.1038/nature21029. PubMed PMID: 28099414; PubMed Central PMCID: PMCPMC5404890.

50. Molofsky AV, Krencik R, Ullian EM, Tsai HH, Deneen B, Richardson WD, et al. Astrocytes and disease: a neurodevelopmental perspective. Genes Dev. 2012;26(9):891-907. Epub 2012/05/03. doi: 10.1101/gad.188326.112. PubMed PMID: 22549954; PubMed Central PMCID: PMCPMC3347787.

51. Yamanaka K, Chun SJ, Boillee S, Fujimori-Tonou N, Yamashita H, Gutmann DH, et al. Astrocytes as determinants of disease progression in inherited amyotrophic lateral sclerosis. Nat Neurosci. 2008;11(3):251-3. Epub 2008/02/05. doi: 10.1038/nn2047. PubMed PMID: 18246065; PubMed Central PMCID: PMCPMC3137510.

52. Lioy DT, Garg SK, Monaghan CE, Raber J, Foust KD, Kaspar BK, et al. A role for glia in the progression of Rett's syndrome. Nature. 2011;475(7357):497-500. Epub 2011/07/01. doi: 10.1038/nature10214. PubMed PMID: 21716289; PubMed Central PMCID: PMCPMC3268776.

53. Tian GF, Azmi H, Takano T, Xu Q, Peng W, Lin J, et al. An astrocytic basis of epilepsy. Nat Med. 2005;11(9):973-81. Epub 2005/08/24. doi: 10.1038/nm1277. PubMed PMID: 16116433; PubMed Central PMCID: PMCPMC1850946.

54. Windrem MS, Osipovitch M, Liu Z, Bates J, Chandler-Militello D, Zou L, et al. Human iPSC Glial Mouse Chimeras Reveal Glial Contributions to Schizophrenia. Cell Stem Cell. 2017;21(2):195-208 e6. Epub 2017/07/25. doi: 10.1016/j.stem.2017.06.012. PubMed PMID: 28736215; PubMed Central PMCID: PMCPMC5576346.

55. Krencik R, Hokanson KC, Narayan AR, Dvornik J, Rooney GE, Rauen KA, et al. Dysregulation of astrocyte extracellular signaling in Costello syndrome. Sci Transl Med. 2015;7(286):286ra66. Epub 2015/05/08. doi: 10.1126/scitranslmed.aaa5645. PubMed PMID: 25947161; PubMed Central PMCID: PMCPMC4474402.

56. Laug D, Huang TW, Huerta NAB, Huang AY, Sardar D, Ortiz-Guzman J, et al. Nuclear factor I-A regulates diverse reactive astrocyte responses after CNS injury. J Clin Invest. 2019;129(10):4408-18. Epub 2019/09/10. doi: 10.1172/JCI127492. PubMed PMID: 31498149; PubMed Central PMCID: PMCPMC6763246.

57. Ballas N, Lioy DT, Grunseich C, Mandel G. Non-cell autonomous influence of MeCP2-deficient glia on neuronal dendritic morphology. Nat Neurosci. 2009;12(3):311-7. Epub 2009/02/24. doi: 10.1038/nn.2275. PubMed PMID: 19234456; PubMed Central PMCID: PMCPMC3134296.

58. Gandal MJ, Haney JR, Parikshak NN, Leppa V, Ramaswami G, Hartl C, et al. Shared molecular neuropathology across major psychiatric disorders parallels polygenic overlap. Science. 2018;359(6376):693-7. Epub 2018/02/14. doi: 10.1126/science.aad6469. PubMed PMID: 29439242; PubMed Central PMCID: PMCPMC5898828.

59. Gandal MJ, Zhang P, Hadjimichael E, Walker RL, Chen C, Liu S, et al. Transcriptome-wide isoform-level dysregulation in ASD, schizophrenia, and bipolar disorder. Science.

2018;362(6420). Epub 2018/12/14. doi: 10.1126/science.aat8127. PubMed PMID: 30545856; PubMed Central PMCID: PMCPMC6443102.

60. Howland DS, Liu J, She Y, Goad B, Maragakis NJ, Kim B, et al. Focal loss of the glutamate transporter EAAT2 in a transgenic rat model of SOD1 mutant-mediated amyotrophic lateral sclerosis (ALS). Proc Natl Acad Sci U S A. 2002;99(3):1604-9. Epub 2002/01/31. doi: 10.1073/pnas.032539299. PubMed PMID: 11818550; PubMed Central PMCID: PMCPMC122237.

61. Guo H, Lai L, Butchbach ME, Stockinger MP, Shan X, Bishop GA, et al. Increased expression of the glial glutamate transporter EAAT2 modulates excitotoxicity and delays the onset but not the outcome of ALS in mice. Hum Mol Genet. 2003;12(19):2519-32. Epub 2003/08/14. doi: 10.1093/hmg/ddg267. PubMed PMID: 12915461.

62. de Majo M, Koontz M, Rowitch D, Ullian EM. An update on human astrocytes and their role in development and disease. Glia. 2020;68(4):685-704. Epub 2020/01/12. doi: 10.1002/glia.23771. PubMed PMID: 31926040.

63. Oberheim NA, Takano T, Han X, He W, Lin JH, Wang F, et al. Uniquely hominid features of adult human astrocytes. J Neurosci. 2009;29(10):3276-87. Epub 2009/03/13. doi: 10.1523/JNEUROSCI.4707-08.2009. PubMed PMID: 19279265; PubMed Central PMCID: PMCPMC2819812.

64. Oberheim NA, Wang X, Goldman S, Nedergaard M. Astrocytic complexity distinguishes the human brain. Trends Neurosci. 2006;29(10):547-53. Epub 2006/08/30. doi: 10.1016/j.tins.2006.08.004. PubMed PMID: 16938356.

65. Zhang Y, Sloan SA, Clarke LE, Caneda C, Plaza CA, Blumenthal PD, et al. Purification and Characterization of Progenitor and Mature Human Astrocytes Reveals Transcriptional and Functional Differences with Mouse. Neuron. 2016;89(1):37-53. Epub 2015/12/22. doi: 10.1016/j.neuron.2015.11.013. PubMed PMID: 26687838; PubMed Central PMCID: PMCPMC4707064.

66. Li J, Pan L, Pembroke WG, Rexach JE, Godoy MI, Condro MC, et al. Conservation and divergence of vulnerability and responses to stressors between human and mouse astrocytes. Nat Commun. 2021;12(1):3958. Epub 2021/06/27. doi: 10.1038/s41467-021-24232-3. PubMed PMID: 34172753; PubMed Central PMCID: PMCPMC8233314.

67. Han X, Chen M, Wang F, Windrem M, Wang S, Shanz S, et al. Forebrain engraftment by human glial progenitor cells enhances synaptic plasticity and learning in adult mice. Cell Stem Cell. 2013;12(3):342-53. Epub 2013/03/12. doi: 10.1016/j.stem.2012.12.015. PubMed PMID: 23472873; PubMed Central PMCID: PMCPMC3700554.

68. Dobin A, Davis CA, Schlesinger F, Drenkow J, Zaleski C, Jha S, et al. STAR: ultrafast universal RNA-seq aligner. Bioinformatics. 2013;29(1):15-21. Epub 2012/10/30. doi: 10.1093/bioinformatics/bts635. PubMed PMID: 23104886; PubMed Central PMCID: PMCPMC3530905.

69. Anders S, Pyl PT, Huber W. HTSeq--a Python framework to work with high-throughput sequencing data. Bioinformatics. 2015;31(2):166-9. Epub 2014/09/28. doi: 10.1093/bioinformatics/btu638. PubMed PMID: 25260700; PubMed Central PMCID: PMCPMC4287950.

70. Love MI, Huber W, Anders S. Moderated estimation of fold change and dispersion for RNA-seq data with DESeq2. Genome Biol. 2014;15(12):550. Epub 2014/12/18. doi: 10.1186/s13059-014-0550-8. PubMed PMID: 25516281; PubMed Central PMCID: PMCPMC4302049.

71. Weng Q, Wang J, Wang J, He D, Cheng Z, Zhang F, et al. Single-Cell Transcriptomics Uncovers Glial Progenitor Diversity and Cell Fate Determinants during Development and Gliomagenesis. Cell Stem Cell. 2019;24(5):707-23 e8. Epub 2019/04/16. doi: 10.1016/j.stem.2019.03.006. PubMed PMID: 30982771; PubMed Central PMCID: PMCPMC6669001.

72. Yu W, Clyne M, Khoury MJ, Gwinn M. Phenopedia and Genopedia: disease-centered and gene-centered views of the evolving knowledge of human genetic associations. Bioinformatics. 2010;26(1):145-6. Epub 2009/10/30. doi: 10.1093/bioinformatics/btp618. PubMed PMID: 19864262; PubMed Central PMCID: PMCPMC2796820.

73. Clarke LE, Liddelow SA, Chakraborty C, Munch AE, Heiman M, Barres BA. Normal aging induces A1-like astrocyte reactivity. Proc Natl Acad Sci U S A. 2018;115(8):E1896-E905. Epub 2018/02/14. doi: 10.1073/pnas.1800165115. PubMed PMID: 29437957; PubMed Central PMCID: PMCPMC5828643.

74. Boisvert MM, Erikson GA, Shokhirev MN, Allen NJ. The Aging Astrocyte Transcriptome from Multiple Regions of the Mouse Brain. Cell Rep. 2018;22(1):269-85. Epub 2018/01/04. doi: 10.1016/j.celrep.2017.12.039. PubMed PMID: 29298427; PubMed Central PMCID: PMCPMC5783200.

75. Ximerakis M, Lipnick SL, Innes BT, Simmons SK, Adiconis X, Dionne D, et al. Single-cell transcriptomic profiling of the aging mouse brain. Nat Neurosci. 2019;22(10):1696-708. Epub 2019/09/26. doi: 10.1038/s41593-019-0491-3. PubMed PMID: 31551601.

76. Zhou Y, Zhou B, Pache L, Chang M, Khodabakhshi AH, Tanaseichuk O, et al. Metascape provides a biologist-oriented resource for the analysis of systems-level datasets. Nat Commun. 2019;10(1):1523. Epub 2019/04/05. doi: 10.1038/s41467-019-09234-6. PubMed PMID: 30944313; PubMed Central PMCID: PMCPMC6447622.

77. Heiland DH, Ravi VM, Behringer SP, Frenking JH, Wurm J, Joseph K, et al. Tumor-associated reactive astrocytes aid the evolution of immunosuppressive environment in glioblastoma. Nat Commun. 2019;10(1):2541. Epub 2019/06/13. doi: 10.1038/s41467-019-10493-6. PubMed PMID: 31186414; PubMed Central PMCID: PMCPMC6559986.

78. Ashburner M, Ball CA, Blake JA, Botstein D, Butler H, Cherry JM, et al. Gene ontology: tool for the unification of biology. The Gene Ontology Consortium. Nat Genet. 2000;25(1):25-

9. Epub 2000/05/10. doi: 10.1038/75556. PubMed PMID: 10802651; PubMed Central PMCID: PMCPMC3037419.

79. Gene Ontology C. The Gene Ontology resource: enriching a GOld mine. Nucleic Acids Res. 2021;49(D1):D325-D34. Epub 2020/12/09. doi: 10.1093/nar/gkaa1113. PubMed PMID: 33290552; PubMed Central PMCID: PMCPMC7779012.

80. Carbon S, Ireland A, Mungall CJ, Shu S, Marshall B, Lewis S, et al. AmiGO: online access to ontology and annotation data. Bioinformatics. 2009;25(2):288-9. Epub 2008/11/27. doi: 10.1093/bioinformatics/btn615. PubMed PMID: 19033274; PubMed Central PMCID: PMCPMC2639003.

81. Xie Z, Janczyk PL, Zhang Y, Liu A, Shi X, Singh S, et al. A cytoskeleton regulator AVIL drives tumorigenesis in glioblastoma. Nat Commun. 2020;11(1):3457. Epub 2020/07/12. doi: 10.1038/s41467-020-17279-1. PubMed PMID: 32651364; PubMed Central PMCID: PMCPMC7351761.

82. Raore B, Schniederjan M, Prabhu R, Brat DJ, Shu HK, Olson JJ. Metastasis infiltration: an investigation of the postoperative brain-tumor interface. Int J Radiat Oncol Biol Phys. 2011;81(4):1075-80. Epub 2010/10/26. doi: 10.1016/j.ijrobp.2010.07.034. PubMed PMID: 20971574.

83. Quail DF, Joyce JA. The Microenvironmental Landscape of Brain Tumors. Cancer Cell. 2017;31(3):326-41. Epub 2017/03/16. doi: 10.1016/j.ccell.2017.02.009. PubMed PMID: 28292436; PubMed Central PMCID: PMCPMC5424263.

84. Yang Y, Gozen O, Watkins A, Lorenzini I, Lepore A, Gao Y, et al. Presynaptic regulation of astroglial excitatory neurotransmitter transporter GLT1. Neuron. 2009;61(6):880-94. Epub 2009/03/28. doi: 10.1016/j.neuron.2009.02.010. PubMed PMID: 19323997; PubMed Central PMCID: PMCPMC2743171.

85. Tanaka K, Watase K, Manabe T, Yamada K, Watanabe M, Takahashi K, et al. Epilepsy and exacerbation of brain injury in mice lacking the glutamate transporter GLT-1. Science.

1997;276(5319):1699-702. Epub 1997/06/13. doi: 10.1126/science.276.5319.1699. PubMed PMID: 9180080.

86. Kofuji P, Newman EA. Potassium buffering in the central nervous system. Neuroscience. 2004;129(4):1045-56. Epub 2004/11/25. doi: 10.1016/j.neuroscience.2004.06.008. PubMed PMID: 15561419; PubMed Central PMCID: PMCPMC2322935.

87. Reichold M, Zdebik AA, Lieberer E, Rapedius M, Schmidt K, Bandulik S, et al. KCNJ10 gene mutations causing EAST syndrome (epilepsy, ataxia, sensorineural deafness, and tubulopathy) disrupt channel function. Proc Natl Acad Sci U S A. 2010;107(32):14490-5. Epub 2010/07/24. doi: 10.1073/pnas.1003072107. PubMed PMID: 20651251; PubMed Central PMCID: PMCPMC2922599.

88. Englot DJ, Chang EF, Vecht CJ. Epilepsy and brain tumors. Handb Clin Neurol. 2016;134:267-85. Epub 2016/03/08. doi: 10.1016/B978-0-12-802997-8.00016-5. PubMed PMID: 26948360; PubMed Central PMCID: PMCPMC4803433.

89. Sattler R, Tyler B, Hoover B, Coddington LT, Recinos V, Hwang L, et al. Increased expression of glutamate transporter GLT-1 in peritumoral tissue associated with prolonged survival and decreases in tumor growth in a rat model of experimental malignant glioma. J Neurosurg. 2013;119(4):878-86. Epub 2013/08/06. doi: 10.3171/2013.6.JNS122319. PubMed PMID: 23909244; PubMed Central PMCID: PMCPMC4086647.

90. Bausch-Fluck D, Goldmann U, Muller S, van Oostrum M, Muller M, Schubert OT, et al. The in silico human surfaceome. Proc Natl Acad Sci U S A. 2018;115(46):E10988-E97. Epub 2018/10/31. doi: 10.1073/pnas.1808790115. PubMed PMID: 30373828; PubMed Central PMCID: PMCPMC6243280.

91. Nguyen PT, Dorman LC, Pan S, Vainchtein ID, Han RT, Nakao-Inoue H, et al. Microglial Remodeling of the Extracellular Matrix Promotes Synapse Plasticity. Cell.

2020;182(2):388-403 e15. Epub 2020/07/03. doi: 10.1016/j.cell.2020.05.050. PubMed PMID: 32615087; PubMed Central PMCID: PMCPMC7497728.

92. Winkler J, Abisoye-Ogunniyan A, Metcalf KJ, Werb Z. Concepts of extracellular matrix remodelling in tumour progression and metastasis. Nat Commun. 2020;11(1):5120. Epub 2020/10/11. doi: 10.1038/s41467-020-18794-x. PubMed PMID: 33037194; PubMed Central PMCID: PMCPMC7547708.

93. Kelley KW, Nakao-Inoue H, Molofsky AV, Oldham MC. Variation among intact tissue samples reveals the core transcriptional features of human CNS cell classes. Nat Neurosci. 2018;21(9):1171-84. Epub 2018/08/30. doi: 10.1038/s41593-018-0216-z. PubMed PMID: 30154505; PubMed Central PMCID: PMCPMC6192711.

94. Park BS, Lee JO. Recognition of lipopolysaccharide pattern by TLR4 complexes. Exp Mol Med. 2013;45:e66. Epub 2013/12/07. doi: 10.1038/emm.2013.97. PubMed PMID: 24310172; PubMed Central PMCID: PMCPMC3880462.

95. Vaure C, Liu Y. A comparative review of toll-like receptor 4 expression and functionality in different animal species. Front Immunol. 2014;5:316. Epub 2014/07/30. doi: 10.3389/fimmu.2014.00316. PubMed PMID: 25071777; PubMed Central PMCID: PMCPMC4090903.

96. Gaitanis JN, Donahue J. Focal cortical dysplasia. Pediatr Neurol. 2013;49(2):79-87. Epub 2013/07/19. doi: 10.1016/j.pediatrneurol.2012.12.024. PubMed PMID: 23859852.

97. Sofroniew MV, Vinters HV. Astrocytes: biology and pathology. Acta Neuropathol. 2010;119(1):7-35. Epub 2009/12/17. doi: 10.1007/s00401-009-0619-8. PubMed PMID: 20012068; PubMed Central PMCID: PMCPMC2799634.

98. Huang YH, Sinha SR, Tanaka K, Rothstein JD, Bergles DE. Astrocyte glutamate transporters regulate metabotropic glutamate receptor-mediated excitation of hippocampal interneurons. J Neurosci. 2004;24(19):4551-9. Epub 2004/05/14. doi:

10.1523/JNEUROSCI.5217-03.2004. PubMed PMID: 15140926; PubMed Central PMCID: PMCPMC6729403.

99. Pinter A, Hevesi Z, Zahola P, Alpar A, Hanics J. Chondroitin sulfate proteoglycan-5 forms perisynaptic matrix assemblies in the adult rat cortex. Cell Signal. 2020;74:109710. Epub 2020/07/13. doi: 10.1016/j.cellsig.2020.109710. PubMed PMID: 32653642.

100. Nakaya N, Sultana A, Munasinghe J, Cheng A, Mattson MP, Tomarev SI. Deletion in the N-terminal half of olfactomedin 1 modifies its interaction with synaptic proteins and causes brain dystrophy and abnormal behavior in mice. Exp Neurol. 2013;250:205-18. Epub 2013/10/08. doi: 10.1016/j.expneurol.2013.09.019. PubMed PMID: 24095980; PubMed Central PMCID: PMCPMC3875227.

101. Westergaard N, Waagepetersen HS, Belhage B, Schousboe A. Citrate, a Ubiquitous Key Metabolite with Regulatory Function in the CNS. Neurochem Res. 2017;42(6):1583-8. Epub 2017/01/07. doi: 10.1007/s11064-016-2159-7. PubMed PMID: 28058526.

102. Zamanian JL, Xu L, Foo LC, Nouri N, Zhou L, Giffard RG, et al. Genomic analysis of reactive astrogliosis. J Neurosci. 2012;32(18):6391-410. Epub 2012/05/04. doi: 10.1523/JNEUROSCI.6221-11.2012. PubMed PMID: 22553043; PubMed Central PMCID: PMCPMC3480225.

103. Werling DM, Geschwind DH. Sex differences in autism spectrum disorders. Curr Opin Neurol. 2013;26(2):146-53. Epub 2013/02/15. doi: 10.1097/WCO.0b013e32835ee548. PubMed PMID: 23406909; PubMed Central PMCID: PMCPMC4164392.

104. Gillies GE, Pienaar IS, Vohra S, Qamhawi Z. Sex differences in Parkinson's disease. Front Neuroendocrinol. 2014;35(3):370-84. Epub 2014/03/13. doi: 10.1016/j.yfrne.2014.02.002. PubMed PMID: 24607323; PubMed Central PMCID: PMCPMC4096384.

105. Westerlind H, Bostrom I, Stawiarz L, Landtblom AM, Almqvist C, Hillert J. New data identify an increasing sex ratio of multiple sclerosis in Sweden. Mult Scler. 2014;20(12):1578-83.

Epub 2014/05/21. doi: 10.1177/1352458514530021. PubMed PMID: 24842964; PubMed Central PMCID: PMCPMC4230455.

106. Seshadri S, Wolf PA, Beiser A, Au R, McNulty K, White R, et al. Lifetime risk of dementia and Alzheimer's disease. The impact of mortality on risk estimates in the Framingham Study. Neurology. 1997;49(6):1498-504. Epub 1997/12/31. doi: 10.1212/wnl.49.6.1498. PubMed PMID: 9409336.

107. McLean CP, Asnaani A, Litz BT, Hofmann SG. Gender differences in anxiety disorders: prevalence, course of illness, comorbidity and burden of illness. J Psychiatr Res. 2011;45(8):1027-35. Epub 2011/03/29. doi: 10.1016/j.jpsychires.2011.03.006. PubMed PMID: 21439576; PubMed Central PMCID: PMCPMC3135672.

108. Tricarico R, Nicolas E, Hall MJ, Golemis EA. X- and Y-Linked Chromatin-Modifying Genes as Regulators of Sex-Specific Cancer Incidence and Prognosis. Clin Cancer Res. 2020;26(21):5567-78. Epub 2020/08/01. doi: 10.1158/1078-0432.CCR-20-1741. PubMed PMID: 32732223; PubMed Central PMCID: PMCPMC7642178.

109. Zablotsky B, Black LI, Blumberg SJ. NCHS Data Brief No. 291: Estimated Prevalence of Children With Diagnosed Developmental Disabilities in the United States, 2014–2016. 2017.

110. McCarthy KD, de Vellis J. Preparation of separate astroglial and oligodendroglial cell cultures from rat cerebral tissue. J Cell Biol. 1980;85(3):890-902. Epub 1980/06/01. doi: 10.1083/jcb.85.3.890. PubMed PMID: 6248568; PubMed Central PMCID: PMCPMC2111442.

111. Foo LC, Allen NJ, Bushong EA, Ventura PB, Chung WS, Zhou L, et al. Development of a method for the purification and culture of rodent astrocytes. Neuron. 2011;71(5):799-811. Epub 2011/09/10. doi: 10.1016/j.neuron.2011.07.022. PubMed PMID: 21903074; PubMed Central PMCID: PMCPMC3172573.

112. Rossini L, Garbelli R, Gnatkovsky V, Didato G, Villani F, Spreafico R, et al. Seizure activity per se does not induce tissue damage markers in human neocortical focal epilepsy. Ann Neurol. 2017;82(3):331-41. Epub 2017/07/28. doi: 10.1002/ana.25005. PubMed PMID: 28749594.

113. Venkataramani V, Tanev DI, Strahle C, Studier-Fischer A, Fankhauser L, Kessler T, et al. Glutamatergic synaptic input to glioma cells drives brain tumour progression. Nature. 2019;573(7775):532-8. Epub 2019/09/20. doi: 10.1038/s41586-019-1564-x. PubMed PMID: 31534219.

114. Venkatesh HS, Morishita W, Geraghty AC, Silverbush D, Gillespie SM, Arzt M, et al. Electrical and synaptic integration of glioma into neural circuits. Nature. 2019;573(7775):539-45. Epub 2019/09/20. doi: 10.1038/s41586-019-1563-y. PubMed PMID: 31534222; PubMed Central PMCID: PMCPMC7038898.

115. Zeng Q, Michael IP, Zhang P, Saghafinia S, Knott G, Jiao W, et al. Synaptic proximity enables NMDAR signalling to promote brain metastasis. Nature. 2019;573(7775):526-31. Epub 2019/09/20. doi: 10.1038/s41586-019-1576-6. PubMed PMID: 31534217; PubMed Central PMCID: PMCPMC6837873.

116. Chaboub LS, Manalo JM, Lee HK, Glasgow SM, Chen F, Kawasaki Y, et al. Temporal Profiling of Astrocyte Precursors Reveals Parallel Roles for Asef during Development and after Injury. J Neurosci. 2016;36(47):11904-17. Epub 2016/11/25. doi: 10.1523/JNEUROSCI.1658-16.2016. PubMed PMID: 27881777; PubMed Central PMCID: PMCPMC5125245.

117. Kang P, Lee HK, Glasgow SM, Finley M, Donti T, Gaber ZB, et al. Sox9 and NFIA coordinate a transcriptional regulatory cascade during the initiation of gliogenesis. Neuron. 2012;74(1):79-94. Epub 2012/04/17. doi: 10.1016/j.neuron.2012.01.024. PubMed PMID: 22500632; PubMed Central PMCID: PMCPMC3543821.

118. Li J, Khankan RR, Caneda C, Godoy MI, Haney MS, Krawczyk MC, et al. Astrocyte-to-astrocyte contact and a positive feedback loop of growth factor signaling regulate astrocyte maturation. Glia. 2019;67(8):1571-97. Epub 2019/04/30. doi: 10.1002/glia.23630. PubMed PMID: 31033049; PubMed Central PMCID: PMCPMC6557696.

119. Huttenlocher PR. Synaptic density in human frontal cortex - developmental changes and effects of aging. Brain Res. 1979;163(2):195-205. Epub 1979/03/16. doi: 10.1016/0006-8993(79)90349-4. PubMed PMID: 427544.

120. Huttenlocher PR, Dabholkar AS. Regional differences in synaptogenesis in human cerebral cortex. J Comp Neurol. 1997;387(2):167-78. Epub 1997/10/23 22:34. doi: 10.1002/(sici)1096-9861(19971020)387:2<167::aid-cne1>3.0.co;2-z. PubMed PMID: 9336221.

121. Petanjek Z, Judas M, Simic G, Rasin MR, Uylings HB, Rakic P, et al. Extraordinary neoteny of synaptic spines in the human prefrontal cortex. Proc Natl Acad Sci U S A. 2011;108(32):13281-6. Epub 2011/07/27. doi: 10.1073/pnas.1105108108. PubMed PMID: 21788513; PubMed Central PMCID: PMCPMC3156171.

122. Johnson RT, Breedlove SM, Jordan CL. Sex differences and laterality in astrocyte number and complexity in the adult rat medial amygdala. J Comp Neurol. 2008;511(5):599-609. Epub 2008/10/15. doi: 10.1002/cne.21859. PubMed PMID: 18853427; PubMed Central PMCID: PMCPMC2592304.

123. Mong JA, McCarthy MM. Ontogeny of sexually dimorphic astrocytes in the neonatal rat arcuate. Brain Res Dev Brain Res. 2002;139(2):151-8. Epub 2002/12/14. doi: 10.1016/s0165-3806(02)00541-2. PubMed PMID: 12480129.

Chapter 2

Lymphocyte Deficiency Alters the Transcriptomes of Oligodendrocytes, but Not Astrocytes or Microglia

2.1 Abstract

Though the brain was long characterized as an immune-privileged organ, findings in recent years have shown extensive communications between the brain and peripheral immune cells. We now know that alterations in the peripheral immune system can affect the behavioral outputs of the central nervous system, but we do not know which brain cells are affected by the presence of peripheral immune cells. Glial cells including microglia, astrocytes, oligodendrocytes, and oligodendrocyte precursor cells (OPCs) are critical for the development and function of the central nervous system. In a wide range of neurological and psychiatric diseases, the glial cell state is influenced by infiltrating peripheral lymphocytes. However, it remains largely unclear whether the development of the molecular phenotypes of glial cells in the healthy brain is regulated by lymphocytes. To answer this question, we acutely purified each type of glial cell from immunodeficient $Rag2^{-/-}$ mice. Interestingly, we found that the transcriptomes of microglia, astrocytes, and OPCs developed normally in $Rag2^{-/-}$ mice without reliance on lymphocytes. In contrast, there are modest transcriptome differences between the oligodendrocytes from $Rag2^{-/-}$ and control mice. Furthermore, the subcellular localization of the RNA-binding protein Quaking, is altered in oligodendrocytes. These results demonstrate that the molecular attributes of glial cells develop largely without influence from lymphocytes and highlight potential interactions between lymphocytes and oligodendrocytes.

2.2 Introduction

The immune system and the nervous system are two vital and intricate biological systems. In recent decades an additional layer in their complexity is emerging as accumulating evidence suggests how these two systems interact and influence one another. Although the brain has been traditionally considered an immune-privileged organ, researchers have reported the presence of immune cells in the protective layers surrounding the brain, the meninges, as well as in the perivascular space and choroid plexus [1-4]. Some meningeal immune cells are

produced locally in the skull bone marrow and display different properties than immune cells derived from the periphery, suggesting brain-specific roles for the immune cells that occupy this niche [5, 6]. These meningeal immune cells are poised for direct signaling to the brain through secreted factors or indirect signaling via border cells. Several lines of evidence implicate meningeal immune cells in homeostatic brain function. Limiting immune cell migration across the blood-meningeal barrier using VLA-4 integrin antibody results in cognitive impairment, and disrupting meningeal T cells via eliminating the deep cervical lymph nodes also impairs learning [7-9]. One recent study found that meningeal γδ T cells induce anxiety-like behavior through the secretion of IL-17a through activation of receptors on glutamatergic cortical neurons [10]. As the peripheral immune cells influence the brain, the brain in turn regulates the immune system in several ways, including the production of hormones. Activation of the hypothalamic-pituitary-adrenal axis results in the secretion of corticosteroids that inhibit many immune responses [11, 12].

Although the impact of peripheral immune cells on the behavioral output of the central nervous system (CNS) has been demonstrated, how immune cells affect the cellular state in the CNS remains elusive. Glial cells including microglia, astrocytes, oligodendrocytes, and oligodendrocyte precursor cells (OPCs) make up a large portion of brain cells and play key roles in the development and function of the CNS[13-29]. Of particular note in this study, microglia are CNS-resident innate immune cells and key players in CNS pathogen defense, homeostasis, and developmental synapse engulfment and neural circuit refinement [30-39]. Oligodendrocytes form insulating myelin sheaths around axons, accelerate the propagation of action potentials along axons, and provide metabolic support to axons [40-48]. Under pathological conditions in a wide range of neurological disorders, such as stroke, trauma, and CNS autoimmunity, infiltrating peripheral immune cells release cytokines that impact levels of neuroinflammation and glial cell states [49]. State changes of glial cells in turn contribute to neuroinflammation, tissue homeostasis, and neural repair [50]. A long-standing question that remains largely unanswered

is whether the cellular states of glial cells are regulated by immune cells under homeostatic conditions in the healthy brain.

Like glia, lymphocytes play a powerful role in many neurological pathologies. Most notably, lymphocytes have been implicated in the prototypic inflammatory disease, multiple sclerosis (MS). Lymphocytes are implicated in the causal pathology of MS due to a variety of experimental observations[51]. Activated myelin-specific T lymphocytes are sufficient to generate brain lesions in the popular mouse model of MS, experimental autoimmune encephalomyelitis (EAE)[52]. Though exceedingly rare in homeostasis, peripheral immune cells can migrate into the brain in a variety of neurological disease states, including stroke, cancer, where they become central players in the pathology[53, 54]. Peripheral myeloid cells and neutrophils can be found in the brains of Alzheimer disease patients, and peripheral immune composition shows changes in Parkinson disease[55, 56]. Inflammation, and therefore immune cells, are known or suspected to play a role in a huge array of CNS diseases. While their many roles in disease garner widespread attention, relatively little is known about how immune cells effect the brain in the absence of disease.

$Rag2^{-/-}$ mice are a particularly useful tool for assessing the impact of peripheral immune cells on the CNS as they lack mature lymphocytes, the central players in adaptive immunity. Lymphocytes, including T and B cells, serve to recognize potentially hazardous antigens, and they accomplish this task by expressing a great diversity of receptors to identify the many possible antigens they may need to detect. Rather than expressing an impossibly large number of distinct receptor genes, this receptor diversity is accomplished by physical recombination of a small number of antigen receptor genes; Rag1 and Rag2 are the recombinase enzymes required for this recombination [57]. In the absence of Rag2, this recombination cannot take place, so lymphocytes will not create the appropriate receptor array and therefore fail to mature into functional T and B cells [58]. In the absence of these lymphocytes, researchers have reported a diverse set of changes in learning and behavior. When trained to associate a tone

with a foot shock, Rag2$^{-/-}$ mice show significantly less freezing when presented with the tone, indicating a fear learning deficit[59]. The freezing response was partially recovered in Rag2$^{-/-}$ that had been reconstituted with CD4+ T-cells. In a social interaction test, Rag2$^{-/-}$ mice spent significantly less time interacting with a conspecific mouse than wildtype mice, and this phenotype was also rescued with reconstitution of functional lymphocytes[60]. Reconstituted Rag2$^{-/-}$ also showed less anxiety behavior than naïve Rag2$^{-/-}$ mice, as measured by time in the open arm of an elevated plus maze. These studies demonstrate that lymphocytes can shape behavior outside of pathological conditions, though it remains unclear how this influence is exerted.

In this study we sought to determine whether the homeostatic transcriptome states of CNS glial cells require signals from lymphocytes. To that end, we acutely purified cortical oligodendrocytes, OPCs, astrocytes, and microglia by the immunopanning method from immunodeficient Rag2$^{-/-}$ mice and immunocompetent littermates. We performed RNA-sequencing to characterize the transcriptome profiles of each of the glial cell types. We found modest changes in gene expression among oligodendrocytes, though gross myelin development appears normal. However, we did identify altered localization of an RNA-binding protein, Quaking, in oligodendrocytes, which binds transcripts for a key myelin gene, *MBP*[61]. Microg lia, OPCs, and astrocytes show little to no alterations in gene expression in the cortex, despite a previous study suggesting that lymphocyte depletion altered microglial gene signatures[62]. Overall, we find little evidence that lymphocytes influence CNS function by majorly altering the transcriptome profiles of microglia, astrocytes, and OPCs in the healthy cortex.

2.3 Materials and Methods

Experimental animals

All animal care and experimentation were approved by the Animal Research Committee at the University of California, Los Angeles (UCLA) under the approved protocol #R-16-080. We obtained Rag2$^{-/-}$ mice from Jackson Laboratory (B6.Cg-Rag2$^{tm1.1Cgn}$/J, #008449) and crossed with C57BL/6J to establish the breeding colony used in all sequencing and immunostaining experiments. We ordered 8-week-old male Rag2$^{-/-}$ mice (B6.Cg-Rag2$^{tm1.1Cgn}$/J, #008449) and controls (C57BL/6J, #000664) from Jackson Laboratory for western blot experiments. Mice were housed in autoclaved cages and received sterilized food and water. Both male and female mice were used for experimentation. We used 3-month-old mice for RNA-sequencing experiments, and approximately 1-year-old mice for RNAscope experiments.

Purification of brain cells

Four classes of brain cells (microglia, OPCs, oligodendrocytes, and astrocytes) were purified using immunopanning, as described in Zhang 2016 and Zhang 2014 [63, 64]. Briefly, we anesthetized animals with isofluorane and performed transcardial perfusions with phosphate buffered saline (PBS) and subsequently dissected cortical grey matter. The tissue was digested enzymatically with papain (12 units/mL) at 34.5°C for 45 minutes, followed by mechanical trituration to generate a single cell suspension. Cells were treated with enzymatic inhibitor to end digestion. We incubated this single cell suspension for 10-15 minutes at room temperature on a series of petri dishes that were pre-coated with cell-specific antibodies. After incubation, we washed each dish with PBS to remove contaminants, applied TRIzol to release the RNA, and flash froze the resulting sample in liquid nitrogen for storage at -80°C. We used the following series of antibodies to purify each cell class in this order: microglia, anti-CD45 x3 plates (BD Pharmingen 550539); OPCs, anti-PDGFRα x1 plate (BD Sciences 558774) (harvested for RNA-sequencing) and O4 hybridoma x2 plates (to further deplete OPCs, not harvested for RNA-sequencing); oligodendrocytes, GalC hybridoma x2-3 plates; astrocytes, HepaCAM x1 plate (R&D Systems MAB4108). Of note, anti-CD45 can also bind a population of peripheral macrophages, though this population was reduced by perfusion prior to brain

dissection. The following sample sizes were collected for each cell class: astrocyte n = 12 [6 control, 6 Rag2-knockout (KO)], microglia n = 12 (6 control, 6 KO), OPC = 11 (6 control, 5 KO), and oligodendrocyte = 8 (4 control, 4 KO). Samples also included both males and females: astrocyte 7 male, 5 female; microglia 7 male, 5 female; OPC 7 male, 4 female; oligodendrocyte 5 male, 3 female.

RNA-sequencing library construction and sequencing

RNA was purified from frozen samples using the miRNeasy kit (Qiagen 217004) according to the manufacturer's protocol. The resulting RNA was converted to cDNA and amplified using the Nugen Ovation RNAseq System V2 (Nugen 7102-32), and fragmented using a Covaris S220 focused-ultrasonicator (Covaris 500217). Final libraries were prepared using the NEB Next Ultra RNA Library Prep Kit (New England Biolabs E7530S) and NEBNext multiplex oligos for Illumina (NEB E7335S) according to manufacturer's protocol. Libraries from the same cell type from all mice were pooled and sequenced on the same lane using the Illumina NovaSeq 600 System to obtain 23.2 ± 5.74 (s.d.) million 2x50 bp reads per sample. RNA integrity was measured using the 2200 TapeStation System (Agilent G2964AA) and the RNA high sensitivity assay (Agilent 5067-5579). All samples had RIN > 7, though some samples were out of the measurable range.

Read alignment and quantification

We mapped the reads using the STAR package v2.7.8a and genome assembly GRCm39 (Ensembl, release 104) [65]. Samples had 73.7% ± 2.97 (s.d.) uniquely aligned reads. Reads were quantified using HTSeq v0.13.5 to obtain counts for downstream analysis [66]. Quantified RNA-seq data can be found in supplemental information (S1).

Differential gene expression analysis with DESeq2

We analyzed differential gene expression of each cell type using gene counts and the DESeq2 (v1.26.0) package in R [67]. We built our linear model using only two binary variables: sex and genotype. Full differential gene expression results are reported in the supplemental

information (S2, S3). Male- and female-enriched genes in oligodendrocytes were also passed into the online database STRING to identify functional enrichment of these gene sets[68].

Gene Set enrichment analysis (GSEA)

We downloaded GSEA software from www.gsea-msigdb.org, version 4.2.3 [69, 70]. We used the default settings with the following exceptions. We entered normalized counts for our expression data, which we calculated using the DESeq2 functions estimateSizeFactors() and counts(). "Permutation type" was set to "gene_set". We built our own gene sets based on scRNAseq analysis published in Pasciuto 2020 [62]. They sequenced cells from MHCII knock-out mice which have a different form of lymphocyte deficiency[71]. We extracted the genes they found to be differentially expressed among all $MHCII^{-/-}$ microglia vs all control microglia. We made one gene set of upregulated genes and one gene set of downregulated genes. The gene sets were trimmed to the top 500 genes ranked by p-values to meet the recommended gene set size.

Principal components analysis

Principal components analysis (PCA) was performed to visualize RNAseq results in a low-dimensional space. In R, we converted raw read counts using a $\log_2$ transformation with the function "rlogcounts" followed by PCA using the function "prcomp". Resulting plots are shown in supplemental data, SI2-5.

RNAscope in situ hybridization

In situ hybridization of microglial markers was performed using the RNAscope Multiplex Fluorescent V2 Assay (ACDBio 323100). Brain tissue was harvested from approximately 1 year old mice (3 $Rag2^{+/+}$, 3 $Rag2^{-/-}$) after anesthetization with isoflurane and 10-minute transcardial perfusion with 4% paraformaldehyde. Brains were postfixed overnight in 4% PFA at 4°C, then dehydrated in 30% sucrose at 4°C until brains sank. Finally, brains were embedded in OCT compound (Fisher Scientific 23-730-571) and sectioned at 15 µm thickness and mounted onto Superfrost Plus slides (Fisher Scientific 12-550-15) before proceeding to the RNAscope assay.

The assay was conducted as per the manufacturer's protocol. We used the following probes, formulated by ACD Bio: Mm-Tmem119 (cat. 472901), Mm-C1qa-C2 (cat. 441221-C2), and Mm-Junb-O1-C3 (cat. 584761-C3). The cerebral cortex was imaged with a 20x objective in both the upper cortex (layers 2-3) and lower cortex (layers 4-6) in both the motor and dorsal somatosensory regions. Images were quantified using ImageJ (2.0.0-rc-61/1.51n with Java 1.8.0_66) [72]. To quantify fluorescence intensity, regions of interest were manually drawn around microglial soma using microglia-specific markers *Tmem119* and *C1qa*, and intensity was measured using the "Measure" tool. For microglial-specific markers *Tmem119* and *C1qa*, we also quantified the area of staining by first applying an equal threshold to all images before measuring area with the "Measure" tool. Welch's t test was used to assess differences between *Rag2*$^{+/+}$ and *Rag2*$^{-/-}$ tissue.

Data deposition

We deposited all gene expression data to the Gene Expression Omnibus, accession number GSE210580.

Immunohistochemistry

Brain tissue was fixed and embedded as described for RNAscope. Brains were sectioned at 15-20 µm and directly mounted onto Superfrost Plus slides (Fisher Scientific 12-550-15). Sections were permeabilized with a blocking solution made of 0.2% Triton-X and 10% donkey serum in PBS at room temperature for 30 minutes, then they were rinsed and incubated with primary antibody diluted in blocking solution overnight at 4°C. The following day, sections were washed 3 times in PBS and incubated with secondary antibody at room temperature for 90 minutes, followed by 3 PBS washes. Finally, coverslips were added with a mounting solution containing DAPI. Primary antibodies: anti-MBP, 1:200 (Abcam ab7349), anti-APC clone CC1 (Millipore Sigma OP80); Secondary antibodies: anti-rat 647 (Invitrogen A48272), anti-rat 594 (Invitrogen A-21209), anti-mouse 488 (Invitrogen SA5-10166). Staining was quantified in 1-

year-old mice (n = 3/group). MBP was quantified in coronal sections approaching the crossing of the anterior commissure (bregma 0 mm to 0.1 mm).

Western blot

Whole-cell lysates from 2-month-old mouse cortex were lysed RIPA buffer (Thermo Fisher, cat #89901) containing EDTA-free protease inhibitor cocktail (Sigma, cat #4693159001), and centrifuged at 12,000 × g for 10 min to remove cell debris. Whole-cell lysates were then mixed with sodium dodecyl sulfate (SDS) sample buffer (Fisher, cat # AAJ60660AC) and 2-mercaptoethanol before boiling for 5 min. Samples were separated by SDS-polyacrylamide gel electrophoresis, followed by transfer to polyvinylidene difluoride membranes (Thermo Fisher, 88520) via wet transfer at 300 mA for 1.5 hours. Membranes were blocked with clear milk-blocking buffer (Fisher, cat #PI37587) for 1 hour at room temperature and incubated with primary antibodies against MBP (Abcam, cat #ab7349, dilution 1:1000), GAPDH (Sigma, cat #CB1001, dilution 1:5000), and PLP1 (Millipore, cat #MAB388, dilution 1:500) at 4°C overnight. Membranes were washed with tris-buffered saline with Tween 20 (TBST) three times and incubated with either horseradish peroxidase-conjugated secondary antibodies (Mouse, Cell Signaling, cat #7076S; Rat, Cell Signaling, cat #7077S) (for MBP and PLP1) or Donkey anti-Mouse IgG (H+L) Highly Cross-Adsorbed Secondary Antibody, Alexa Fluor™ Plus 647 (Fisher, cat # PIA32787,1:1000) (for GAPDH) for 1 hour at room temperature. After three washes in the TBST buffer, SuperSignal™ West Femto Maximum Sensitivity Substrate (Fisher, cat #PI34095) was added to the membranes, and these signals were visualized using a ChemiDocTM MP Imaging system (BIO-RAD). Images were quantified in ImageJ using the plugin "bandandPeakQuantification" and normalized to Gapdh expression.

Statistics

Differential gene expression and associated statistical testing was performed using DESeq2. Gene set enrichment analysis (GSEA) was performed using GSEA software v4.3.2,

as described above. All other statistical comparisons were performed using Welch's t-test in Excel.

2.4 Results

RNA-sequencing of glia from Rag2$^{-/-}$ mice

Rag2$^{-/-}$ immunodeficient mice and wildtype immunocompetent control mice are typically housed in facilities with different levels of pathogen exposures and other environmental variables. To compare glial cell states in *Rag2*$^{-/-}$ and control mice with minimal environmental confounding factors, we established a single colony of *Rag2*$^{+/-}$ heterozygous mice housed in a clean facility for immunodeficient mice. We crossed heterozygous parents to generate *Rag2*$^{-/-}$ and *Rag2*$^{+/+}$ littermate pairs raised with the same maternal care in the same environment for RNA-sequencing (Fig 2-1A).

We purified each glial cell type from the mouse cerebral cortex using an immunopanning technique [63, 64]. Cells were separated into a single-cell suspension and then passed over plates coated with cell type specific antibodies that pull down the cell types of interest (Fig 2-1B). Compared with the traditional method of culturing glial cells in serum-containing media and separating them based on the layers in which each cell type is enriched, immunopanning allows acute purification of glial cells without exposure to serum and allows cells to remain much closer to a physiological state [63, 64]. Using this method, we collected microglia (anti-CD45), astrocytes (anti-HepaCAM), oligodendrocytes (GalC hybridoma), and OPCs (anti-PDGFRA) from 4-6 littermate pairs of *Rag2*$^{-/-}$ and *Rag2*$^{+/+}$ mice and performed RNA-sequencing. Using a panel of cell type-enriched genes, we found that glial samples enriched via immunopanning have low levels of contamination from other cell types (Fig 2-1C).

Lymphocyte deficiency affects the oligodendrocyte transcriptome and Quaking RNA-binding protein localization

We analyzed each cell type for differential gene expression using DESeq2. We found five or fewer differentially expressed genes (multiple comparison adjusted p-value <0.05) in

astrocytes, OPCs, and microglia from immunocompetent vs. immunodeficient *Rag2*$^{-/-}$ mice. Of note, the gene *Iftap* (encoding intraflagellar transport associated protein) overlaps with *Rag2* in the genome, and *Iftap* is significantly downregulated in all four cell types analyzed. This observation suggests that the coding and/or regulatory sequences of *Iftap* is disrupted in *Rag2*$^{-/-}$ mice.

In contrast to the other three cell classes, oligodendrocytes showed more differentially expressed genes: 19 upregulated and 180 downregulated genes, of which 16 upregulated genes and 71 downregulated genes are protein-coding (Fig 2-2A). This suggests a role of peripheral lymphocytes in maintaining some aspect of oligodendrocyte molecular signatures.

Among the downregulated genes is *Man1a2*, a gene encoding an enzyme involved in N-glycosylation of peptides. N-glycosylation occurs on many important peptides expressed by oligodendrocytes, including myelin oligodendrocyte glycoprotein (MOG) [73]. *Rag2*$^{-/-}$ oligodendrocytes also downregulate *Spx*, which encodes the neuropeptide spexin, also known as neuropeptide Q. Spexin has been implicated in a variety of functions, including nociception and feeding behaviors, though its role in oligodendrocytes has not been described [74].
The upregulated genes include *Sema3b*, a member of the semaphorin family of genes that encode axon guidance cues. Interestingly, we also see observed differential expression of *Ppia*, which encodes an enzyme that catalyzes isomerization of peptide bonds. *Ppia* is sometimes referred to as a housekeeping gene and used as a reference gene in real time quantitative PCR, so its differential expression is interesting to note [75].

Upon further inspection of oligodendrocytes in the immunodeficient mice at the protein level, we found a striking change in CC1, a canonical marker of mature oligodendrocytes. We find that Rag2$^{-/-}$ show altered cellular distribution of CC1 within white matter (Fig 2-2B). In control mice, CC1 labels oligodendrocyte soma, as well as a number of processes. Somatic expression of CC1 remains in Rag2$^{-/-}$ mice, but CC1+ processes virtually disappear. CC1 antibodies specifically recognize the RNA-binding protein Quaking (QKI), specifically isoform

7[76]. QKI in oligodendrocytes is known to bind myelin basic protein (*MBP*) mRNA, and QKI disruption was previously shown to prevent *MBP* export to cytoplasmic processes, ultimately altering myelination[61].

To assess whether MBP levels were altered in conjunction with QKI localization, we performed immunohistochemistry experiments and measured MBP in three myelin-rich regions: the corpus callosum ($p = 0.44$, mean[control, KO] = 922.6, 762.4, SD[control, KO] = 288.1, 46.3), anterior commissure ($p = 0.46$, mean[control, KO] = 809.7, 762.0, SD[control, KO] = 80.1, 61.6), and striatum ($p = 0.32$, mean[control, KO] = 729.7, 698.6, SD[control, KO] = 41.2, 10.1). We found no difference between immunocompetent and immunocompromised mice in any of these regions (Fig 2-3A). To assess myelin protein levels using another method, we used western blots. Again, we found no difference in expression in MBP ($p = 0.69$, mean[control, KO] = 4.25, 4.38, SD[control, KO] = 0.55, 0.33) or another key myelin protein, myelin proteolipid protein, PLP ($p = 0.61$, mean[control, KO] = 0.20, 0.19, SD[control, KO] = 0.018, 0.021; Fig 2-3B). This suggests that lymphocytes are not required for gross myelination.

Sexual dimorphism in glial gene expression

Given the increased incidence of autoimmune disorders in women compared to men, we also examined differential gene expression associated with sex in our dataset. We found genes that were significantly associated with sex in each cell type, many of which were located on the X or Y chromosome (e.g. *Kdm5d*, *Uty*, *Eif2s3y*). Interestingly, oligodendrocytes again showed the most robust difference with 143 female-enriched genes, and 136 male-enriched genes (S3 File). Using a database of protein-protein interactions, STRING, we found that male-enriched genes showed functional enrichment for SNAP/SNARE and endosome terms, while female-enriched genes had functional enrichment for voltage-gated channel and neuronal system terms[68]. Among the other cell types we found the following numbers of female-enriched/male-enriched protein-coding genes: astrocytes 1/13, microglia 3/4, OPCs 2/6. We observed that

Kdm6a expression was significantly higher in female astrocytes compared to males, which agrees with our previous findings from RNAseq of human astrocytes[77].

Lymphocyte deficiency does not affect the maturation of microglia

Our RNA-sequencing data revealed that the expression of mature microglia markers such as *Cx3cr1*, *Tmem119*, *P2ry12*, and *Aif1* do not significantly differ between immunocompetent vs. immunodeficient Rag2$^{-/-}$ mice. This is somewhat surprising given microglia are the brain resident immune cells, and they express high levels of receptors for immune signaling molecules that peripheral lymphocytes could use to pass signals into the brain. To further assess markers of microglia in immune-compromised mice, we performed RNA and protein level analysis of microglial markers. First, we reanalyzed our RNAseq data by identifying a panel of microglial genes, and we generated an aggregate expression score for each sample (Panel C in SI2-4). There were no differences between Rag2$^{-/-}$ and control mice. Second, we performed RNAscope *in situ* hybridization to visualize the expression of genes found in mature microglia: *Tmem119*, *C1qa*, and *Junb*. Once again, we found no differences in gene expression (Panels A, B in SI2-4). Lastly, we performed immunohistochemistry to assess protein levels of the microglial markers Iba1, P2ry12, and Cd68, and we continued to detect no differences in the Rag2$^{-/-}$ mice (Panel D in SI2-4).

Given the striking lack of aberration among these brain resident immune cells, we asked whether microglia responded to other changes in peripheral immunity. One such animal model knocks out a set of major histocompatibility complex class II (MHCII) genes, which results in the loss of CD4+ T cells[71]. Rag2$^{-/-}$ mice, in contrast, lack all mature lymphocytes, including all T cells and B cells for a more complete depletion of adaptive immune cells. MHCII$^{-/-}$ animals show substantial differences in microglia transcription, including downregulation of highly expressed microglial genes including *P2ry12, Itgb5,* and *Tgfb1*[62]. To make a direct comparison between microglial gene expression in total lymphocyte-deficient *Rag2*$^{-/-}$ mice and CD4+ T lymphocyte-deficient MHCII-knockout mice in Pasciuto 2020, we took a more

systematic approach to assess whether the microglial differential gene expression signature observed in T lymphocyte-deficient MHCII-knockout mice is enriched in microglia from *Rag2*$^{-/-}$ mice. We took all the differentially expressed genes in microglia from MHCII-knockout mice from the Pasciuto study and performed gene set enrichment analysis (GSEA) using our RNA-seq data[62]. We found that the up- and down-regulated genes identified in their study did not show global enrichment in our dataset (Fig 2-2C). That is to say, upregulated genes in MHCII-knockout microglia did not trend toward higher expression in *Rag2*$^{-/-}$ microglia, nor did downregulated genes in MHCII-knockout microglia trend toward higher expression in immunocompetent microglia in this current study. This contrast suggests that the exact complement of peripheral lymphocytes can exert highly varied and perhaps surprising changes in the brain.

2.5 Discussion

We generated transcriptomic data of acutely purified glial cells from mice lacking adaptive immune cells and their immunocompetent littermates. We found differentially expressed genes among oligodendrocytes, while the transcriptome of microglia, astrocytes, and OPCs remained largely unaltered by the lack of lymphocytes. In oligodendrocytes, we found altered localization of the RNA-binding protein QKI. Given previous reports of microglia changes in immune-compromised mice [62], we validated our sequencing results with *in situ* hybridization and immunohistochemistry of microglial markers and found no differences in *Rag2*$^{-/-}$ mice. We also performed a bioinformatic analysis of the microglia that failed to detect the previously reported gene signature found in a different T lymphocyte deficiency model. Together, these data shed light on the impacts of peripheral immune cells on the brain, and suggest underappreciated interactions between oligodendrocytes and lymphocytes.

Molecular profile of oligodendrocytes in the absence of adaptive immunity

Oligodendrocytes were the only cell class in this study to show appreciable differential expression in *Rag2*$^{-/-}$ mice. The differentially expressed genes have a wide variety of functional roles in the brain that defy easy classification. Pathway analysis of gene expression, including gene ontology and gene set enrichment analysis, failed to identify larger patterns among these genes. Among the differentially expressed genes were axon guidance cues (*Sema3b*), glycosylation enzymes (*Man1a2*), neuropeptides (*Spx*), transcription factors (*Gli1*), and proteasome components (*Psmd5*).

At the protein level, we found differences in the expression of RNA-binding protein Quaking isoform 7, as shown with the classical oligodendrocyte marker CC1. QKI is important for trafficking various mRNAs, including the key myelin protein gene *MBP*. In Rag2$^{-/-}$ white matter, QKI7 no longer enters the processes, which may be relevant for delivering important oligodendrocyte transcripts like *MBP* to sites of myelination. We find that the overall levels of MBP do not change in adult Rag2$^{-/-}$ mice, but future studies could investigate potential changes during myelination in development that may underlie the behavioral phenotypes observed in these mice.

The link between peripheral immune state and oligodendrocyte transcription may provide a fruitful new avenue for understanding their interactions under pathological conditions. Lymphocyte interactions with oligodendrocytes and their myelin sheaths have long been suspected to be central to the demyelinating pathology of multiple sclerosis [51]. To our knowledge, this is the first evidence that oligodendrocytes are affected by lymphocytes in the healthy brain. Further elucidation of the interactions between oligodendrocytes and lymphocytes in homeostatic conditions could improve our understanding of how these interactions become maladaptive in a disease state.

Homeostatic microglia are unaltered in total lymphocyte deficiency

In this study, we find that microglia in adult *Rag2*$^{-/-}$ mice under homeostatic conditions are indistinguishable from microglia in immunocompetent mice in their transcriptome profiles.

This finding comes in surprising contrast to a previously published report that CD4+ T-cells were required for microglial maturation [62]. In that study, investigators used an MHCII knockout mouse model that lacks several genes that make protein products for the major histocompatibility complex 2. MHCII$^{-/-}$ mice specifically lack CD4+ T-cells, while maintaining other lymphocyte populations including CD8+ T-cells and B cells [71]. Single-cell sequencing of these cells found that MHCII$^{-/-}$ microglia downregulated highly expressed microglial markers including *P2ry12*, *Itgb5*, and *Tgfb1*. They therefore conclude that microglia from MHCII$^{-/-}$ mice are arrested in an immature state.

In contrast, the *Rag2*$^{-/-}$ model used in the current study results in the loss of all mature lymphocytes, including CD4+ T cells, CD8+ T cells, and B cells [58]. Despite a more comprehensive loss of adaptive immune cells, microglia from these mice did not show major transcriptional perturbations. The divergence in these two immunodeficiency models poses several interesting possibilities that should be explored in future studies. First, various lymphocyte classes may exert different or even opposing influences on brain cells. Perhaps the MHCII$^{-/-}$ microglia are altered not just by the absence of CD4+ T-cells, but also the influence of remaining T-cells and B-cells that would otherwise face regulation by CD4+ T-cells. This model could be compatible with unperturbed Rag2$^{-/-}$ microglia, where the relative balance of lymphocyte classes is maintained (i.e. all present or all absent). Alternatively, MHCII$^{-/-}$ may directly alter microglia. Microglia can express MHCII genes and become antigen presenting cells, whereas Rag2 is a lymphocyte-specific protein. However, microglial MHCII expression is largely thought to occur in pathological conditions, and little if any MHCII protein expression has been found in homeostatic microglia. Furthermore, Pasciuto et al. show that reintroduction of CD4+ T-cells to MHCII$^{-/-}$ slice culture can partially rescue some downregulated microglia genes, which argues for a causal role of lymphocytes in MHCII$^{-/-}$ microglia. Still, loss of MHCII genes may exert direct effects on microglia that are absent in the Rag2$^{-/-}$ model. The distinctions

between the MHCII and Rag2 models serve as a fruitful ground for further dissection of lymphocytic influence in the brain.

Neuro-immune interactions represent an exciting frontier of neurobiology that was previously overlooked. While modern studies now suggest influential roles of peripheral immune cells in brain function and behavior [4, 10, 59, 60, 78], it is important to understand the extent and the limits of this influence. These data provide important insight into which brain cells might interface with adaptive immune cells in non-pathological conditions. Of equal importance, this study also points to limits of adaptive immune influence in the central nervous system, and it insinuates that various peripheral immune cells may wield distinct influences within the central nervous system that remain to be explored.

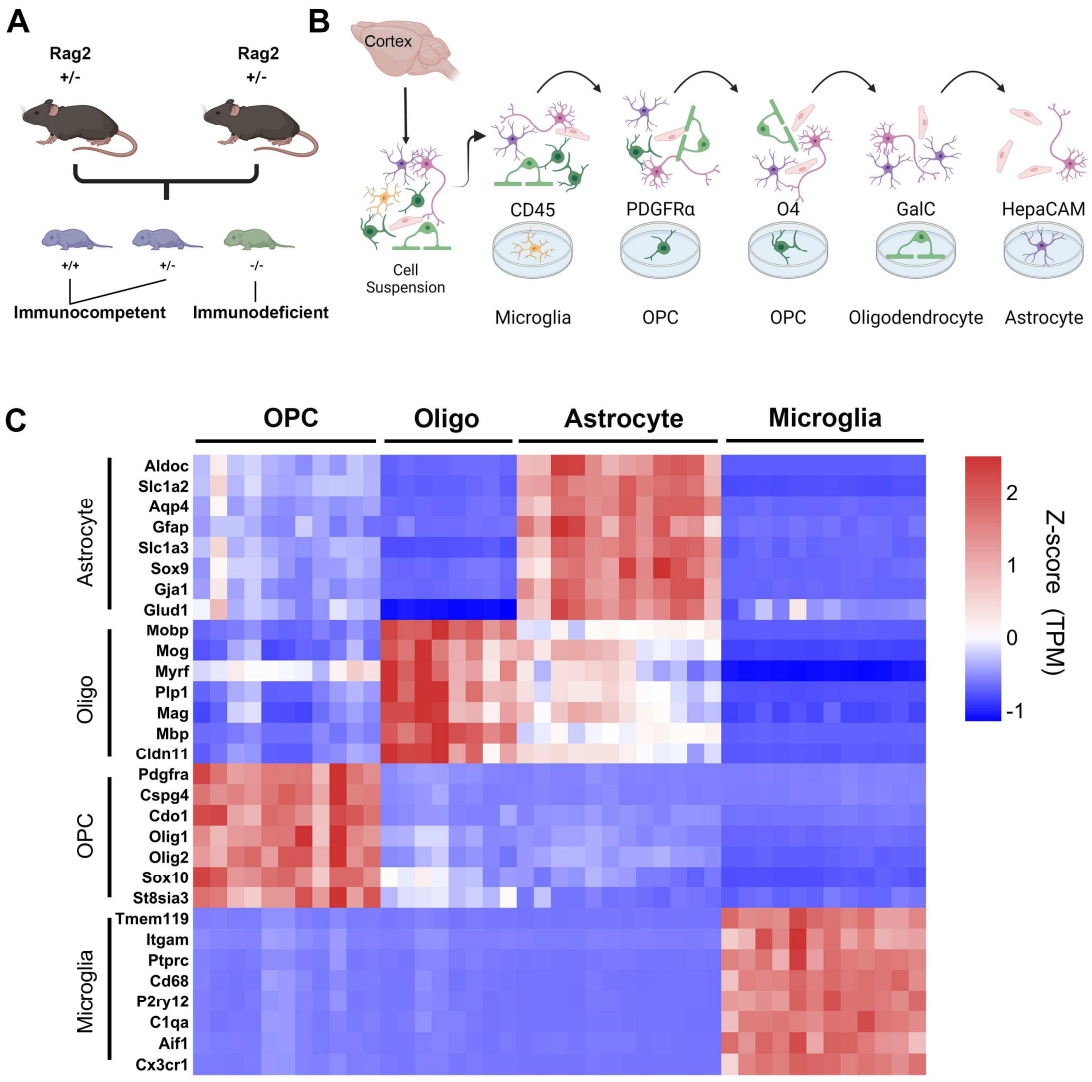

Figure 2-1. Acute purification of glial cell populations from immunodeficient mice. A) Breeding schematic; $Rag2^{+/-}$ parents bore offspring that were immunocompetent ($Rag2^{+/+}$ and $Rag2^{+/-}$) or immunodeficient ($Rag2^{-/-}$). All immunodeficient mice and littermate controls were maintained in the same environment. B) Immunopanning schematic; a single-cell suspension was generated from the cerebral cortex, then passed over a series of plates coated with cell type specific antibodies to enrich for specific glial cell populations. C) Heatmap showing enrichment of cell-specific markers (rows) among the glial samples that we harvested and sequenced (columns); gene expression is quantified as transcripts per million (TPM), and each

gene was further normalized to a z-score, defined as (expression in the sample - the average expression across all samples)/standard deviation; *i.e.*, the number of standard deviations from the average.

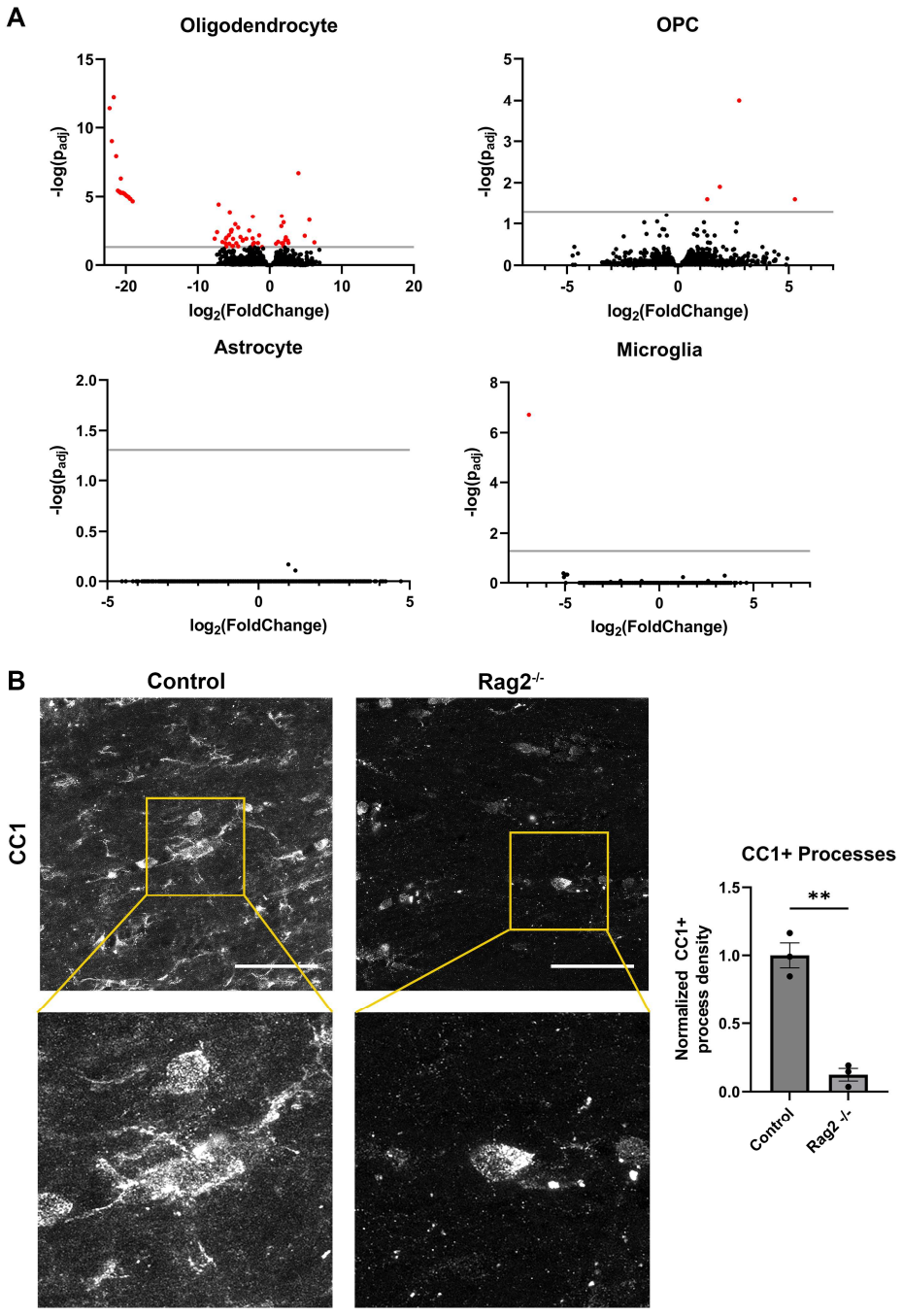

Figure 2-2. Differential gene expression of glial cells in Rag2$^{-/-}$ mice. A) Volcano plots displaying differential gene expression analysis of oligodendrocytes (top-left), OPCs (top-right), astrocytes (bottom-left), and microglia (bottom-right). Differential gene expression was analyzed using DESeq2, and the resulting fold change and statistical significance are plotted on

the x and y axes respectively. Red: $p < 0.05$; gray line: $p = .05$. B) Loss of CC1 expression in cellular processes. Top: Representative images of CC1 in the corpus callosum of control (left) and $Rag2^{-/-}$ (right) mice; Bottom: Insets of control showing CC1+ processes extending from a CC1+ cell bodies and KO showing only CC1+ soma. Right: Quantification of CC1+ process density, normalized to average control levels (right, $p = 0.0034$; mean[control, KO] = 1.0, 0.1246; SD[control, KO] = 0.157, 0.081; error bars = SEM). Scale bar = 50 μm.

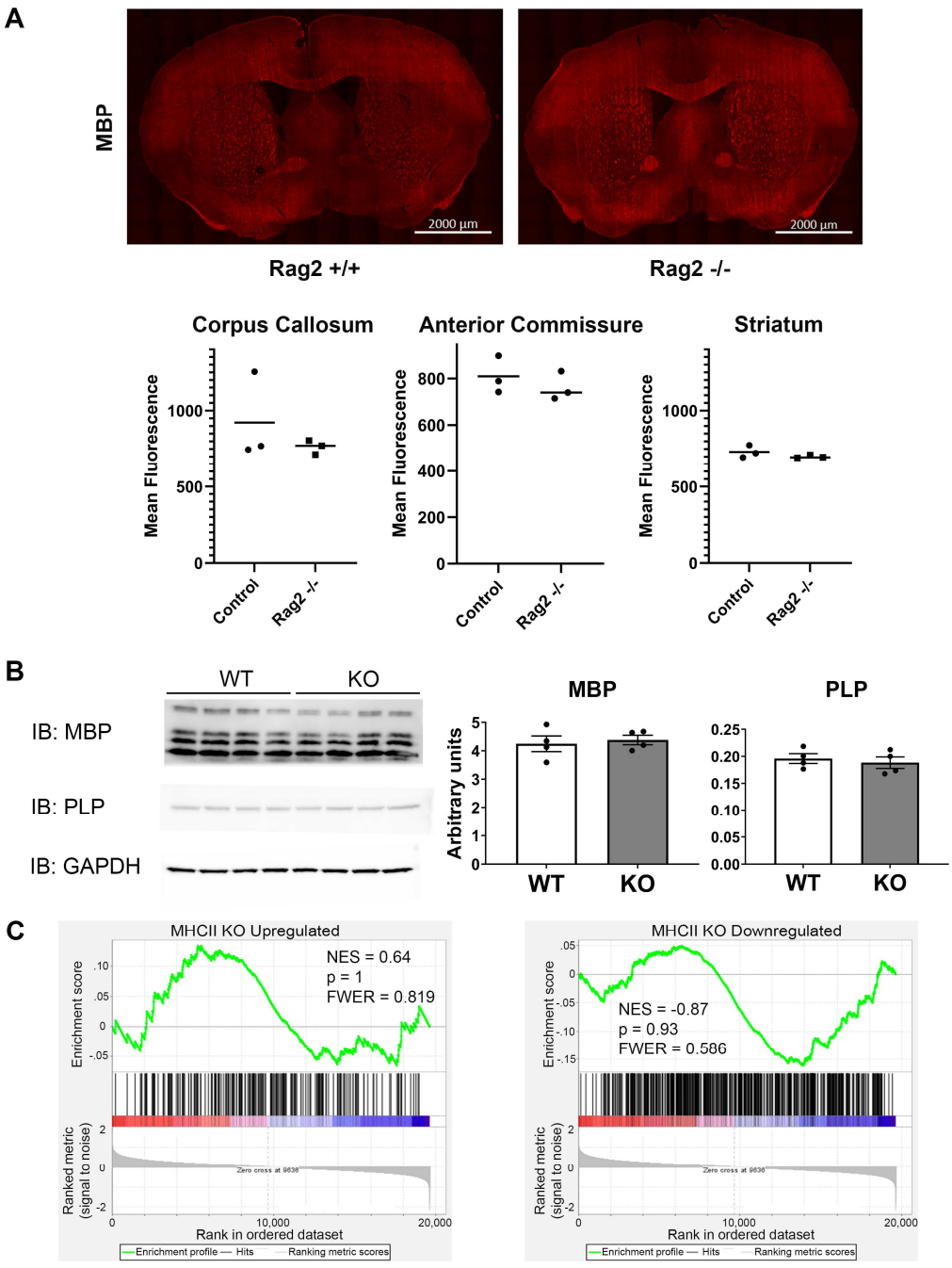

Figure 2-3. Normal myelin proteins and microglial gene signature in Rag2$^{-/-}$ mice. A) Immunostaining of MBP. Top: representative images of MBP immunofluorescence in control (left) and Rag2$^{-/-}$ (right) mice. Bottom: quantification of MBP fluorescence in 3 myelin rich regions; no significant differences. B) Western blots of key myelin proteins MBP and PLP. Left: Images of Western blot of MBP (top), PLP (middle), and reference protein GAPDH (bottom),

Right: Quantification of signal intensity for MBP and PLP, normalized to GAPDH signal. No significant differences. All error bars = SEM. C) GSEA output of genes upregulated (left) or downregulated (right) in MHCII KO microglia reported in Pasciuto 2020. Neither MHCII KO up- nor downregulated genes are significantly enriched in a comparison of $Rag2^{+/+}$ *vs.* $Rag2^{-/-}$ microglia (p = 1, 0.93); NES = normalized enrichment score, FWER = family wise error rate.

2.6 References

1. Kivisakk P, Mahad DJ, Callahan MK, Trebst C, Tucky B, Wei T, et al. Human cerebrospinal fluid central memory CD4+ T cells: evidence for trafficking through choroid plexus and meninges via P-selectin. Proc Natl Acad Sci U S A. 2003;100(14):8389-94. Epub 2003/06/28. doi: 10.1073/pnas.1433000100. PubMed PMID: 12829791; PubMed Central PMCID: PMCPMC166239.
2. Qing Z, Sewell D, Sandor M, Fabry Z. Antigen-specific T cell trafficking into the central nervous system. J Neuroimmunol. 2000;105(2):169-78. Epub 2000/04/01. doi: 10.1016/s0165-5728(99)00265-9. PubMed PMID: 10742559.
3. Alves de Lima K, Rustenhoven J, Kipnis J. Meningeal Immunity and Its Function in Maintenance of the Central Nervous System in Health and Disease. Annu Rev Immunol. 2020;38:597-620. Epub 2020/04/29. doi: 10.1146/annurev-immunol-102319-103410. PubMed PMID: 32340575.
4. Rustenhoven J, Drieu A, Mamuladze T, de Lima KA, Dykstra T, Wall M, et al. Functional characterization of the dural sinuses as a neuroimmune interface. Cell. 2021;184(4):1000-16 e27. Epub 2021/01/29. doi: 10.1016/j.cell.2020.12.040. PubMed PMID: 33508229; PubMed Central PMCID: PMCPMC8487654.
5. Cugurra A, Mamuladze T, Rustenhoven J, Dykstra T, Beroshvili G, Greenberg ZJ, et al. Skull and vertebral bone marrow are myeloid cell reservoirs for the meninges and CNS parenchyma. Science. 2021;373(6553). Epub 2021/06/05. doi: 10.1126/science.abf7844. PubMed PMID: 34083447; PubMed Central PMCID: PMCPMC8863069.
6. Mazzitelli JA, Smyth LCD, Cross KA, Dykstra T, Sun J, Du S, et al. Cerebrospinal fluid regulates skull bone marrow niches via direct access through dural channels. Nat Neurosci. 2022;25(5):555-60. Epub 2022/03/19. doi: 10.1038/s41593-022-01029-1. PubMed PMID: 35301477; PubMed Central PMCID: PMCPMC9081158.

7. Radjavi A, Smirnov I, Derecki N, Kipnis J. Dynamics of the meningeal CD4(+) T-cell repertoire are defined by the cervical lymph nodes and facilitate cognitive task performance in mice. Mol Psychiatry. 2014;19(5):531-3. Epub 2013/06/12. doi: 10.1038/mp.2013.79. PubMed PMID: 23752249; PubMed Central PMCID: PMCPMC3773254.

8. Derecki NC, Cardani AN, Yang CH, Quinnies KM, Crihfield A, Lynch KR, et al. Regulation of learning and memory by meningeal immunity: a key role for IL-4. J Exp Med. 2010;207(5):1067-80. Epub 2010/05/05. doi: 10.1084/jem.20091419. PubMed PMID: 20439540; PubMed Central PMCID: PMCPMC2867291.

9. Herz J, Fu Z, Kim K, Dykstra T, Wall M, Li H, et al. GABAergic neuronal IL-4R mediates T cell effect on memory. Neuron. 2021;109(22):3609-18 e9. Epub 2021/11/19. doi: 10.1016/j.neuron.2021.10.022. PubMed PMID: 34793707; PubMed Central PMCID: PMCPMC9116260.

10. Alves de Lima K, Rustenhoven J, Da Mesquita S, Wall M, Salvador AF, Smirnov I, et al. Meningeal gammadelta T cells regulate anxiety-like behavior via IL-17a signaling in neurons. Nat Immunol. 2020;21(11):1421-9. Epub 2020/09/16. doi: 10.1038/s41590-020-0776-4. PubMed PMID: 32929273; PubMed Central PMCID: PMCPMC8496952.

11. Smith SM, Vale WW. The role of the hypothalamic-pituitary-adrenal axis in neuroendocrine responses to stress. Dialogues Clin Neurosci. 2006;8(4):383-95. Epub 2007/02/13. PubMed PMID: 17290797; PubMed Central PMCID: PMCPMC3181830.

12. Ashwell JD, Lu FW, Vacchio MS. Glucocorticoids in T cell development and function*. Annu Rev Immunol. 2000;18:309-45. Epub 2000/06/03. doi: 10.1146/annurev.immunol.18.1.309. PubMed PMID: 10837061.

13. Chung WS, Clarke LE, Wang GX, Stafford BK, Sher A, Chakraborty C, et al. Astrocytes mediate synapse elimination through MEGF10 and MERTK pathways. Nature.

2013;504(7480):394-400. Epub 2013/11/26. doi: 10.1038/nature12776. PubMed PMID: 24270812; PubMed Central PMCID: PMCPMC3969024.

14. Olsen ML, Sontheimer H. Functional implications for Kir4.1 channels in glial biology: from K+ buffering to cell differentiation. J Neurochem. 2008;107(3):589-601. Epub 2008/08/12. doi: 10.1111/j.1471-4159.2008.05615.x. PubMed PMID: 18691387; PubMed Central PMCID: PMCPMC2581639.

15. Rothstein JD, Dykes-Hoberg M, Pardo CA, Bristol LA, Jin L, Kuncl RW, et al. Knockout of glutamate transporters reveals a major role for astroglial transport in excitotoxicity and clearance of glutamate. Neuron. 1996;16(3):675-86. Epub 1996/03/01. doi: 10.1016/s0896-6273(00)80086-0. PubMed PMID: 8785064.

16. Papouin T, Dunphy JM, Tolman M, Dineley KT, Haydon PG. Septal Cholinergic Neuromodulation Tunes the Astrocyte-Dependent Gating of Hippocampal NMDA Receptors to Wakefulness. Neuron. 2017;94(4):840-54 e7. Epub 2017/05/10. doi: 10.1016/j.neuron.2017.04.021. PubMed PMID: 28479102; PubMed Central PMCID: PMCPMC5484087.

17. Nagai J, Yu X, Papouin T, Cheong E, Freeman MR, Monk KR, et al. Behaviorally consequential astrocytic regulation of neural circuits. Neuron. 2021;109(4):576-96. Epub 2021/01/02. doi: 10.1016/j.neuron.2020.12.008. PubMed PMID: 33385325; PubMed Central PMCID: PMCPMC7897322.

18. Blanco-Suarez E, Liu TF, Kopelevich A, Allen NJ. Astrocyte-Secreted Chordin-like 1 Drives Synapse Maturation and Limits Plasticity by Increasing Synaptic GluA2 AMPA Receptors. Neuron. 2018;100(5):1116-32 e13. Epub 2018/10/23. doi: 10.1016/j.neuron.2018.09.043. PubMed PMID: 30344043; PubMed Central PMCID: PMCPMC6382071.

19. Allen NJ, Bennett ML, Foo LC, Wang GX, Chakraborty C, Smith SJ, et al. Astrocyte glypicans 4 and 6 promote formation of excitatory synapses via GluA1 AMPA receptors.

Nature. 2012;486(7403):410-4. Epub 2012/06/23. doi: 10.1038/nature11059. PubMed PMID: 22722203; PubMed Central PMCID: PMCPMC3383085.

20. Stogsdill JA, Ramirez J, Liu D, Kim YH, Baldwin KT, Enustun E, et al. Astrocytic neuroligins control astrocyte morphogenesis and synaptogenesis. Nature. 2017;551(7679):192-7. Epub 2017/11/10. doi: 10.1038/nature24638. PubMed PMID: 29120426; PubMed Central PMCID: PMCPMC5796651.

21. Vainchtein ID, Chin G, Cho FS, Kelley KW, Miller JG, Chien EC, et al. Astrocyte-derived interleukin-33 promotes microglial synapse engulfment and neural circuit development. Science. 2018;359(6381):1269-73. Epub 2018/02/09. doi: 10.1126/science.aal3589. PubMed PMID: 29420261; PubMed Central PMCID: PMCPMC6070131.

22. Yu X, Taylor AMW, Nagai J, Golshani P, Evans CJ, Coppola G, et al. Reducing Astrocyte Calcium Signaling In Vivo Alters Striatal Microcircuits and Causes Repetitive Behavior. Neuron. 2018;99(6):1170-87 e9. Epub 2018/09/04. doi: 10.1016/j.neuron.2018.08.015. PubMed PMID: 30174118; PubMed Central PMCID: PMCPMC6450394.

23. Anderson MA, Burda JE, Ren Y, Ao Y, O'Shea TM, Kawaguchi R, et al. Astrocyte scar formation aids central nervous system axon regeneration. Nature. 2016;532(7598):195-200. Epub 2016/03/31. doi: 10.1038/nature17623. PubMed PMID: 27027288; PubMed Central PMCID: PMCPMC5243141.

24. Ma Z, Stork T, Bergles DE, Freeman MR. Neuromodulators signal through astrocytes to alter neural circuit activity and behaviour. Nature. 2016;539(7629):428-32. Epub 2016/11/10. doi: 10.1038/nature20145. PubMed PMID: 27828941; PubMed Central PMCID: PMCPMC5161596.

25. Lee JH, Kim JY, Noh S, Lee H, Lee SY, Mun JY, et al. Astrocytes phagocytose adult hippocampal synapses for circuit homeostasis. Nature. 2021;590(7847):612-7. Epub 2020/12/29. doi: 10.1038/s41586-020-03060-3. PubMed PMID: 33361813.

26. Young KM, Psachoulia K, Tripathi RB, Dunn SJ, Cossell L, Attwell D, et al. Oligodendrocyte dynamics in the healthy adult CNS: evidence for myelin remodeling. Neuron. 2013;77(5):873-85. Epub 2013/03/12. doi: 10.1016/j.neuron.2013.01.006. PubMed PMID: 23473318; PubMed Central PMCID: PMCPMC3842597.

27. Bergles DE, Richardson WD. Oligodendrocyte Development and Plasticity. Cold Spring Harb Perspect Biol. 2015;8(2):a020453. Epub 2015/10/23. doi: 10.1101/cshperspect.a020453. PubMed PMID: 26492571; PubMed Central PMCID: PMCPMC4743079.

28. Hill RA, Patel KD, Goncalves CM, Grutzendler J, Nishiyama A. Modulation of oligodendrocyte generation during a critical temporal window after NG2 cell division. Nat Neurosci. 2014;17(11):1518-27. Epub 2014/09/30. doi: 10.1038/nn.3815. PubMed PMID: 25262495; PubMed Central PMCID: PMCPMC4275302.

29. Kang SH, Fukaya M, Yang JK, Rothstein JD, Bergles DE. NG2+ CNS glial progenitors remain committed to the oligodendrocyte lineage in postnatal life and following neurodegeneration. Neuron. 2010;68(4):668-81. Epub 2010/11/26. doi: 10.1016/j.neuron.2010.09.009. PubMed PMID: 21092857; PubMed Central PMCID: PMCPMC2989827.

30. Nimmerjahn A, Kirchhoff F, Helmchen F. Resting microglial cells are highly dynamic surveillants of brain parenchyma in vivo. Science. 2005;308(5726):1314-8. Epub 2005/04/16. doi: 10.1126/science.1110647. PubMed PMID: 15831717.

31. Paolicelli RC, Bolasco G, Pagani F, Maggi L, Scianni M, Panzanelli P, et al. Synaptic pruning by microglia is necessary for normal brain development. Science. 2011;333(6048):1456-8. Epub 2011/07/23. doi: 10.1126/science.1202529. PubMed PMID: 21778362.

32. Schafer DP, Lehrman EK, Kautzman AG, Koyama R, Mardinly AR, Yamasaki R, et al. Microglia sculpt postnatal neural circuits in an activity and complement-dependent

manner. Neuron. 2012;74(4):691-705. Epub 2012/05/29. doi: 10.1016/j.neuron.2012.03.026. PubMed PMID: 22632727; PubMed Central PMCID: PMCPMC3528177.

33. Badimon A, Strasburger HJ, Ayata P, Chen X, Nair A, Ikegami A, et al. Negative feedback control of neuronal activity by microglia. Nature. 2020;586(7829):417-23. Epub 2020/10/02. doi: 10.1038/s41586-020-2777-8. PubMed PMID: 32999463; PubMed Central PMCID: PMCPMC7577179.

34. Squarzoni P, Oller G, Hoeffel G, Pont-Lezica L, Rostaing P, Low D, et al. Microglia modulate wiring of the embryonic forebrain. Cell Rep. 2014;8(5):1271-9. Epub 2014/08/28. doi: 10.1016/j.celrep.2014.07.042. PubMed PMID: 25159150.

35. Block CL, Eroglu O, Mague SD, Smith CJ, Ceasrine AM, Sriworarat C, et al. Prenatal environmental stressors impair postnatal microglia function and adult behavior in males. Cell Rep. 2022;40(5):111161. Epub 2022/08/05. doi: 10.1016/j.celrep.2022.111161. PubMed PMID: 35926455.

36. Cardona AE, Pioro EP, Sasse ME, Kostenko V, Cardona SM, Dijkstra IM, et al. Control of microglial neurotoxicity by the fractalkine receptor. Nat Neurosci. 2006;9(7):917-24. Epub 2006/05/30. doi: 10.1038/nn1715. PubMed PMID: 16732273.

37. Krasemann S, Madore C, Cialic R, Baufeld C, Calcagno N, El Fatimy R, et al. The TREM2-APOE Pathway Drives the Transcriptional Phenotype of Dysfunctional Microglia in Neurodegenerative Diseases. Immunity. 2017;47(3):566-81 e9. Epub 2017/09/21. doi: 10.1016/j.immuni.2017.08.008. PubMed PMID: 28930663; PubMed Central PMCID: PMCPMC5719893.

38. Ulland TK, Song WM, Huang SC, Ulrich JD, Sergushichev A, Beatty WL, et al. TREM2 Maintains Microglial Metabolic Fitness in Alzheimer's Disease. Cell. 2017;170(4):649-63 e13. Epub 2017/08/13. doi: 10.1016/j.cell.2017.07.023. PubMed PMID: 28802038; PubMed Central PMCID: PMCPMC5573224.

39. Gunner G, Cheadle L, Johnson KM, Ayata P, Badimon A, Mondo E, et al. Sensory lesioning induces microglial synapse elimination via ADAM10 and fractalkine signaling. Nat Neurosci. 2019;22(7):1075-88. Epub 2019/06/19. doi: 10.1038/s41593-019-0419-y. PubMed PMID: 31209379; PubMed Central PMCID: PMCPMC6596419.

40. Lee Y, Morrison BM, Li Y, Lengacher S, Farah MH, Hoffman PN, et al. Oligodendroglia metabolically support axons and contribute to neurodegeneration. Nature. 2012;487(7408):443-8. Epub 2012/07/18. doi: 10.1038/nature11314. PubMed PMID: 22801498; PubMed Central PMCID: PMCPMC3408792.

41. Nave KA, Werner HB. Myelination of the nervous system: mechanisms and functions. Annu Rev Cell Dev Biol. 2014;30:503-33. Epub 2014/10/08. doi: 10.1146/annurev-cellbio-100913-013101. PubMed PMID: 25288117.

42. Funfschilling U, Supplie LM, Mahad D, Boretius S, Saab AS, Edgar J, et al. Glycolytic oligodendrocytes maintain myelin and long-term axonal integrity. Nature. 2012;485(7399):517-21. Epub 2012/05/25. doi: 10.1038/nature11007. PubMed PMID: 22622581; PubMed Central PMCID: PMCPMC3613737.

43. Larson VA, Mironova Y, Vanderpool KG, Waisman A, Rash JE, Agarwal A, et al. Oligodendrocytes control potassium accumulation in white matter and seizure susceptibility. Elife. 2018;7. Epub 2018/03/30. doi: 10.7554/eLife.34829. PubMed PMID: 29596047; PubMed Central PMCID: PMCPMC5903864.

44. Mukherjee C, Kling T, Russo B, Miebach K, Kess E, Schifferer M, et al. Oligodendrocytes Provide Antioxidant Defense Function for Neurons by Secreting Ferritin Heavy Chain. Cell Metab. 2020;32(2):259-72 e10. Epub 2020/06/13. doi: 10.1016/j.cmet.2020.05.019. PubMed PMID: 32531201; PubMed Central PMCID: PMCPMC7116799.

45. Saab AS, Tzvetavona ID, Trevisiol A, Baltan S, Dibaj P, Kusch K, et al. Oligodendroglial NMDA Receptors Regulate Glucose Import and Axonal Energy Metabolism. Neuron.

2016;91(1):119-32. Epub 2016/06/14. doi: 10.1016/j.neuron.2016.05.016. PubMed PMID: 27292539; PubMed Central PMCID: PMCPMC9084537.

46. Schirmer L, Mobius W, Zhao C, Cruz-Herranz A, Ben Haim L, Cordano C, et al. Oligodendrocyte-encoded Kir4.1 function is required for axonal integrity. Elife. 2018;7. Epub 2018/09/12. doi: 10.7554/eLife.36428. PubMed PMID: 30204081; PubMed Central PMCID: PMCPMC6167053.

47. Simons M, Nave KA. Oligodendrocytes: Myelination and Axonal Support. Cold Spring Harb Perspect Biol. 2015;8(1):a020479. Epub 2015/06/24. doi: 10.1101/cshperspect.a020479. PubMed PMID: 26101081; PubMed Central PMCID: PMCPMC4691794.

48. Gibson EM, Purger D, Mount CW, Goldstein AK, Lin GL, Wood LS, et al. Neuronal activity promotes oligodendrogenesis and adaptive myelination in the mammalian brain. Science. 2014;344(6183):1252304. Epub 2014/04/15. doi: 10.1126/science.1252304. PubMed PMID: 24727982; PubMed Central PMCID: PMCPMC4096908.

49. Gonzalez H, Elgueta D, Montoya A, Pacheco R. Neuroimmune regulation of microglial activity involved in neuroinflammation and neurodegenerative diseases. J Neuroimmunol. 2014;274(1-2):1-13. Epub 2014/08/06. doi: 10.1016/j.jneuroim.2014.07.012. PubMed PMID: 25091432.

50. Bernaus A, Blanco S, Sevilla A. Glia Crosstalk in Neuroinflammatory Diseases. Front Cell Neurosci. 2020;14:209. Epub 2020/08/28. doi: 10.3389/fncel.2020.00209. PubMed PMID: 32848613; PubMed Central PMCID: PMCPMC7403442.

51. van Langelaar J, Rijvers L, Smolders J, van Luijn MM. B and T Cells Driving Multiple Sclerosis: Identity, Mechanisms and Potential Triggers. Front Immunol. 2020;11:760. Epub 2020/05/28. doi: 10.3389/fimmu.2020.00760. PubMed PMID: 32457742; PubMed Central PMCID: PMCPMC7225320.

52. Stromnes IM, Goverman JM. Passive induction of experimental allergic encephalomyelitis. Nat Protoc. 2006;1(4):1952-60. Epub 2007/05/10. doi: 10.1038/nprot.2006.284. PubMed PMID: 17487182.

53. Iadecola C, Anrather J. The immunology of stroke: from mechanisms to translation. Nat Med. 2011;17(7):796-808. Epub 2011/07/09. doi: 10.1038/nm.2399. PubMed PMID: 21738161; PubMed Central PMCID: PMCPMC3137275.

54. Ratnam NM, Gilbert MR, Giles AJ. Immunotherapy in CNS cancers: the role of immune cell trafficking. Neuro Oncol. 2019;21(1):37-46. Epub 2018/05/18. doi: 10.1093/neuonc/noy084. PubMed PMID: 29771386; PubMed Central PMCID: PMCPMC6303437.

55. Zenaro E, Pietronigro E, Della Bianca V, Piacentino G, Marongiu L, Budui S, et al. Neutrophils promote Alzheimer's disease-like pathology and cognitive decline via LFA-1 integrin. Nat Med. 2015;21(8):880-6. Epub 2015/07/28. doi: 10.1038/nm.3913. PubMed PMID: 26214837.

56. Tansey MG, Wallings RL, Houser MC, Herrick MK, Keating CE, Joers V. Inflammation and immune dysfunction in Parkinson disease. Nat Rev Immunol. 2022;22(11):657-73. Epub 2022/03/06. doi: 10.1038/s41577-022-00684-6. PubMed PMID: 35246670; PubMed Central PMCID: PMCPMC8895080.

57. Oettinger MA, Schatz DG, Gorka C, Baltimore D. RAG-1 and RAG-2, adjacent genes that synergistically activate V(D)J recombination. Science. 1990;248(4962):1517-23. Epub 1990/06/22. doi: 10.1126/science.2360047. PubMed PMID: 2360047.

58. Shinkai Y, Rathbun G, Lam KP, Oltz EM, Stewart V, Mendelsohn M, et al. RAG-2-deficient mice lack mature lymphocytes owing to inability to initiate V(D)J rearrangement. Cell. 1992;68(5):855-67. Epub 1992/03/06. doi: 10.1016/0092-8674(92)90029-c. PubMed PMID: 1547487.

59. Clark SM, Soroka JA, Song C, Li X, Tonelli LH. CD4(+) T cells confer anxiolytic and antidepressant-like effects, but enhance fear memory processes in Rag2(-/-) mice. Stress. 2016;19(3):303-11. Epub 2016/06/15. doi: 10.1080/10253890.2016.1191466. PubMed PMID: 27295202; PubMed Central PMCID: PMCPMC4960826.

60. Clark SM, Vaughn CN, Soroka JA, Li X, Tonelli LH. Neonatal adoptive transfer of lymphocytes rescues social behaviour during adolescence in immune-deficient mice. Eur J Neurosci. 2018;47(8):968-78. Epub 2018/02/13. doi: 10.1111/ejn.13860. PubMed PMID: 29430738; PubMed Central PMCID: PMCPMC5902418.

61. Larocque D, Pilotte J, Chen T, Cloutier F, Massie B, Pedraza L, et al. Nuclear retention of MBP mRNAs in the quaking viable mice. Neuron. 2002;36(5):815-29. Epub 2002/12/07. doi: 10.1016/s0896-6273(02)01055-3. PubMed PMID: 12467586.

62. Pasciuto E, Burton OT, Roca CP, Lagou V, Rajan WD, Theys T, et al. Microglia Require CD4 T Cells to Complete the Fetal-to-Adult Transition. Cell. 2020;182(3):625-40 e24. Epub 2020/07/24. doi: 10.1016/j.cell.2020.06.026. PubMed PMID: 32702313.

63. Zhang Y, Chen K, Sloan SA, Bennett ML, Scholze AR, O'Keeffe S, et al. An RNA-sequencing transcriptome and splicing database of glia, neurons, and vascular cells of the cerebral cortex. J Neurosci. 2014;34(36):11929-47. Epub 2014/09/05. doi: 10.1523/JNEUROSCI.1860-14.2014. PubMed PMID: 25186741; PubMed Central PMCID: PMCPMC4152602.

64. Zhang Y, Sloan SA, Clarke LE, Caneda C, Plaza CA, Blumenthal PD, et al. Purification and Characterization of Progenitor and Mature Human Astrocytes Reveals Transcriptional and Functional Differences with Mouse. Neuron. 2016;89(1):37-53. Epub 2015/12/22. doi: 10.1016/j.neuron.2015.11.013. PubMed PMID: 26687838; PubMed Central PMCID: PMCPMC4707064.

65. Dobin A, Davis CA, Schlesinger F, Drenkow J, Zaleski C, Jha S, et al. STAR: ultrafast universal RNA-seq aligner. Bioinformatics. 2013;29(1):15-21. Epub 2012/10/30. doi:

10.1093/bioinformatics/bts635. PubMed PMID: 23104886; PubMed Central PMCID: PMCPMC3530905.

66. Anders S, Pyl PT, Huber W. HTSeq--a Python framework to work with high-throughput sequencing data. Bioinformatics. 2015;31(2):166-9. Epub 2014/09/28. doi: 10.1093/bioinformatics/btu638. PubMed PMID: 25260700; PubMed Central PMCID: PMCPMC4287950.

67. Love MI, Huber W, Anders S. Moderated estimation of fold change and dispersion for RNA-seq data with DESeq2. Genome Biol. 2014;15(12):550. Epub 2014/12/18. doi: 10.1186/s13059-014-0550-8. PubMed PMID: 25516281; PubMed Central PMCID: PMCPMC4302049.

68. Szklarczyk D, Gable AL, Nastou KC, Lyon D, Kirsch R, Pyysalo S, et al. The STRING database in 2021: customizable protein-protein networks, and functional characterization of user-uploaded gene/measurement sets. Nucleic Acids Res. 2021;49(D1):D605-D12. Epub 2020/11/26. doi: 10.1093/nar/gkaa1074. PubMed PMID: 33237311; PubMed Central PMCID: PMCPMC7779004.

69. Mootha VK, Lindgren CM, Eriksson KF, Subramanian A, Sihag S, Lehar J, et al. PGC-1alpha-responsive genes involved in oxidative phosphorylation are coordinately downregulated in human diabetes. Nat Genet. 2003;34(3):267-73. Epub 2003/06/17. doi: 10.1038/ng1180. PubMed PMID: 12808457.

70. Subramanian A, Tamayo P, Mootha VK, Mukherjee S, Ebert BL, Gillette MA, et al. Gene set enrichment analysis: a knowledge-based approach for interpreting genome-wide expression profiles. Proc Natl Acad Sci U S A. 2005;102(43):15545-50. Epub 2005/10/04. doi: 10.1073/pnas.0506580102. PubMed PMID: 16199517; PubMed Central PMCID: PMCPMC1239896.

71. Madsen L, Labrecque N, Engberg J, Dierich A, Svejgaard A, Benoist C, et al. Mice lacking all conventional MHC class II genes. Proc Natl Acad Sci U S A. 1999;96(18):10338-43.

Epub 1999/09/01. doi: 10.1073/pnas.96.18.10338. PubMed PMID: 10468609; PubMed Central PMCID: PMCPMC17889.

72. Schneider CA, Rasband WS, Eliceiri KW. NIH Image to ImageJ: 25 years of image analysis. Nat Methods. 2012;9(7):671-5. Epub 2012/08/30. doi: 10.1038/nmeth.2089. PubMed PMID: 22930834; PubMed Central PMCID: PMCPMC5554542.

73. Clements CS, Reid HH, Beddoe T, Tynan FE, Perugini MA, Johns TG, et al. The crystal structure of myelin oligodendrocyte glycoprotein, a key autoantigen in multiple sclerosis. Proc Natl Acad Sci U S A. 2003;100(19):11059-64. Epub 2003/09/10. doi: 10.1073/pnas.1833158100. PubMed PMID: 12960396; PubMed Central PMCID: PMCPMC196926.

74. Lv SY, Zhou YC, Zhang XM, Chen WD, Wang YD. Emerging Roles of NPQ/Spexin in Physiology and Pathology. Front Pharmacol. 2019;10:457. Epub 2019/05/28. doi: 10.3389/fphar.2019.00457. PubMed PMID: 31133851; PubMed Central PMCID: PMCPMC6514225.

75. Munoz JJ, Anauate AC, Amaral AG, Ferreira FM, Watanabe EH, Meca R, et al. Ppia is the most stable housekeeping gene for qRT-PCR normalization in kidneys of three Pkd1-deficient mouse models. Sci Rep. 2021;11(1):19798. Epub 2021/10/07. doi: 10.1038/s41598-021-99366-x. PubMed PMID: 34611276; PubMed Central PMCID: PMCPMC8492864.

76. Bin JM, Harris SN, Kennedy TE. The oligodendrocyte-specific antibody 'CC1' binds Quaking 7. J Neurochem. 2016;139(2):181-6. Epub 2016/07/28. doi: 10.1111/jnc.13745. PubMed PMID: 27454326.

77. Krawczyk MC, Haney JR, Pan L, Caneda C, Khankan RR, Reyes SD, et al. Human Astrocytes Exhibit Tumor Microenvironment-, Age-, and Sex-Related Transcriptomic Signatures. J Neurosci. 2022;42(8):1587-603. Epub 2022/01/07. doi:

10.1523/JNEUROSCI.0407-21.2021. PubMed PMID: 34987109; PubMed Central PMCID: PMCPMC8883850.

78. Radjavi A, Smirnov I, Kipnis J. Brain antigen-reactive CD4+ T cells are sufficient to support learning behavior in mice with limited T cell repertoire. Brain Behav Immun. 2014;35:58-63. Epub 2013/09/10. doi: 10.1016/j.bbi.2013.08.013. PubMed PMID: 24012647; PubMed Central PMCID: PMCPMC3858511.

Chapter 3

Serpin E2 Regulates Antimicrobial Gene Expression by Microglia

3.1 Abstract

Microglia are the brain-resident immune cells responsible for surveilling and protecting the central nervous system. These cells can express a wide array of immune genes, and that expression can become highly dynamic in response to changes in the environment, such as traumatic injury or neurological disease. Though microglial immune responses are well studied, we still do not know many mechanisms and regulators underlying all the varied microglial responses. Serpin E2 is a serine protease inhibitor that acts on a wide variety of serine proteases, with particularly potent affinity for the blood clotting enzyme thrombin. In the brain, Serpin E2 is highly expressed by many cell types, especially glia, and loss of Serpin E2 leads to behavioral changes as well as deficits in synaptic plasticity. To determine whether Serpin E2 is important for maintaining homeostasis in glia, we performed RNA sequencing of microglia and astrocytes from Serpin E2-deficient mice in a healthy state or under immune activation due to lipopolysaccharide (LPS) injection. We found that microglia in Serpin E2-deficient mice had higher expression of antimicrobial genes, while astrocytes did not display any robust changes in transcription. Furthermore, the lack of Serpin E2 did not affect transcriptional responses to LPS in either microglia or astrocytes. Overall, we find that Serpin E2 is a regulator of antimicrobial genes in microglia.

3.2 Introduction

As the resident immune cells of the brain, microglia play indispensable roles in immune surveillance and defense in the central nervous system. Accordingly, microglia can dynamically express a broad array of antimicrobial genes to initiate and mount an immune response. While we often refer to microglia as “activated” or “reactive” while undergoing an inflammatory response, there are myriad genes and pathways involved and which change based on the particular environmental stimuli[1-4]. Given the underlying diversity of microglial responses to pathology, it is important to untangle these responses and identify underlying regulatory mechanisms that control specific portions of the immune response. While much is known about

the innate immune functions including antimicrobial functions of microglia, the signals that regulate the expression of antimicrobial genes by microglia remain largely unidentified.

Serpin Family E Member 2 (Serpin E2, aka Protease-Nexin 1/PN1 or Glia-derived Nexin 1) is a serine protease inhibitor that can inhibit a number of enzymes[5-9]. In mice, it has particularly high RNA expression in the brain across most major cell types, including microglia, astrocytes, neurons, oligodendrocyte-lineage cells, and endothelial cells[10, 11]. Transgenic mice overexpressing Serpin E2 in neurons or lack Serpin E2 entirely develop epileptic activity *in vivo* and *in vitro*[12]. Overexpressing mice showed increases in long-term potentiation in the hippocampus, while deficient mice showed a reduction[12]. Serpin E2-deficient mice also showed a deficit in fear extinction after learning to associate a tone with a foot shock, as well as reduced availability of NR1 subunits in NMDA receptors, suggesting a potential NMDA-dependent mechanism underlying the behavioral changes[13, 14].

The mechanisms of Serpin E2 activity in the brain are complex and likely multifaceted. As Serpin E2 can act on several serine proteases, it may modulate the activity of many cellular signaling pathways [15]. Serpin E2 is a particularly potent inhibitor of thrombin, a key molecule in the formation of blood clots[5]. Thrombin also participates in other forms of signaling, including binding with the thrombin receptor PAR1. Experimental activation of PAR1 has been shown to induce amnesia and reduce LTP in hippocampal slices[16]. Other studies observed that the loss of Serpin E2 led to upregulation of Sonic hedgehog target genes *in vivo*[17]. In a cancer model, Serpin E2 may promote invasiveness via MMP9 and receptor LRP1 activity[18]. Taken together, Serpin E2 is a versatile protein with great potential to regulate a number of cellular processes.

Serpin E2-overexpressing mice under the Thy1 promoter demonstrate a functional role of neuronal Serpin E2, but the *Serpine2* gene is more highly expressed among glia[10, 11]. Whether and how Serpin E2 impacts glial cells is unknown. In this study, we use *Serpine2* deficient mice to examine the impact of Serpin E2 on the transcriptome of astrocyte and

microglia in healthy and reactive states. We purified microglia and astrocytes from *Serpine2* deficient and control mice undergoing inflammatory responses to lipopolysaccharide (LPS) injection and mice who received a control saline injection. Upon RNA sequencing and subsequent analysis, we found that loss of *Serpine2* results in the upregulation of numerous antimicrobial genes in microglia. Astrocytes did not show appreciable *Serpine2*-dependent changes in transcription, nor did *Serpine2* deficiency result in robust changes in LPS-induced gene expression. Overall, we identify Serpin E2 as a regulator of antimicrobial genes in microglia, without altering astrocyte transcription or glial responses to inflammatory stimuli.

3.3 Materials and Methods

Experimental animals

All animals were used in compliance with the Animal Research Committee at the University of California, Los Angeles (UCLA) under the approved protocol #R-16-080. We obtained *Serpine2*$^{-/-}$ mice from the lab of Dr. Thomas Mariani at the University of Rochester. We injected two cohorts of mice with 10 mg/kg lipopolysaccharides (LPS) or a control saline solution (Sigma L6529). Both cohorts consisted of 12 mice, where mice differed by genotype (*Serpine2*$^{+/+}$ vs. *Serpine2*$^{-/-}$) and treatment (LPS *vs.* saline), resulting in 4 treatment groups with 3 mice per group. The microglia cohort was approximately 1 month old and received IP injections 48 hours before purifying and harvesting microglia RNA. The astrocyte cohort was approximately 2 months old and received IP injections 24 hours before purifying and harvesting astrocyte RNA. The microglia and astrocyte cohorts consisted of 7 males, 5 females and 8 males, 4 females respectively. 30- and 60-day old mice were also used to perform immunostaining of microglia, detailed under “Immunohistochemistry”.

Purification of microglia and astrocytes

We purified microglia and astrocytes using two distinct approaches. For microglia, we followed a previously published protocol using douncing and immunopanning that aimed to

minimize microglial reactive response to the brain dissociation process[19]. Animals received transcardiac perfusions of ice-cold DPBS (Fisher 14-040-182) for 10 minutes to remove blood cells from the brain. After harvesting the whole brain, we removed olfactory bulbs before roughly chopping the tissue and douncing on ice in DPBS supplemented with DNase I (Worthington LS002007). To remove myelin debris, we brought the dounced cell suspension to 25 mL in a 20% Percoll solution (GE Healthcare 17-0891-01). We spun down the cell suspension for 15 minutes at 500 g and 4°C to isolate and remove myelin debris. Cells were resuspended in DPBS with 2 mg/mL milk peptone solids (Sigma P6838). The cell suspension was incubated for 20 minutes at room temperature on a plastic petri dish coated with anti-CD11b antibody to bind microglia (Biolegend 101202). The dish was washed with PBS and the cells were immediately scraped off the dish using 700 µL TRIzol (ThermoFisher 15596018), which was flash frozen using liquid nitrogen and stored at -80°C.

For astrocytes, we utilized our standard immunopanning protocol. Briefly, we dissected out the cerebral cortex (a large region with relatively little myelin debris), roughly chopped the tissue and incubated it for 45 minutes in a papain solution (12 u/mL, Worthington LS003126) while heated to 34.5°C. Digestion was halted using a trypsin ovomucoid inhibitor (Worthington LS003086), and tissue was further digested using mechanical trituration with a serological pipette. The resulting solution was passed through a Nitex filter and spun down at 300 g for 5 minutes. Cells were resuspended in DPBS and incubated on a series of antibody-coated petri dishes. The cell suspension was incubated on a series of dishes for 10 mins each: anti-CD45 x2-3 to remove microglia (BD Biosciences 550539), anti-O4 hybridoma supernatant x2-3 to remove oligodendrocyte progenitors, and anti-GalC hybridoma supernatant x2-3 to remove oligodendrocytes. Finally, the astrocyte-enriched cell suspension was passed to an anti-HepaCAM dish to pull down astrocytes (R&D Systems MAB4108), and it was incubated at room temperature for 20 minutes. The dish was rinsed with PBS, and astrocytes were scraped off the dish with 700 µL TRIzol and immediately flash frozen in liquid nitrogen.

RNA-sequencing library construction and sequencing

RNA was purified from TRIzol lysates using the Qiagen miRNeasy kit (Qiagen 217004) according to the manufacturer's protocol. Purified RNA was converted to cDNA using the Ovation RNAseq System V2 (Nugen 7102-32), specifically designed for low input. We fragmented the cDNA using a Covaris S220 focused-ultrasonicator (Covaris 500217), and final libraries were constructed using the NEB Next Ultra RNA Library Prep Kit (New England Biolabs E7530S) along with appropriate indexing primers (NEB E7335S). Libraries from the same cell type were pooled and sequenced together on an Illumina NovaSeq 600 System to obtain paired-end 50 bp reads. The sequenced libraries had 40M ± 13M (s.d.) reads per microglia sample and 38M ± 8.7M reads per astrocyte sample.

Read alignment and quantification

Sequencing data was demultiplexed and aligned to the mouse genome (astrocytes: GRCm38, release 100, microglia: GRCm39, release 103) using the program STAR (astrocytes: v2.6.0c, microglia: 2.7.8a)[20]. Microglia samples had 80.0% ± 2.1 (s.d.) uniquely aligned reads, and astrocyte samples had 69.1% ± 6.6 uniquely aligned reads. After alignment, we obtained read counts using HTSeq v0.13.5 in RStudio[21]. Full RNA-seq expression data can be found in the supplemental information (SI 3-1).

Differential gene expression analysis with DESeq2

We performed differential gene expression (DGE) analysis in RStudio using the DESeq2 package (v1.26.0)[22]. For both astrocytes and microglia, we analyzed all samples from the same cell type together using a linear model that included terms for genotype (wild-type or *Serpine2*$^{-/-}$) and treatment (LPS or saline). For microglia, we also included a term for sex (male or female) and RNA integrity, as measured by the 2200 TapeStation System (Agilent G2964AA) and the RNA high sensitivity assay (Agilent 5067-5579). The resulting analyses of differentially expressed genes associated with genotype and LPS can be found in supplemental information (SI 3-2).

Gene set enrichment analysis (GSEA)

We performed gene set enrichment analysis using GSEA software version 4.2.3 downloaded from www.gsea-msigdb.org [23]. We used the default settings, with the following specifications. We input gene counts that were normalized using the estimateSizeFactors() and counts() functions from the DESeq2 package v1.26.0. Based on our DGE results, we compared saline-injected wild-type and mutant mice to find transcriptional patterns associated with *Serpine2*. We used all gene ontology (GO) datasets that were built into the GSEA software (c5.all.v7.5.1).

Data deposition

We will deposit all gene expression data to the Gene Expression Omnibus when this work is submitted as a peer-reviewed manuscript.

Immunohistochemistry

Mice received transcardial perfusions of PBS (10 mins) followed by 4% paraformaldehyde (10 mins). Brains were post-fixed in 4% PFA overnight at 4°C before being stored in 30% sucrose for 1-2 nights at 4°C until brains sank. Brains were embedded in OCT compound (Fisher Scientific 23-730-571) and sectioned at 30 μm thickness and stored as free-floating sections at 4°C prior to staining and mounting. For immunostaining, sections were blocked and permeabilized with a blocking solution (0.2% Triton X-100 and 10% donkey serum in PBS) for one hour at room temperature, and then slides were incubated in similar blocking solution with primary antibodies overnight at 4°C (0.5% Triton X-100 for Iba1, 0.05% Triton X-100 for P2ry12 and 10% donkey serum in PBS). The following day, primary antibodies were washed off with PBS, and sections were incubated with secondary antibodies in blocking solution for 90 minutes at room temperature. Slices were mounted onto Superfrost Plus slides (Fisher Scientific 12-550-15) and coverslipped with a DAPI-containing media. Primary antibodies: anti-Iba1 (1:200 AbCam ab5076), anti-P2ry12 (1:500 Anaspec AS-55043A);

Secondary antibodies: Donkey anti-rabbit 488 (1:1000 Life Technologies A21206), dokey anti-goat 488 (1:1000 Life Technologies A11055).

Iba1 and P2ry12 staining was performed with 3 pairs of mice at P30 and 3 pairs of mice at P60, and images were acquired in the cerebral cortex using a confocal microscope using a 20x lens. Signal intensity of Iba1 and P2ry12 was measured with the resulting images in ImageJ after masking with a manual binary threshold to eliminate background. We further quantified aspects of microglial morphology using images of P2ry12 staining in 3 pairs of mice at P60. Images were analyzed using the “filaments” function in Imaris software. Following automatic detection of processes, "over-detected" filaments that did not represent microglial processes were manually deleted. Measurements of process number and length were quantified and exported for statistical analysis.

Statistics

Statistical analyses for immunohistochemistry were performed using either R or Excel, using Welch’s t-test. Statistical analysis of differential gene expression was carried out within the DESeq2 package, and gene set enrichment analysis was performed using GSEA software v4.3.2, as previously described.

3.4 Results

Transcriptome profiling of microglia and astrocytes from Serpine2$^{-/-}$ mice

To examine how the loss of *Serpine2* may impact the transcriptome of astrocytes and microglia, we obtained and bred a colony of *Serpine2* knockout mice. We bred sibling pairs of 1 month (microglia) or 2 month (astrocyte) old mice consisting of a *Serpine2*$^{-/-}$ mouse and a *Serpine2*$^{+/+}$ or *Serpine2*$^{+/-}$ littermate. Of the 6 pairs collected per cell type, half were injected with saline while the other half were given injections of lipopolysaccharides (LPS) to induce systemic inflammation. This allowed us to ask not only whether *Serpine2* impacts homeostatic

transcription but also whether *Serpine2* is required for the robust inflammatory responses that microglia and astrocytes normally exhibit in response to LPS [24, 25].

We acutely harvested microglia through a combination of douncing and immunopanning (Fig 3-1A, top). Microglia can rapidly alter their transcription during cell purification protocols in a temperature dependent manner[26]. To combat technical artifacts, we performed most of the cell extraction over ice with pre-chilled reagents. Mice were perfused and dissected using ice-cold PBS. Then, tissue was dounced over ice, which results in the death of most brain cell types while preserving microglia. Myelin debris was removed by spinning the cell suspension down through a Percoll solution at 4°C. Finally, the cell suspension was passed over a petri dish coated with a microglia-binding antibody Cd11b. RNA was harvested from the bound microglia using TRIzol, which was followed by sequencing.

For astrocytes, we acutely purified cells using an immunopanning method (Fig 3-1A, bottom). We dissected out the cerebral cortex to exclude myelin rich regions and improve purification. Tissue was then enzymatically digested in papain before mechanical trituration to create a single-cell suspension. We passed the cell suspension over a series of antibody-coated petri dishes to remove unwanted cell types (microglia, oligodendrocyte progenitor cells, and oligodendrocytes), and we pulled down astrocytes on a dish covered with an astrocyte-binding antibody for HepaCAM. As with the microglia samples, RNA was harvested using TRIzol, purified, and sequenced for analysis.

Serpine2$^{-/-}$ microglia upregulate antimicrobial genes

After sequencing, we performed differential gene expression analysis of *Serpine2$^{-/-}$* microglia using the DESeq2 package in R. When comparing *Serpine2$^{-/-}$* microglia to controls, we found numerous genes upregulated in *Serpine2*-deficient microglia, in addition to the highly significant downregulation of *Serpine2* itself. There were 12 protein-coding genes differentially expressed, and all of them had higher transcription in *Serpine2$^{-/-}$* compared to controls (Fig 3-2A, SI 3-2). Among these genes was *Lyz2*, which codes for an enzyme that damages bacterial

cell walls to promote lysis and eliminate microbes[27, 28]. *Hp* is another upregulated gene that encodes a protein with antibacterial properties, haptoglobin. Haptoglobin binds hemoglobin and therefore acts as an iron scavenger that impairs bacterial survival[29]. *Seprine2*$^{-/-}$ microglia also increased transcription of *Lgals3*, which encodes Galectin 3, yet another protein with noted antimicrobial activity. One proposed mechanism of action is that Galectin 3 mediates the destruction of pathogen containing vacuoles where microbes sometimes propagate within a host cell[30]. *S100a8* encodes a protein that forms a heterodimer with S100A9 with antimicrobial properties named calprotectin[31]. *Camp* encodes cathelicidin antimicrobial peptide, which is a member of the cathelicidin family of proteins known primarily for their capacity to kill microbes[32, 33]. Lastly, *Serpine2*$^{-/-}$ mice also upregulate *Clec4e*, the gene encoding the protein Mincle which binds microbial ligands and helps initiate the activation of antigen presenting cells[34].

While examining differentially expressed genes individually, we clearly observed repeated annotations of antibacterial activity among these upregulated genes. To better describe this pattern with an unbiased approach, we performed Gene Set Enrichment Analysis (GSEA)[23]. GSEA uses all the expression data from control and knockout microglia to test whether various pathways are up- or down-regulated. We tested our data against a over 15,000 ontology gene sets, and we found that *Serpine2*$^{-/-}$ microglia show greater expression of 21 gene sets (FDR = 0.05), while no gene sets demonstrated higher expression in control microglia (Fig 3-2B, SI 3-3).

All the significant gene sets pertaining to biological processes concerned immune and antimicrobial responses, e.g. defense response to bacterium (Fig 3-2C), antibacterial humoral response, immune response in mucosa. This directly aligns with the results of our differential gene expression analysis, which also identified upregulation of antimicrobial genes in transgenic microglia. With the combined results of these analyses, we found that microglia have increased transcription of antimicrobial genes in the absence of Serpin E2.

Microglia are known to make distinct morphological changes when they are reactive, such as thicker and shorter processes[35]. To test whether changes in immune response genes we observed had corresponding changes in morphology, we performed immunostaining of canonical microglial markers Iba1 and P2ry12 (Fig 3-3A,C). We found no difference in the average intensity or area of Iba1 staining ($p = 0.95$) or P2ry12 staining ($p = 0.87$, Fig 3-3B&D). We used P2ry12 staining to quantify aspects of microglial morphology, namely branch number ($p = 0.51$) and branch length ($p = 0.88$, Fig 3-3D). None of these measures showed differences in transgenic mice compared to controls, indicating that *Serpine2* is dispensable for microglial morphology.

Astrocyte transcriptome is unchanged in the absence of Serpine2

Using a similar methodology, we also employed DESeq2 to identify differential gene expression in astrocytes from *Serpine2*$^{-/-}$ vs. control mice. In this comparison, there was only one gene that showed differential expression, aside from the highly significant downregulation of *Serpine2* (Fig 3-1A). However, this gene, *Scg2*, is only lowly expressed in astrocytes and much more highly expressed in neurons[10, 11]. Therefore, we did not find evidence that astrocytes alter their transcriptomes in the absence of Serpin E2. This is somewhat surprising, given that we previously found astrocytes highly express *Serpine2*[10, 11].

Microglia and astrocytes respond robustly to LPS in the absence of Serpine2

Microglia and astrocytes are two important classes of glia that are known for their abilities to dynamically change state in response to environmental stimuli. This is a well-studied phenomenon variously referred to as “activation” or “reactivity”[35]. Whether or not Serpin E2 played an important role in these cells during homeostasis, it is also critical to know whether it modulates their responses to pathological conditions. To test this question, we induced a systemic inflammatory response in *Serpine2*$^{-/-}$ and control animals with injections of lipopolysaccharides, which are major surface components of many bacteria that trigger a robust response.

Differential gene expression analysis found that LPS successfully induced large transcriptomic changes in both astrocytes and microglia, as expected (Fig 3-1A). Microglia had over 800 differentially expressed gene entries, while astrocytes had over 2,000. However, when we looked among LPS-treated animals and compared *Serpine2*$^{-/-}$ to controls, we saw virtually no evidence that Serpin E2 regulates glial responses to LPS. LPS-treated astrocytes showed no differential expression associated with genotype, other than *Serpine2* itself. LPS-treated microglia showed a short list of genes associated with genotype, though only three entries were protein-coding and all had very low levels of gene expression (SI 3-2). Additionally, none of these genes were among the genes that were associated with genotype in our previous analysis of microglia. Taken together, we find that the loss of *Serpine2* can alter gene expression by microglia in the healthy brain, but it does not change microglial or astrocytic responses to inflammatory stimuli, at least under the conditions we tested.

3.5 Discussion

We collected and analyzed transcriptomic data from mice lacking the gene for the serine protease Serpin E2. We examined both microglia and astrocytes, two major populations of glia with appreciable expression of this gene. Through differential gene expression analysis, we found that microglia increase the expression of numerous antimicrobial genes, and we further confirmed this pattern in a follow-up analysis using GSEA. Gross microglial morphology did not accompany these changes. Despite our previous observation that *Serpine2* was expressed highly in astrocytes, *Serpine2*$^{-/-}$ astrocytes did not change in gene expression[10, 11, 36]. Furthermore, astrocytes and microglia could both become reactive in response to an inflammatory stimulus, but the presence or absence of *Serpine2* did not affect these responses. Taken together, these findings demonstrate that *Serpine2* expression is a regulator of antimicrobial genes in microglia in the healthy brain, but not an important regulator of astrocyte transcription or glial responses to inflammatory stimuli.

Microglia in Serpine2$^{-/-}$ mice

In our previous studies, microglia appeared to have lower *Serpine2* expression when compared with astrocytes in both mouse and human tissue[10, 11]. Interestingly, this study finds that microglia do in fact upregulate numerous genes in the absence of *Serpine2*. A clear majority of them are involved in immune responses, particularly antimicrobial responses (*Lyz2*, *Hp*, *Lgals3, S100a8, Camp, Clec4e*). This pattern was further demonstrated by GSEA, which found a number of immune response pathways upregulated in *Serpine2*$^{-/-}$ microglia, particularly pathways associated with antimicrobial responses (defense response to bacterium, antibacterial humoral response, etc.) Based on these data, we conclude that *Serpine2* is a regulator of antimicrobial genes in microglia.

Further experimentation demonstrated the limitations of *Serpine2*'s influence in microglia. Microglia did not change in morphology or expression of two major markers, P2ry12 and Iba1. This refutes the idea that these microglia are partially reactive, or "primed", despite the increased expression of several immune response genes. In fact, the presence of *Serpine2* failed to affect the transcription of immune response genes in microglia after we induced systemic inflammation with LPS. Therefore, *Serpine2* is not a necessary component of microglial LPS responses, which are multifaceted and arise through many other signaling pathways. Nevertheless, we have found that *Serpine2* is capable of exerting an influence on microglia through a mechanism that remains unclear. It is possible that *Serpine2* plays a more substantial role in regulating microglial responses in other contexts not explored in this study, such as development, where microglia play vital roles in refining neuronal circuitry[37, 38]. Indeed, some evidence already suggests that *Serpine2* affects neuronal progenitor proliferation in this epoch[39].

Astrocytes in Serpine2$^{-/-}$ mice

This study did not find evidence that astrocyte transcription is altered by the presence or absence of *Serpine2*. Given the high expression of this gene in our previous astrocyte studies,

this came as a surprise[10, 11]. We also previously reported that *Serpine2* itself was dynamically expressed in human astrocytes in a tumor context, so we hypothesized that *Serpine2* might play some part in astrocyte reactivity[36]. Interestingly, there was no gene expression associated with the loss of *Serpine2*, even when astrocytes did show a robust response to an inflammatory stimulus.

This raises the question of the function of *Serpine2* transcription in astrocytes. Importantly, Serpin E2 is a secreted molecule and it is expressed by many cell types in the brain, so astrocytes may produce Serpin E2 for it to act elsewhere in the brain. As Serpin E2 is a potent thrombin inhibitor involved in the blood clotting pathway, and astrocytic endfeet line blood vessels of the brain, perhaps expression of *Serpine2* is a preemptory strategy for addressing potential brain bleeds[40]. It would be interesting for future studies to assess whether *Serpine2* expression in astrocytes plays a role in hemorrhagic stroke responses.

Overall, this present study elucidates aspects of microglial biology as well as providing further knowledge of a protein that is ubiquitously transcribed in the brain. Our findings show that *Serpine2* regulates the expression of antimicrobial genes in microglia. It also describes limits to the influence of *Serpine2*, which is important knowledge given the broad expression and myriad protein-protein interactions of the Serpin E2 protein in the brain. At the same time, we have uncovered a novel regulator of immune response genes in microglia, and these discoveries will in turn increase our knowledge of neuroimmune interactions and ultimately the roles of microglia in neuropathology.

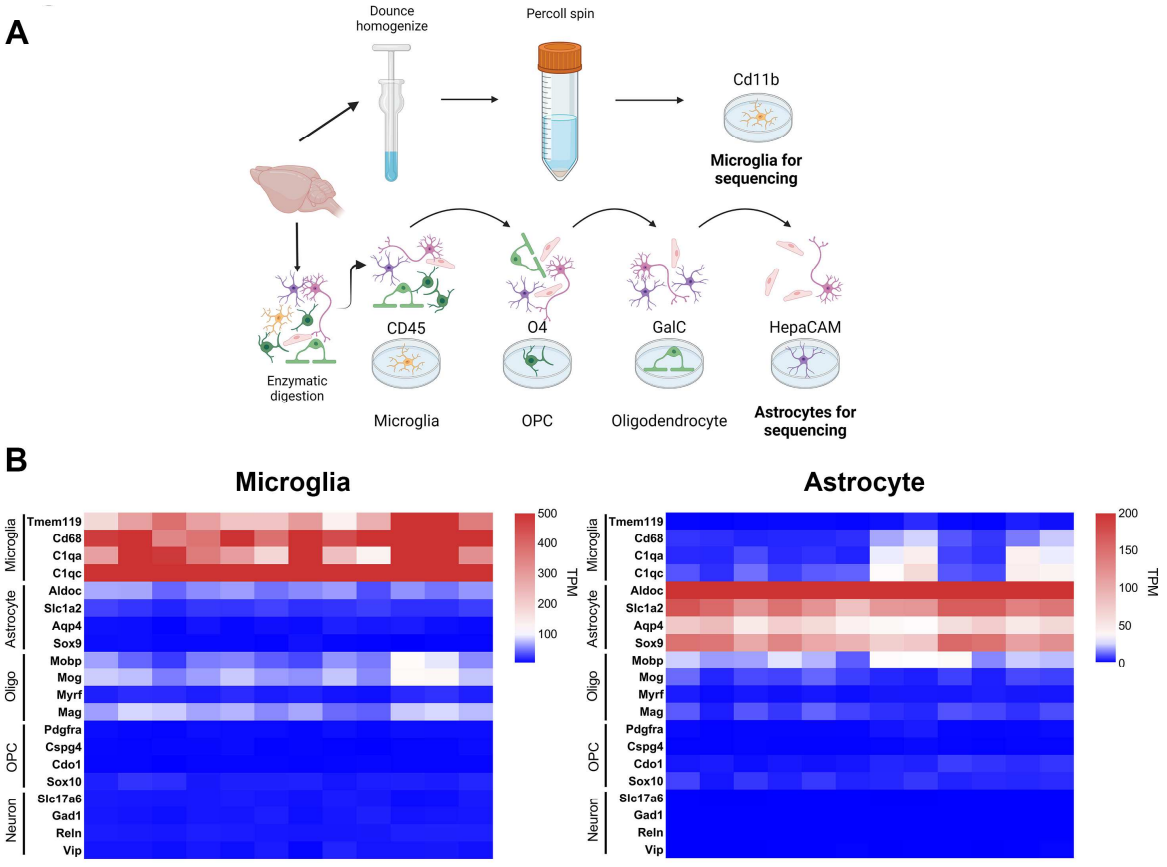

Figure 3-1. Acute purification of microglia and astrocytes from *Serpine2*$^{-/-}$ mice. A) Cell purification schematic; top: microglia were collected with a combination of douncing and immunopanning with anti-Cd11b antibody, bottom: astrocytes were collected with an enzymatic digestion followed by immunopanning that depleted other cell types before binding astrocytes using anti-HepaCAM antibody. B) Heatmap of brain cell-specific markers (rows) detected in immunopanning purified microglia (left) and astrocytes (right) as determined by RNA-sequencing; gene expression is quantified as Transcripts per Million (TPM).

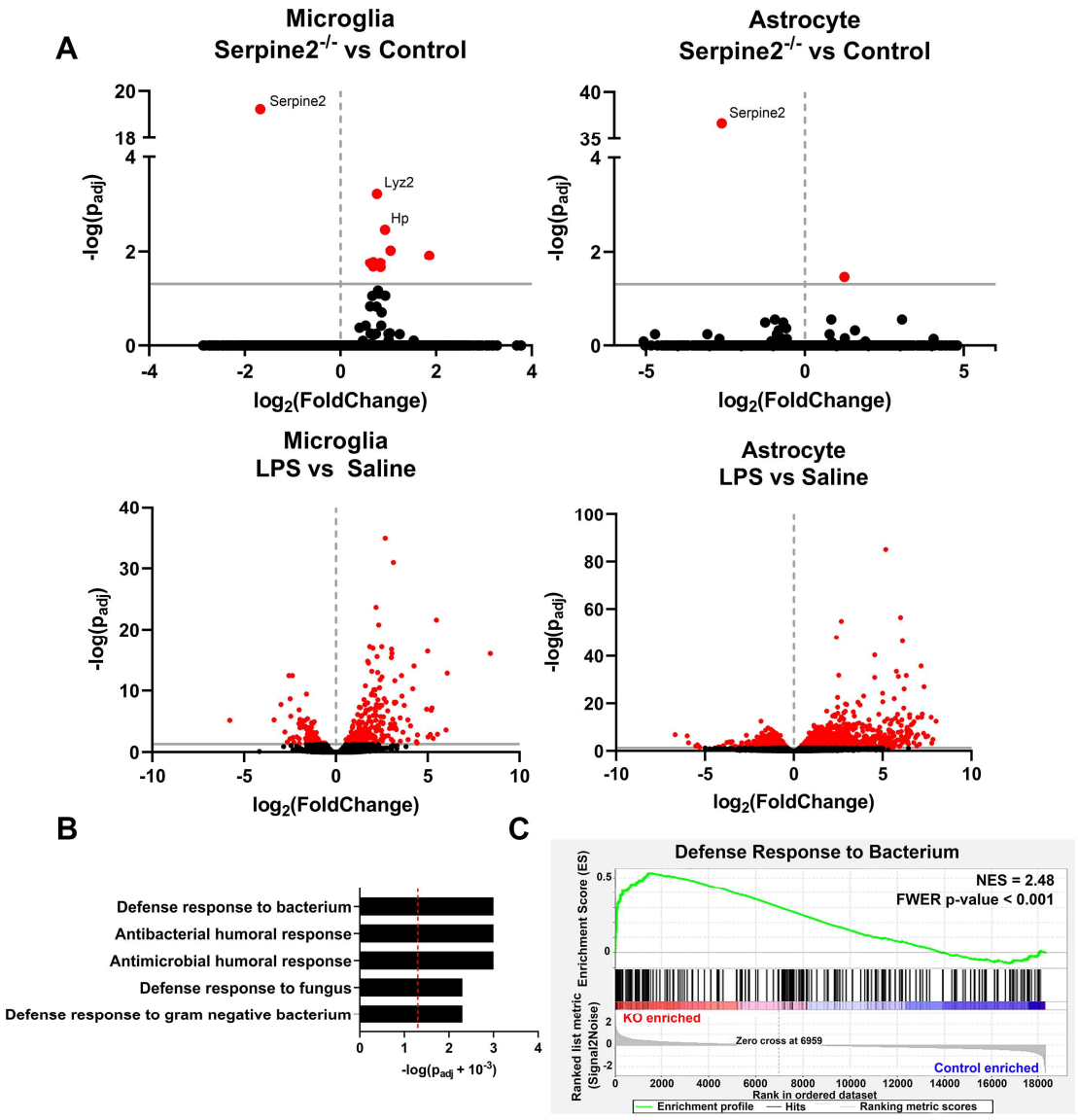

Figure 3-2. Transcriptomes of microglia and astrocytes in *Serpine2*$^{-/-}$ mice. A) Volcano plots of the differential gene expression analysis results for microglia (top) and astrocytes (bottom) with respect to genotype (left) and LPS response (right). Red = p-adjusted < 0.05. B) Gene set enrichment analysis (GSEA) results for *Serpine2*$^{-/-}$ microglia, selected terms with significant enrichment. Dashed line marks p = 0.05 C) GSEA detailed results of one term significantly enriched in *Serpine2*$^{-/-}$ microglia; NES = normalized enrichment score, FWER = family-wise error rate.

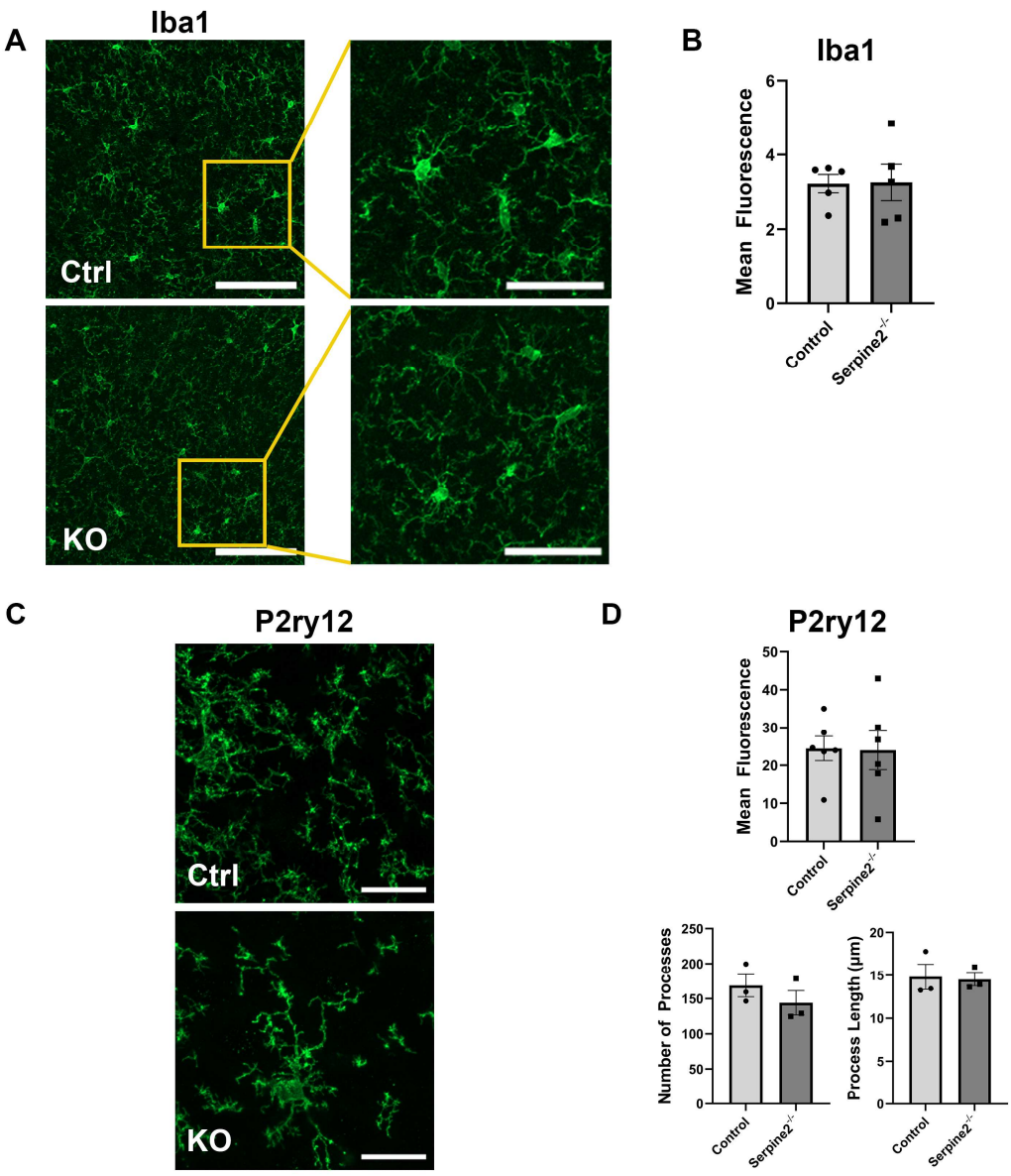

Figure 3-3. Microglial morphology in *Serpine2*$^{-/-}$ mice. A) Example images of microglial marker Iba1 in *Serpine2*$^{-/-}$ and control mice and high magnification insets. Full image scale bar = 100 µm, inset scale bar = 50 µm. B) Quantification of Iba1 fluorescence in *Serpine2*$^{-/-}$ vs. control animals. C) Example images of microglial marker P2ry12. Scale bar = 20 µm. D) Quantification of P2ry12 fluorescence (top) and microglial process morphology as analyzed with Imaris using images of P2ry12 fluorescence.

3.6 References

1. Perry VH, Cunningham C, Holmes C. Systemic infections and inflammation affect chronic neurodegeneration. Nat Rev Immunol. 2007;7(2):161-7. Epub 2007/01/16. doi: 10.1038/nri2015. PubMed PMID: 17220915.
2. Schwartz M, Butovsky O, Bruck W, Hanisch UK. Microglial phenotype: is the commitment reversible? Trends Neurosci. 2006;29(2):68-74. Epub 2006/01/13. doi: 10.1016/j.tins.2005.12.005. PubMed PMID: 16406093.
3. Morgan D, Gordon MN, Tan J, Wilcock D, Rojiani AM. Dynamic complexity of the microglial activation response in transgenic models of amyloid deposition: implications for Alzheimer therapeutics. J Neuropathol Exp Neurol. 2005;64(9):743-53. Epub 2005/09/06. doi: 10.1097/01.jnen.0000178444.33972.e0. PubMed PMID: 16141783.
4. Herber DL, Maloney JL, Roth LM, Freeman MJ, Morgan D, Gordon MN. Diverse microglial responses after intrahippocampal administration of lipopolysaccharide. Glia. 2006;53(4):382-91. Epub 2005/11/17. doi: 10.1002/glia.20272. PubMed PMID: 16288481.
5. Scott RW, Bergman BL, Bajpai A, Hersh RT, Rodriguez H, Jones BN, et al. Protease nexin. Properties and a modified purification procedure. J Biol Chem. 1985;260(11):7029-34. Epub 1985/06/10. PubMed PMID: 3997857.
6. Eaton DL, Scott RW, Baker JB. Purification of human fibroblast urokinase proenzyme and analysis of its regulation by proteases and protease nexin. J Biol Chem. 1984;259(10):6241-7. Epub 1984/05/25. PubMed PMID: 6373753.
7. Evans DL, McGrogan M, Scott RW, Carrell RW. Protease specificity and heparin binding and activation of recombinant protease nexin I. J Biol Chem. 1991;266(33):22307-12. Epub 1991/11/25. PubMed PMID: 1939253.
8. Knauer DJ, Majumdar D, Fong PC, Knauer MF. SERPIN regulation of factor XIa. The novel observation that protease nexin 1 in the presence of heparin is a more potent inhibitor of

factor XIa than C1 inhibitor. J Biol Chem. 2000;275(48):37340-6. Epub 2000/09/07. doi: 10.1074/jbc.M003909200. PubMed PMID: 10973954.

9. Hermans JM, Stone SR. Interaction of activated protein C with serpins. Biochem J. 1993;295 (Pt 1)(Pt 1):239-45. Epub 1993/10/01. doi: 10.1042/bj2950239. PubMed PMID: 8216224; PubMed Central PMCID: PMCPMC1134845.

10. Zhang Y, Chen K, Sloan SA, Bennett ML, Scholze AR, O'Keeffe S, et al. An RNA-sequencing transcriptome and splicing database of glia, neurons, and vascular cells of the cerebral cortex. J Neurosci. 2014;34(36):11929-47. Epub 2014/09/05. doi: 10.1523/JNEUROSCI.1860-14.2014. PubMed PMID: 25186741; PubMed Central PMCID: PMCPMC4152602.

11. Zhang Y, Sloan SA, Clarke LE, Caneda C, Plaza CA, Blumenthal PD, et al. Purification and Characterization of Progenitor and Mature Human Astrocytes Reveals Transcriptional and Functional Differences with Mouse. Neuron. 2016;89(1):37-53. Epub 2015/12/22. doi: 10.1016/j.neuron.2015.11.013. PubMed PMID: 26687838; PubMed Central PMCID: PMCPMC4707064.

12. Luthi A, Van der Putten H, Botteri FM, Mansuy IM, Meins M, Frey U, et al. Endogenous serine protease inhibitor modulates epileptic activity and hippocampal long-term potentiation. J Neurosci. 1997;17(12):4688-99. Epub 1997/06/15. PubMed PMID: 9169529; PubMed Central PMCID: PMCPMC6573330.

13. Meins M, Herry C, Muller C, Ciocchi S, Moreno E, Luthi A, et al. Impaired fear extinction in mice lacking protease nexin-1. Eur J Neurosci. 2010;31(11):2033-42. Epub 2010/06/10. doi: 10.1111/j.1460-9568.2010.07221.x. PubMed PMID: 20529116.

14. Kvajo M, Albrecht H, Meins M, Hengst U, Troncoso E, Lefort S, et al. Regulation of brain proteolytic activity is necessary for the in vivo function of NMDA receptors. J Neurosci. 2004;24(43):9734-43. Epub 2004/10/29. doi: 10.1523/JNEUROSCI.3306-04.2004. PubMed PMID: 15509762; PubMed Central PMCID: PMCPMC6730139.

15. Monard D. SERPINE2/Protease Nexin-1 in vivo multiple functions: Does the puzzle make sense? Semin Cell Dev Biol. 2017;62:160-9. Epub 2016/08/23. doi: 10.1016/j.semcdb.2016.08.012. PubMed PMID: 27545616.

16. Itzekson Z, Maggio N, Milman A, Shavit E, Pick CG, Chapman J. Reversal of trauma-induced amnesia in mice by a thrombin receptor antagonist. J Mol Neurosci. 2014;53(1):87-95. Epub 2013/12/20. doi: 10.1007/s12031-013-0200-8. PubMed PMID: 24352712.

17. Vaillant C, Michos O, Orolicki S, Brellier F, Taieb S, Moreno E, et al. Protease nexin 1 and its receptor LRP modulate SHH signalling during cerebellar development. Development. 2007;134(9):1745-54. Epub 2007/04/06. doi: 10.1242/dev.02840. PubMed PMID: 17409116.

18. Fayard B, Bianchi F, Dey J, Moreno E, Djaffer S, Hynes NE, et al. The serine protease inhibitor protease nexin-1 controls mammary cancer metastasis through LRP-1-mediated MMP-9 expression. Cancer Res. 2009;69(14):5690-8. Epub 2009/07/09. doi: 10.1158/0008-5472.CAN-08-4573. PubMed PMID: 19584287.

19. Bohlen CJ, Bennett FC, Bennett ML. Isolation and Culture of Microglia. Curr Protoc Immunol. 2019;125(1):e70. Epub 2018/11/11. doi: 10.1002/cpim.70. PubMed PMID: 30414379; PubMed Central PMCID: PMCPMC6510657.

20. Dobin A, Davis CA, Schlesinger F, Drenkow J, Zaleski C, Jha S, et al. STAR: ultrafast universal RNA-seq aligner. Bioinformatics. 2013;29(1):15-21. Epub 2012/10/30. doi: 10.1093/bioinformatics/bts635. PubMed PMID: 23104886; PubMed Central PMCID: PMCPMC3530905.

21. Anders S, Pyl PT, Huber W. HTSeq--a Python framework to work with high-throughput sequencing data. Bioinformatics. 2015;31(2):166-9. Epub 2014/09/28. doi: 10.1093/bioinformatics/btu638. PubMed PMID: 25260700; PubMed Central PMCID: PMCPMC4287950.

22. Love MI, Huber W, Anders S. Moderated estimation of fold change and dispersion for RNA-seq data with DESeq2. Genome Biol. 2014;15(12):550. Epub 2014/12/18. doi: 10.1186/s13059-014-0550-8. PubMed PMID: 25516281; PubMed Central PMCID: PMCPMC4302049.

23. Subramanian A, Tamayo P, Mootha VK, Mukherjee S, Ebert BL, Gillette MA, et al. Gene set enrichment analysis: a knowledge-based approach for interpreting genome-wide expression profiles. Proc Natl Acad Sci U S A. 2005;102(43):15545-50. Epub 2005/10/04. doi: 10.1073/pnas.0506580102. PubMed PMID: 16199517; PubMed Central PMCID: PMCPMC1239896.

24. Zamanian JL, Xu L, Foo LC, Nouri N, Zhou L, Giffard RG, et al. Genomic analysis of reactive astrogliosis. J Neurosci. 2012;32(18):6391-410. Epub 2012/05/04. doi: 10.1523/JNEUROSCI.6221-11.2012. PubMed PMID: 22553043; PubMed Central PMCID: PMCPMC3480225.

25. Pulido-Salgado M, Vidal-Taboada JM, Barriga GG, Sola C, Saura J. RNA-Seq transcriptomic profiling of primary murine microglia treated with LPS or LPS + IFNgamma. Sci Rep. 2018;8(1):16096. Epub 2018/11/02. doi: 10.1038/s41598-018-34412-9. PubMed PMID: 30382133; PubMed Central PMCID: PMCPMC6208373.

26. Marsh SE, Walker AJ, Kamath T, Dissing-Olesen L, Hammond TR, de Soysa TY, et al. Dissection of artifactual and confounding glial signatures by single-cell sequencing of mouse and human brain. Nat Neurosci. 2022;25(3):306-16. Epub 2022/03/10. doi: 10.1038/s41593-022-01022-8. PubMed PMID: 35260865.

27. Fleming A. On a remarkable bacteriolytic element found in tissues and secretions. Proc R Soc Lond B. 1922;(93):306–17. doi: https://doi.org/10.1098/rspb.1922.0023.

28. Cross M, Mangelsdorf I, Wedel A, Renkawitz R. Mouse lysozyme M gene: isolation, characterization, and expression studies. Proc Natl Acad Sci U S A. 1988;85(17):6232-6.

Epub 1988/09/01. doi: 10.1073/pnas.85.17.6232. PubMed PMID: 3413093; PubMed Central PMCID: PMCPMC281943.

29. Eaton JW, Brandt P, Mahoney JR, Lee JT, Jr. Haptoglobin: a natural bacteriostat. Science. 1982;215(4533):691-3. Epub 1982/02/05. doi: 10.1126/science.7036344. PubMed PMID: 7036344.

30. Feeley EM, Pilla-Moffett DM, Zwack EE, Piro AS, Finethy R, Kolb JP, et al. Galectin-3 directs antimicrobial guanylate binding proteins to vacuoles furnished with bacterial secretion systems. Proc Natl Acad Sci U S A. 2017;114(9):E1698-E706. Epub 2017/02/15. doi: 10.1073/pnas.1615771114. PubMed PMID: 28193861; PubMed Central PMCID: PMCPMC5338555.

31. Zackular JP, Chazin WJ, Skaar EP. Nutritional Immunity: S100 Proteins at the Host-Pathogen Interface. J Biol Chem. 2015;290(31):18991-8. Epub 2015/06/10. doi: 10.1074/jbc.R115.645085. PubMed PMID: 26055713; PubMed Central PMCID: PMCPMC4521021.

32. Scheenstra MR, van Harten RM, Veldhuizen EJA, Haagsman HP, Coorens M. Cathelicidins Modulate TLR-Activation and Inflammation. Front Immunol. 2020;11:1137. Epub 2020/06/26. doi: 10.3389/fimmu.2020.01137. PubMed PMID: 32582207; PubMed Central PMCID: PMCPMC7296178.

33. Gallo RL, Kim KJ, Bernfield M, Kozak CA, Zanetti M, Merluzzi L, et al. Identification of CRAMP, a cathelin-related antimicrobial peptide expressed in the embryonic and adult mouse. J Biol Chem. 1997;272(20):13088-93. Epub 1997/05/16. doi: 10.1074/jbc.272.20.13088. PubMed PMID: 9148921.

34. Schoenen H, Bodendorfer B, Hitchens K, Manzanero S, Werninghaus K, Nimmerjahn F, et al. Cutting edge: Mincle is essential for recognition and adjuvanticity of the mycobacterial cord factor and its synthetic analog trehalose-dibehenate. J Immunol. 2010;184(6):2756-

60. Epub 2010/02/19. doi: 10.4049/jimmunol.0904013. PubMed PMID: 20164423; PubMed Central PMCID: PMCPMC3442336.

35. Raivich G, Bohatschek M, Kloss CU, Werner A, Jones LL, Kreutzberg GW. Neuroglial activation repertoire in the injured brain: graded response, molecular mechanisms and cues to physiological function. Brain Res Brain Res Rev. 1999;30(1):77-105. Epub 1999/07/17. doi: 10.1016/s0165-0173(99)00007-7. PubMed PMID: 10407127.

36. Krawczyk MC, Haney JR, Pan L, Caneda C, Khankan RR, Reyes SD, et al. Human Astrocytes Exhibit Tumor Microenvironment-, Age-, and Sex-Related Transcriptomic Signatures. J Neurosci. 2022;42(8):1587-603. Epub 2022/01/07. doi: 10.1523/JNEUROSCI.0407-21.2021. PubMed PMID: 34987109; PubMed Central PMCID: PMCPMC8883850.

37. Paolicelli RC, Bolasco G, Pagani F, Maggi L, Scianni M, Panzanelli P, et al. Synaptic pruning by microglia is necessary for normal brain development. Science. 2011;333(6048):1456-8. Epub 2011/07/23. doi: 10.1126/science.1202529. PubMed PMID: 21778362.

38. Schafer DP, Lehrman EK, Kautzman AG, Koyama R, Mardinly AR, Yamasaki R, et al. Microglia sculpt postnatal neural circuits in an activity and complement-dependent manner. Neuron. 2012;74(4):691-705. Epub 2012/05/29. doi: 10.1016/j.neuron.2012.03.026. PubMed PMID: 22632727; PubMed Central PMCID: PMCPMC3528177.

39. Lino MM, Vaillant C, Orolicki S, Sticker M, Kvajo M, Monard D. Newly generated cells are increased in hippocampus of adult mice lacking a serine protease inhibitor. BMC Neurosci. 2010;11:70. Epub 2010/06/10. doi: 10.1186/1471-2202-11-70. PubMed PMID: 20529321; PubMed Central PMCID: PMCPMC2896953.

40. Simard M, Arcuino G, Takano T, Liu QS, Nedergaard M. Signaling at the gliovascular interface. J Neurosci. 2003;23(27):9254-62. Epub 2003/10/10. doi:

10.1523/JNEUROSCI.23-27-09254.2003. PubMed PMID: 14534260; PubMed Central PMCID: PMCPMC6740832.